AUTOPHAGY IN ANTIVIRAL IMMUNITY

APPROVED BY SUPERVISORY COMMITTEE

Beth Levine, M.D.

James Chen, Ph.D.

Beatriz Fontoura, Ph.D.

Lora Hooper, Ph.D.

ACKNOWLEDGMENTS

I would like to acknowledge the many people who made to this work possible. Without the advice, input, collaboration, and support of these people, my efforts alone would have been meaningless. The number of people that helped me is too many to name here, so I thank you and apologize if I have omitted your name.

First, I would like to thank my mentor, Dr. Beth Levine, for trusting that I would be successful with the considerable amount of resources she provided. Her enthusiasm, perceptiveness, and dedication were a constant motivation while completing this work. I thank her for exposing me to the fascinating field of autophagy, training me to be a better scientist, allowing me to travel the world to meet experts in this field, and preparing me for the next phase of my career. I would also like to thank the Levine lab members, who all contributed to this work in some way. Most of all I thank Dr. Rhea Sumpter; his unquenchable curiosity about infection and immunity made every day in the lab enjoyable. Moreover, Rhea performed a number of crucial experiments and followed up on my preliminary observations regarding the mechanism of SMURF1. I thank former post-doctoral fellows, Zolt Tallóczy and Sarah MacPherson, for initiating and laying the groundwork for the studies on HSV-1 and Sindbis virus, respectively. Qihua Sun and Zhongju Zou provided excellent technical support and assisted with a number of experiments in our studies. The other lab members provided a diverse and intellectually stimulating research environment.

I would like to thank other individuals at UT Southwestern and elsewhere who collaborated on this work. Shuguang Wei, Mridula Vishwanath, Dr. Bruce Posner, Dr. Michael Roth, and others in the High Throughput Screening center were instrumental in

developing and implementing our screen. Abhijit Bugde and Dr. Kathrine Luby-Phelps provided support in Live Cell Imaging core facility, and Dr. Luby-Phelps provided her invaluable expertise on microscopy and image analysis. Dr. Guanghua Xiao and Dr. Yang Xie performed statistical analysis of our screen data. Dr. Aylwin Ng and Dr. Ramnik Xavier collaborated on bioinformatic analysis of our screening data. Dr. Diane Alexander and Dr. David Leib provided HSV-1 mutant strains and performed PKR KO mouse experiments. I would like to thank members of my thesis committee, Dr. Beatriz Fontoura, Dr. Lora Hooper, and Dr. James Chen, for the advice and critiques that made our work stronger.

I am grateful for my future wife, Dr. Melanie Yarbrough. I have known you as a colleague, collaborator, and friend. I thank you for your understanding, and for always being there for me even when work consumed me. You taught me to slow down every now and again, enjoy the moment, and not take myself so seriously! I love you very much.

Lastly, I would like to thank my family. Without the love and support of my parents, I would have never been in a position to seize the many opportunities I was provided. Both of you taught me the value of education and instilled in me my work ethic. To my mother, you taught me patience and an appreciation of nature's beauty. To my father, you taught me perseverance and nutured my academic interests. This work is a testament to these things you both taught me, and I can never thank you enough.

AUTOPHAGY IN ANTIVIRAL IMMUNITY

by

ANTHONY WALTER ORVEDAHL

DISSERTATION

Presented to the Faculty of the Graduate School of Biomedical Sciences

The University of Texas Southwestern Medical Center at Dallas

In Partial Fulfillment of the Requirements

For the Degree of

DOCTOR OF PHILOSOPHY

The University of Texas Southwestern Medical Center at Dallas

Dallas, Texas

May, 2012

AUTOPHAGY IN ANTIVIRAL IMMUNITY

ANTHONY WALTER ORVEDAHL, Ph.D.

The University of Texas Southwestern Medical Center at Dallas, 2012

BETH LEVINE, M.D.

Autophagy is an evolutionarily conserved pathway in which cytoplasmic material is sequestered in a double-membrane vesicle and delivered to the lysosome for degradation. During times of starvation, autophagy functions to generate essential nutrients through the degradation of non-essential cytoplasmic contents. It is also the only known mechanism for removal of damaged or superfluous organelles and cytoplasmic contents that are too large to be degraded by the proteasome. Given the critical role for autophagy in response to stress and in maintaining cell cytoplasmic quality control, it is not surprising that autophagy plays an essential role in the host response to infection, and that microbes have evolved mechanisms to counteract or evade autophagy. In this work,

we studied the role of autophagy inhibition in a mouse model of herpes simplex virus type I (HSV-1) encephalitis, investigated the role of autophagy in protection against Sindbis virus infection of the central nervous system (CNS), and identified novel host genes involved in targeting viral proteins to the autophagy pathway. We found that the HSV-1 encoded neurovirulence protein ICP34.5 interacted with the host autophagy protein Beclin 1, and that this interaction was essential for HSV-1 neurovirulence. This was the first example of a viral virulence protein that targets host autophagy, and provided evidence that autophagy functions in innate immunity to viruses. In a second study, we found that the host autophagy gene *Atg5* was required to protect against lethal Sindbis virus CNS disease. We found that autophagy targeted viral proteins for degradation in brains of infected mice and cells *in vitro*, and that the autophagy adaptor protein p62 was involved in targeting viral proteins for autophagic degradation. This study demonstrated that degradation of viral proteins by autophagy was an important mechanism for cellular and organismal survival. Lastly, we performed a genome-wide siRNA screen to identify novel host factors required for autophagic targeting of viral proteins. We identified cellular networks and genes that were previously unappreciated to be involved in targeting viral proteins for autophagy. One of these factors, SMURF1, is an E3 ubiquitin ligase that not only functioned to target viral proteins, but was also involved in targeting damaged mitochondria for autophagic clearance.

TABLE OF CONTENTS

PUBLICATIONS

Orvedahl, A.*, Sumpter, Jr., R.*, Xiao, G.[#], Ng, A.[#], Zou, Z., Tang, Yi., Narimatsu, M., Gilpin, C., Sun, Q., Roth, M., Forst, C. V., Wrana, J. L., Tang, Y., Zhang, Y. E., Luby-Phelps, K., Xavier, R., Xie, Y., Levine, B. (2011) Image-based genome-wide siRNA screen identifies selective autophagy factors. Nature *480*, 113-7.

Bodemann, B.O., **Orvedahl, A.**, Cheng, T., Ram, R.R., Ou, Y.H., Formstecher, E., Maiti, M., Hazelett, C.C., Wauson, E.M., Balakireva, M., Camonis, J.H., Yeaman, C., Levine, B., White, M.A. (2011) RalB and the exocyst mediate the cellular starvation response by direct activation of autophagosome assembly. Cell *144*, 253-67.

Orvedahl, A.*, MacPherson, S.*, Sumpter, Jr., R., Zou, Z., Tallóczy, Z., and Levine, B. (2010) Autophagy protects against Sindbis virus infection of the central nervous system. Cell Host & Microbe *7*, 115-27.

Orvedahl, A. and Levine, B. (2009) "Autophagy in mammalian antiviral immunity" in Autophagy in Infection and Immunity, Curr. Top. Microbiol. Immunol. ed. by Levine, B., Yoshimori, T., and Deretic, V. Springer-Verlag, *335*, 267-85.

Orvedahl, A. and Levine, B. (2009) Eating the enemy within: Autophagy in infectious diseases. Cell Death Differ. *16,* 57-69.

Burdette, D.*, Yarbrough, M.*, **Orvedahl, A.**, Gilpin, C., and Orth, K. (2008) *Vibrio parahaemolyticus* orchestrates a multifaceted host cell infection by induction of autophagy, cell rounding and then cell lysis. Proc Natl Acad Sci USA. *105*, 12497-502.

Orvedahl, A. and Levine, B. (2008). Autophagy and viral neurovirulence. Cell Microbiol. *10*, 1747-56.

Orvedahl, A. and Levine, B. (2008). Viral evasion of autophagy. Autophagy *4*, 280-5.

Orvedahl, A.*, Alexander, D.*, Tallóczy, Z., Sun, Q., Wei, Y., Zhang, W., Burns, D., Lieb, D.A., and Levine, B. (2007). HSV-1 ICP34.5 confers neurovirulence by targeting the Beclin 1 autophagy protein. Cell Host & Microbe *1*, 23-35.

He, C., and **Orvedahl, A.** (2007). Meeting report: 2007 Keystone Symposium on Autophagy in Health and Disease. Autophagy *3*, 527-36.

*, [#] These authors contributed equally to this work.

LIST OF FIGURES

LIST OF TABLES

LIST OF ABBREVIATIONS

3-MA	3-methyladenine
Atg	Autophagy-related gene
Bcl-2	B-cell lymphoma 2
BHK-21	Baby hamster kidney cell
CCCP	Carbonyl cyanide *m*-chlorophenyl hydrazone
CMV	Cytomegalovirus
CNS	Central nervous system
DMEM	Dulbecco's Modified Eagle Medium
EDTA	Ethylenediaminetetraacetic acid
eIF2α	eukaryotic initiation factor 2α
EM	Electron microscopy
ES	Embryonic stem cells
FBS	Fetal bovine serum
GADD34	Growth arrest and DNA damage-inducible protein 34
GFP	Green flourescent protein
H&E	Hematoxylin and eosin
HBSS	Hanks buffered salt solution
HEPES	4-(2-hydroxyethyl)-1-piperazineethanesulfonic acid
HSV-1	Herpes simplex virus type I
ICP34.5	Infected cell protein 34.5
IFN	Interferon
KSHV	Kaposi's sarcoma-associated virus

LC3	Microtubule-associate protein light chain 3
MAPK	Mitogen associated protein kinase
MEF	Mouse embryonic fibroblast
MOI	Multiplicity of infection
PAGE	Polyacrylamide gel electrophoresis
PAMP	Pathogen associated molecular pattern
PBS	Phosphate buffered saline
PE	Phosphatidyl ethanolamine
PFU	Plaque forming unit
PI3	Phosphoinositide-3-phosphate
PKR	Protein kinase R
PRR	Pattern recognition receptor
PVDF	Polyvinylidene difluoride
RFWD3	Ring finger, WD repeat 3
SIN	Sindbis virus
siRNA	small-interfering RNA
SMURF1	SMAD specific E3 ubiquitin protein ligase 1
TLR	Toll-like receptor
TUNEL	Terminal dUTP nick end labeling
VPS	Vacuolar protein sorting
VSV	Vesicular stomatitis virus
YFP	Yellow fluorescent protein
γ-HV68	gamma-herpes virus 68

CHAPTER ONE
Introduction and Literature Review

General Introduction

Autophagy (derived from Greek roots auto, meaning 'self', and phagy, 'to eat') is a highly evolutionarily conserved pathway in which cytoplasmic material is sequestered in a double-membrane vesicle and delivered to the lysosome for degradation. Autophagy genes are found in almost every eukaryotic species, from yeast to humans, with the exception of protozoan parasites that derive nutrients from their hosts (Hughes and Rusten, 2007). The wide conservation of the autophagy machinery suggests that this pathway arose very early during eukaryotic cellular evolution and underscores its fundamental role in cellular physiology. Indeed, an expanding body of evidence suggests that autophagy plays diverse roles in normal cellular homeostasis, and defects of which may lead to an array of diseases ranging from neurodegeneration, to cancer, to infectious diseases.

Viruses, as obligate intracellular parasites, rely on the host cell protein translation machinery, nucleic acids, and membranes for their replication. Viruses are evolutionarily ancient, and thus the competition for resources between cells and viruses is also an ancient driving force in evolution (Koonin et al., 2006). It is therefore not surprising that autophagy, as an important stress response and cytosolic quality control pathway, has emerged as an integral component of the cellular response to viral infection. In addition to the pro-survival and recycling

functions of autophagy, the sequestration of foreign infectious agents (termed ‘xenophagy’, or ‘to eat what is foreign’ (Levine, 2005)) may facilitate delivery of microbial products to the vesicular compartments involved in innate and adaptive immune activation. Given the central role of autophagy in the cellular response to infection, successful pathogens have inevitably evolved mechanisms to target the host autophagy machinery and counteract the immune functions of autophagy to cause disease.

The Autophagy Machinery

The autophagy pathway is regulated and executed by a conserved core set of genes, first identified in yeast (termed ‘Atg’ genes) (Mizushima et al., 1998; Tsukada and Ohsumi, 1993). Formation of the autophagosome is thought to involve a membrane nucleation step, followed by membrane expansion around cytoplasmic cargo, and closure to form the characteristic double-membrane vesicle (Fig. 1). Autophagosomes are trafficked through the cell to fuse with lysosomes, and the inner membrane and sequestered material are degraded. In addition to regulation at steps of vesicle closure and lysosomal fusion, a large and growing number of signaling pathways have been identified that converge on the vesicle nucleation machinery to modulate levels of autophagy.

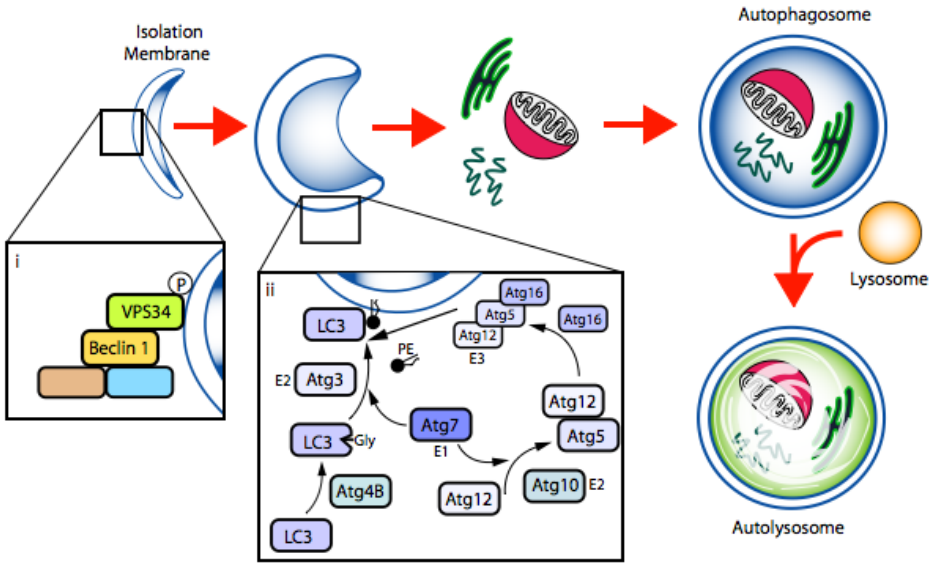

Fig. 1. The Autophagy Pathway and Machinery. Schematic showing the initiation complex (i), which contains Beclin 1, VPS34, and other regulatory proteins (not shown, for review see (He and Levine, 2010)), which nucleates the membrane and recruits the elongation and fusion machinery (ii). The pathway is completed after autophagosome fusion with lysosomes to form autolysosomes in which the contents are degraded.

Initiation of autophagosome formation in mammals involves a complex containing the ortholog of yeast *ATG6*, Beclin 1, and a Class III PI3 kinase, VPS34 (reviewed in (He and Levine, 2010)) (Fig. 1i). Generation of phosphoinositol-3-phosphate by VPS34 is thought to recruit two ubiquitin-like conjugation systems that ultimately result in covalent linkage of the mammalian ortholog of yeast *ATG8*, microtubule light chain 3 (LC3), to phosphatidylethanolamine (PE) in the growing isolation membrane (Geng and Klionsky, 2008). Atg7 functions as an E1 ligase in both reactions, by transferring both LC3 and Atg12 to their E2 ligases, Atg3 and Atg10, respectively. Atg12 is conjugated to Atg5, which associates with Atg16 in a tetramer of trimers. The Atg5-12-16 complex functions as an E3 itself to facilitate transfer of LC3 from

Atg3 to PE (Hanada et al., 2007), and specify its location in the membrane (Fujita et al., 2008b) (Fig 1ii). Autophagosome closure is facilitated by removal of LC3 from the outer membrane by Atg4 (Fujita et al., 2008a), which is also required for initial activation of LC3 by removal of its C-terminal glycine (Tanida et al., 2004)(Fig. 1). Activation of the autophagy machinery can be assayed by biochemical detection of the PE-conjugated form of LC3 (as a lower migrating form, referred to as LC3-II, compared to unconjugated LC3-I), or by fluorescence microscopy (with N-terminal fluorescent protein fusions or by immunofluorescence of LC3) where LC3 is observed to redistribute from a diffuse pattern to punctate pattern upon autophagy stimulation (Klionsky et al., 2008). Autophagic flux can be assayed by treating cells with lysosomal protease inhibitors, in which case accumulation of additional LC3 indicates that lysosomal turnover is intact. In addition to generating tools to measure autophagy regulation, identification of autophagy genes has provided the ability to dissect the roles of this ancient pathway in health and disease.

Functions of Autophagy

Autophagosomes were first described in the 1960's in ultrastructural studies of tissues from developing and stressed animals (De Duve and Wattiaux, 1966). Nutrient deprivation was also demonstrated to induce autophagy in yeast (Takeshige et al., 1992), and the first genetic screen in yeast to identify autophagy genes revealed an essential role for autophagy in yeast survival during starvation

(Tsukada and Ohsumi, 1993). Since the early observations of autophagy in starved animals and initial identification of autophagy genes, there has been an explosion of knowledge about the roles of autophagy in processes ranging from multicellular organismal development, to specific elimination of organelles, to involvement in non-classical release of cytoplasmic contents. This section will highlight basic functions of autophagy that have been shown or are predicted to also be important during infection (discussed below).

Eukaryotic cells possess two pathways to degrade cytosolic proteins: the ubiquitin-proteasome and the autolysosomal pathway. While short-lived proteins are thought to be degraded primarily by the proteasome, long-lived proteins are turned over by constitutive autophagy of the cytosol (Korolchuk et al., 2010). Protein turnover by autophagy functions to prevent accumulation of damaged oxidized proteins in the cell, and also prevents accumulation of mutant aggregate-prone proteins (Kubota, 2009). Additionally, as mentioned above, during nutrient-limiting conditions autophagy can be upregulated to degrade cytosolic material and generate metabolites for energy production and to maintain essential functions.

Genetic knockout studies have demonstrated that mammalian autophagy is important both during the starvation response and to prevent accumulation of aggregated proteins. *Atg5* and *Atg7* knockout mice, which survive embryonic development, die early after birth presumably due to a failure to adapt to the *ex utero* nutrient limiting environment (Komatsu et al., 2005; Kuma et al., 2004).

Using tissue-specific knockout animals, two groups subsequently demonstrated that endogenous mammalian autophagy genes are important to maintain cytosolic protein quality control and prevent aggregate formation. Neuronal-specific deletion of either *Atg5* (Hara et al., 2006), or *Atg7* (Komatsu et al., 2006), results in progressive accumulation of ubiquitinated proteins and intracellular inclusions. Moreover, these mice develop progressive neurodegenerative disease, underscoring the essential role of cytosolic protein quality control through autophagy in post-mitotic cellular homeostasis and survival (Hara et al., 2006; Komatsu et al., 2006).

In addition to routine organelle and protein quality control functions, autophagy is important in preventing the accumulation of aggregate-prone disease-causing proteins (Kubota, 2009). In *Caenorhabditis elegans*, autophagy prevents mutant polyQ-containing protein aggregate accumulation and neurodegeneration (Jia et al., 2007; Khan et al., 2008). Mammalian cells may target ubiquitinated proteins, including the polyQ-containing mutant huntingtin disease protein (htt), for autophagy by the adaptor protein, p62/SQSTM1 (Bjorkoy et al., 2005), which contains a ubiquitin-binding motif and also directly interacts with the autophagosomal protein, LC3 (Pankiv et al., 2007). Importantly, upregulation of autophagy enhances the clearance of mutant htt and tau proteins in Drosophila models of neurodegeneration (Berger et al., 2006; Ravikumar et al., 2002). There are also data suggesting that autophagy may play a role in preventing Alzheimer's disease (AD) (Nixon, 2007). In worms, autophagy

promotes the clearance of AD-related protein (Florez-McClure et al., 2007). These findings extend to mice and humans, in which Beclin 1 expression is decreased in brain tissue from human patients with AD, and β-amyloid accumulation and AD pathology are exacerbated by heterozygous deletion of beclin 1 in mice (Pickford et al., 2008). Together, these findings indicate that autophagy is likely essential for maintaining normal neuronal function and for the prevention of neurodegenerative diseases.

The role of autophagy in cell survival and death is complex, though the balance of evidence weighs heavily towards a prosurvival role for autophagy (Maiuri et al., 2007). The term "autophagic cell death" has been used to describe many instances of dying cells where autophagy has been observed, though few studies determine if autophagy is induced or if autophagosomes accumulate due to decreased turnover, or whether cells are dying "with autophagy" (where the pathway is upregulated as a 'last ditch' survival mechanism) or "by autophagy" (where the cell is literally consuming its contents at a level incompatible with survival) (Kroemer and Levine, 2008). One study that highlights the dual roles of autophagy in survival and death characterized the regulation of Beclin 1 by Bcl-2, and revealed that autophagy is tightly controlled so that homeostatic levels promote cell survival, while unregulated autophagy can lead to autophagic cell death (Pattingre et al., 2005).

Selective sequestration of autophagic substrates is increasingly being recognized as a specialization of autophagy that determines cytoplasmic makeup.

Cargo recognized for selective autophagy includes organelles (mitochondria, peroxisomes, endoplasmic reticulum (ER)), ubiquitinated protein aggregates, specific cytosolic proteins, ribosomes, and pathogens. The ability to discriminate between substrates intended for autolysosomal degradation and non-intended substrates enables the efficient clearance of substrates and spares essential cellular components from degradation. This form of autophagy may be important during times of stress, when non-essential substrates can be broken down to support essential processes, sparing cellular components that are crucial to maintain survival. Conversely, targeted elimination of vital cellular contents may be one mechanism by which autophagy promotes cell death (Yu et al., 2006). Selecting appropriate targets may also be essential when material is sequestered in order to be delivered to compartments other than lysosomes, such as immune compartments, or even the extracellular space (Duran et al., 2010; Manjithaya et al., 2010).

Together, the cellular functions of autophagy (clearance of cytosolic contents, mediation of cellular survival, and selective sequestration of substrates) position this pathway as an ideal mechanism to cope with the invasion and replication of microbial pathogens. Great strides have been made in recent years towards understanding the multifaceted role of autophagy in host immunity. In addition to utilizing the canonical functions of autophagy to combat infection, it is becoming clear that many unique aspects of autophagy may exist during infection in terms of pathway regulation and effector functions. The subsequent sections

will focus on the role of autophagy during infection, with particular focus on viral infection.

Immune Signaling and Autophagy

Many aspects of the autophagy pathway during infection may be unique, including the regulatory pathways (pattern recognition receptors (PRRs), pathogen-associated molecular patterns (PAMPs), and downstream signaling pathways), substrates for autophagosome sequestration (i.e., xenophagy of microbes and/or specific cellular contents), and potentially the events in autophagosome formation (Orvedahl and Levine, 2009b; Sumpter and Levine, 2010). Innate sensing and signaling pathways regulate autophagy induction, and an important effector function of autophagosomes may be to deliver ligands for innate and adaptive immune activation.

A front line of defense against invading pathogens is the well-conserved recognition of PAMPs by PRRs, including Toll-like receptors (TLRs)(Takeuchi and Akira, 2010), and these essential innate immune receptors have recently been demonstrated to regulate autophagy. One of the first immune signaling pathways shown to regulate autophagy was the cytosolic double-stranded viral RNA-sensing kinase PKR, which acts through phosphorylation of eIF2α (Talloczy et al., 2002). The first study to describe a function of TLRs in autophagy induction found that a component of the Gram-negative bacterial cell wall, lipopolysaccharide (LPS), induces autophagy through its cognate receptor TLR4

in macrophages (Xu et al., 2007). LPS-induced autophagy requires the TLR4 adaptor TRIF, but not MyD88, and the downstream components RIP1 and p38 mitogen-activated protein kinase (MAPK). Further, LPS stimulation increases the localization of *Mycobacterium tuberculosis* within autophagosomes suggesting a functional role of LPS signaling in autophagy-mediated pathogen control. Subsequently, Deretic and colleagues (Delgado et al., 2008) extended the known repertoire of TLRs and their ligands that induce autophagy to include TLR3/Poly I:C and TLR7/imiquimod and ssRNA, and confirmed TLR4/LPS induction of autophagy. They also demonstrated that TLR7-induced autophagy decreases *M. tuberculosis* var. *bovis* Bacille Calmette-Guérin (BCG) survival, and requires the TLR7 adaptor MyD88. An additional recent study suggested a novel function of autophagy in mediating TLR signaling in phagosome maturation (Sanjuan et al., 2007). Sanjuan et al. found that LPS induces autophagy as well as phagosome maturation (confirming the findings of Xu et al. (Xu et al., 2007) and Delgado et al. (Delgado et al., 2008)) but, in contrast to Delgado et al., found that autophagy is also stimulated with TLR2 agonists. It is possible that different cell types or agonist preparations may account for these differences, but further studies are needed to more clearly define the full spectrum of PAMPs and PRRs involved in autophagy regulation. Nonetheless, the studies described above convincingly link pathogen recognition, an essential component of innate immunity, with autophagy induction and also underscore the potential importance of autophagy as an innate immune effector in response to PAMPs.

In addition to TLRs, other PAMP-PRR interactions are important for autophagy regulation. In response to measles virus and *Streptococcus* binding, the cell surface complement receptor CD46 induces autophagy through interactions with a scaffolding protein GOPC and the Beclin 1/VPS34 complex (Joubert et al., 2009). Though the specific receptor remains unidentified, the vesicular stomatitis virus (VSV) glycoprotein G was isolated as a virion component that can induce autophagy in cultured Drosophila hemocytes (Shelly et al., 2009). It is likely that a specific PRR recognizes the VSV glycoprotein, though further work is required to identify this receptor. Another recent study in Drosophila further underscores the importance of specific PRRs not only in autophagy induction, but also in mediating autophagic control of bacterial replication in vivo (Yano et al., 2008). The PRR molecule PGRP-LE (analogous to Nod-like receptor (NLR) signaling in mammals) was identified as a crucial component of the host antimicrobial autophagic response in Drosophila (Yano et al., 2008). Yano et al. demonstrated that PGRP-LE mutant flies or flies expressing hemocyte-specific RNAi for PGRP-LE or the autophagy gene *Atg5* were hypersusceptible to lethal infection with *Listeria monocytogenes*. Signaling through the IMD and Toll pathways was dispensable for PGRP-LE-mediated autophagy and restriction of bacterial survival in primary hemocytes (Yano et al., 2008). Additionally, autophagy induction in hemocytes treated with purified tracheal cytotoxin and diaminopimelic-containing peptidoglycan ligands, but not lysine-type peptidoglycan, required PGRP-LE (Yano et al., 2008). Thus, it will be interesting

to determine the precise signaling pathways linking PGRP-LE to the autophagy machinery, and the identity of additional PRRs that are involved in autophagy induction in Drosophila.

Beyond the recognition of PAMPs by PRRs, there is a complex interplay between other immune signals and autophagy regulation. For example, NF-κB may negatively regulate TNF-mediated autophagy (Djavaheri-Mergny et al., 2006), whereas autophagy may negatively regulate NF-κB, in turn, through selective degradation of the upstream activators IκB kinase (Qing et al., 2006) and NF-κB inducing kinase (Qing et al., 2007). Additionally, interferon (IFN)γ-mediated autophagy and BCG killing requires the p47 immunity-related GTPase, IRGM1 (Singh et al., 2006). In contrast, TH2 cytokines (e.g., IL-4 and IL-13) negatively regulate IFNγ-mediated autophagic killing of mycobacteria in a STAT6-dependent manner (Harris et al., 2007). A recent report suggests that B-cell receptor signaling can recruit TLR9 to autophagosomes to promote synergistic signaling through p38 MAPK, and that formation of these compartments requires microtubules and phospholipase D activity (Chaturvedi et al., 2008). Thus, autophagy can be positively and negatively regulated by different immune signaling pathways. Studies in animal models should help to dissect the relative physiological importance of these different immune signaling pathways in the regulation of autophagy during different infectious diseases.

Effector Functions of Autophagy in Immunity

Not only do immune signals regulate autophagy, but autophagy also functions in innate and adaptive immune activation. Autophagy samples certain cytosolic antigens to present on class II MHC molecules for activation of the adaptive immune response (Dengjel et al., 2005; Nimmerjahn et al., 2003; Paludan et al., 2005; Schmid et al., 2007). and may also deliver viral antigens for MHC class I presentation (English et al., 2009). Further, specific strategies to target cytosolic antigens to autophagosomes may lead to enhanced vaccine efficacy, as an influenza virus antigen fused to the autophagosomal membrane protein, LC3, elicits higher levels of CD4+ T-cell responses than the antigen alone (Schmid et al., 2007). Autophagy also functions to deliver cytosolic viral replication intermediates to TLR7-containing endosomes to activate type I IFN production (Lee et al., 2007). The study by Delgado et al., which demonstrated that TLR7 itself activates autophagy (Delgado et al., 2008), raises the possibility that this may represent a positive feedback loop.

In addition to regulation of immune signaling, an important function of autophagy is direct targeting and degradation of invading pathogens (xenophagy). Bacterial pathogens that invade into the cytoplasm or disrupt phagolysosomal fusion are the most well characterized class of microbes that are targeted by autophagy. The first nearly simultaneous findings demonstrating this function of autophagy were with the pathogens, *M. tuberculosis* (Gutierrez et al., 2004) and Group A *Streptococcus* (Nakagawa et al., 2004). Gutierrez et al. found that induction of autophagy with physiological (starvation), pharmacological

(rapamycin), and immune (IFNγ and LRG-47) stimulation increased maturation of mycobacterial-containing vesicles and localization to autophagosomes, and decreased mycobacterial survival (Gutierrez et al., 2004). Nakagawa et al. demonstrated that autophagic targeting degrades Group A *Streptococci* that escape from the endosome and invade intracellularly, as delayed bacterial clearance is observed in *Atg5*-deficient cells (Nakagawa et al., 2004). Subsequent studies have demonstrated an important function of autophagy in targeting other intracellular bacterial pathogens including *Shigella flexneri, Listeria monocytogenes, Salmonella enterica, Francisella tularensis, and Burkholderia pseudomallei* (Birmingham et al., 2006; Checroun et al., 2006; Cullinane et al., 2008; Ogawa et al., 2005; Py et al., 2007; Yano et al., 2008). The biological significance of *Francisella* entry into autophagic compartments is unclear, but a recent study suggests that these compartments may also include MHC class II molecules (Hrstka et al., 2007). The recent study by Yano et al. of *Listeria* infection in Drosophila (discussed above) is an important first demonstration that the xenophagic targeting of bacteria can be an integral innate immune effector pathway *in vivo* (Yano et al., 2008).

Mechanisms by which bacteria can be targeted by autophagy are beginning to be uncovered. Studies with *Shigella* provided the first evidence that the autophagy machinery could associate with bacteria (Ogawa et al., 2005). The authors found that Atg5 could associate with the bacterial surface protein VirG, but a bacterially encoded effector, IcsB, disrupts this interaction to evade

targeting. More recent studies suggest that ubiquitin-binding autophagy adaptors, can recruit ubiquitinated or ubiquitin associated bacteria to the autophagosome. Somewhat similar to *Shigella* escape, *Legionella*-encoded ActA recruits the host Arp2/3 complex and Ena/VASP to the bacterial surface and shields the bacteria from ubiquitination, p62 and LC3 recruitment, and autophagic sequestration (Yoshikawa et al., 2009). Zheng *et al*. demonstrated that ubiquitinated proteins associate with the damaged *Salmonella*-containing vacuole, to which p62 is recruited, and that p62 is required for efficient autophagic clearance of the bacteria (Zheng et al., 2009). A novel ubiquitin-binding autophagy adaptor, NDP52, also links ubiquitin-associated *Salmonella* to Tank binding kinase (TBK1), and both NDP52 and TBK1 are required for autophagic targeting of the bacteria (Thurston et al., 2009). Autophagic regulation of *Shigella* invasion extends beyond direct bacterial targeting, as p62-mediated autophagic clearance of ubiquitinated vacuolar remnants modulates the inflammatory response to these byproducts of invasion (Dupont et al., 2009). Lastly, an F-BAR-containing protein, FNBPL1, with predicted membrane curvature activity, was demonstrated to be required for xenophagy of *Salmonella*, but was dispensable for other forms of autophagy (Huett et al., 2009). Together, these studies suggest that host cells may use tags (ie. ubiquitin) and adaptors (ie. p62) that are common to other forms of autophagy (ie. protein aggregates), as well as unique infection-specific molecules (NDP52 and FNBPL1) to target bacterial pathogens.

In addition to bacteria, protozoans may be targeted by autophagy. *Toxoplasma gondii* resides in parasitophorous vacuoles (PV) within macrophages and prevents their fusion with the lysosome. Two nearly simultaneous studies indicated that autophagy could function to overcome this block and restrict *T. gondii* survival. Andrade *et al.* found that stimulation of the CD40 receptor on macrophages resulted in localization of parasites to GFP-LC3-positive vesicles, vesicle maturation, and decreased intracellular microbial survival (Andrade et al., 2006). On the basis of ultrastructural studies and chemical autophagy inhibition studies, Ling *et al.* proposed a model in which the PV and parasite membranes are stripped before autophagic sequestration and lysosomal degradation (Ling et al., 2006). A non-canonical role for Atg5 in promotion of PV destruction has also been demonstrated (Zhao et al., 2008), underscoring the diversity of functions of the autophagy pathway and machinery in intracellular immunity.

Autophagy in Antiviral Immunity

Given the multifaceted role of autophagy in cell biology, and potential additional specializations of autophagy during immunity, it is likely that autophagy plays a pleiotropic role in protecting against viral infection (Orvedahl and Levine, 2009a). As an important function of autophagy is to maintain cellular homeostasis through its recycling functions and metabolite generation during stress, it is possible that autophagy promotes cell survival during viral infection. Additionally, autophagy can serve as a conduit for delivering cytoplasmic

material to endolysosomal compartments, which may deliver viral proteins and nucleic acids for immune activation and/or lysosomal degradation (as discussed above). While studies have shown that autophagy protects against infection with viruses from different classes in species ranging from flies to mammals, a number of key questions about the role of autophagy in viral infection remained unanswered.

The first genetic evidence that autophagy may function as an antiviral pathway (and an antimicrobial pathway in general) was provided by studies with the neurotropic alphavirus Sindbis virus. Expression of Beclin 1, the mammalian ortholog of yeast Atg6, from a double-subgenomic viral promoter protected mice against fatal Sindbis virus encephalitis, reduced neuronal cell death, and restricted viral replication in infected mouse brains (Liang et al., 1998). In plants, silencing of the autophagy genes *BECLIN 1*, *PI3K/VPS34*, *ATG3*, and *ATG7* resulted in the unrestricted cell death of uninfected cells during the hypersensitive response to tobacco mosaic virus infection (Liu et al., 2005). Additionally, *ATG*-silenced plants had increased viral replication at sites of infection, suggesting that autophagy functions to control virus production (Liu et al., 2005). In Drosophila, knockdown of *Atg7*, *12*, and *18* results in increased susceptibility to infection with vesicular stomatitis virus (VSV) (Shelly et al., 2009). Together these studies suggest that autophagy may function in regulating viral replication and/ or in promoting cell survival during infection.

Histopathologic studies of mouse brains infected with Sindbis virus suggested that one important function of autophagy is the prevention of virus-induced cell death. Compared to mouse brains infected with a virus containing a control insert, mouse brains infected with Sindbis virus overexpressing Beclin 1 exhibit decreased levels of apoptotic neuronal nuclei, while those infected with a virus expressing Beclin 1 with its Bcl-2 interaction domain deleted exhibit increased neuronal death (Liang et al., 1998). Thus, Bcl-2 regulation of Beclin 1 function may be required for autophagy to be neuroprotective rather than neurotoxic. Indeed, Pattingre and colleagues subsequently demonstrated that Bcl-2 regulation of Beclin 1 maintains autophagy within physiological levels that are compatible with cellular survival; expression of Beclin 1 mutants that cannot bind to Bcl-2 results in unregulated autophagy and increased cell death that is inhibitable by knockdown of autophagy genes (Pattingre et al., 2005). Interestingly, some viruses may have captured the autophagy regulatory functions of Bcl-2 and evolved to suppress Beclin 1 autophagy function more effectively than their cellular counterparts (discussed below).

In addition to promoting infected cell survival, autophagy also likely functions to restrict viral replication. In the Sindbis virus encephalitis model, increased levels of Beclin 1 directly correlated with decreased viral titers in infected brains (Liang et al., 1998). In cells infected with herpes simplex virus type 1 (HSV-1) lacking an essential neurovirulence factor ICP34.5 (Δ34.5), Tallóczy and colleagues found that PKR-mediated autophagy could function to

degrade virions and viral proteins (Talloczy et al., 2006). An increased rate of viral protein degradation was observed in biochemical analyses, and increased autophagosomal capturing of virions was observed in ultrastructural analyses in wild-type neurons infected with HSV-1 Δ34.5 compared to $pkr^{-/-}$ neurons infected with HSV-1 Δ34.5 or in wild-type neurons infected with wild-type virus (Talloczy et al., 2006). Sindbis virions are also frequently observed in autophagosomes in wild-type but not in $pkr^{-/-}$ neurons, whereas single-membraned viral replication vacuoles are more numerous in $pkr^{-/-}$ neurons, suggesting increased viral replication in the setting of deficient autophagic capturing of the virus (unpublished data). Additionally, in both plants (Liu et al., 2005), and Drosophila (Shelly et al., 2009), autophagy gene silencing resulted in increased viral replication.

These observations raise a number of questions with respect to xenophagic degradation of viruses. First, do selective mechanisms exist to identify and sequester virions and viral proteins in autophagosomes, or does degradation of viral components merely result from bulk cytosolic autophagy? Examples of substrates for selective autophagy in mammalian cells include cytosolic proteins and organelles, as well as bacteria (discussed above), and it seems likely that mechanisms may also exist to specifically target viral components. In evolutionary terms, the selective targeting of viral components for degradation would be advantageous since host metabolites that have been parasitized by the virus would be reclaimed, while host proteins and organelles essential for

maintaining cellular homeostasis would be spared. Yet, in ultrastructural studies of the two mammalian viruses for which autophagy has been suggested to limit viral replication, Sindibis virus and HSV-1, both cytoplasmic contents and viral components are observed in autophagosomes. Thus, it is possible that host cells may not encode factors to specifically target viral proteins and exclude host factors, but host factors may exist that ensure that viruses are included during the selection of cellular substrates such as organelles and/or specific host proteins, by trafficking, tethering, or binding viral components to these host structures. A related question is whether viral proteins or intact virions are targeted by xenophagy. Tallóczy et al. found that the degradation of total levels of HSV-1 proteins was enhanced by PKR-dependent autophagic degradation, and autophagic vacuoles also appeared to degrade intact HSV-1 virions and HSV-1 viral vesicles (Talloczy et al., 2006). Therefore, ultrastructural evidence indicates that intact virions, and by extension viral proteins, can be sequestered and degraded by autophagy, though it remains to be determined whether viral proteins can also be targeted before their incorporation into viral particles.

Second, during which steps in the viral life cycle does autophagy function to target viral components? During Sindbis virus infection, replication complexes are associated with single-membrane vesicles in the cytoplasm, while it is thought that nucleocapsids form freely during genome packaging in the cytosol before budding at the plasma membrane (Strauss and Strauss, 1994). Thus, autophagy may potentially target alphavirus replication complexes or naked nucleocapsid

virions in the cytoplasm. Although the precise route is controversial, HSV-1 nucleocapsids are thought to enter the cytoplasm after egressing through the nuclear membrane and secondarily acquire their envelope from cytoplasmic vesicles (Mettenleiter et al., 2006). Both cytoplasmic virions and cytoplasmic vesicles containing virions are observed in autophagosomes during HSV-1 infection. Thus it appears that viral proteins, virions, and viral vesicles can be targeted by autophagy, but it is not yet known whether specific mechanisms exist to target viral components during different steps in the replication cycle.

To date, the models in which autophagy has been shown to protect against viral infection demonstrate a protective role relatively late during the viral life cycle. Expression of Beclin 1 from a Sindbis virus double-subgenomic promoter corresponds with viral structural protein synthesis, which occurs after viral entry, uncoating, and genome replication. The temporal association between antiviral effector functions of autophagy and viral structural protein expression suggest that an important function of autophagy may be to target viral structural proteins or forming virions for degradation. However, an important related but unanswered question is whether autophagy targets viruses during entry and uncoating, which could not be addressed with the Sindbis virus model described above. Autophagy targets bacterial pathogens that escape endosomes or phagosomes upon entry into the cytoplasm (discussed above), and xenophagic targeting of uncoating viruses may partially explain the high ratios of viral particles to infectious units that are observed in most viral infections. Also, it should be noted that autophagy in

infected cells may contribute to non-cell-autonomous antiviral responses, including activation of innate and adaptive immunity, both of which may also restrict viral replication. It is also possible that autophagy restricts viral replication through mechanisms other than xenophagic degradation of viral proteins and/or particles, perhaps through the degradation of essential host factors required for replication. This latter possibility could potentially explain why, unlike with intracellular bacteria, all ultrastructural studies performed to date demonstrate cytoplasmic components in addition to viral components inside autophagolysosomal structures in virally infected cells.

In addition to promoting survival and restricting viral replication in infected cells, autophagy may protect against infection through immune activation. These functions may contribute to host antiviral responses, and may represent an attractive strategy for vaccine enhancement, as has been demonstrated by fusion of influenza matrix protein to Atg8/LC3 (Schmid et al., 2007). Neurons, the predominant target cell during Sindbis virus infection, do not express MHC class II molecules; however, it is possible that autophagy in glial cells in infected brains may play a role in antigen presentation and protection against viral encephalitides. Autophagy may also function to deliver viral replication intermediates to TLR-7-containing vesicles for innate immune activation and interferon production (Lee et al., 2007). Lee and colleagues demonstrated this function in plasmacytoid dendritic cells, but it remains possible that autophagy in neurons or glial cells can also deliver viral MAMPs for TLR

recognition and interferon production. Thus, it is likely that autophagy may exert multiple protect functions during viral infection, though the relative contribution of each during viral infection *in vivo* remains unclear.

Viral Evasion and Subversion of Autophagy

Pathogens that successfully infect host cells must overcome barriers to infection, and this is illustrated by the evolution of viral mechanisms that exploit or evade host autophagy. With respect to autophagy evasion, there is now evidence that all families of herpesviruses possess mechanisms to block host autophagy. As discussed above, HSV-1, an α-herpesvirus, encodes an essential neurovirulence factor, ICP34.5, that was shown to antagonize autophagy by reversal of PKR-mediated eIF2α phosphorylation (Talloczy et al., 2002). ICP34.5 antagonism of autophagy may be important to restrict xenophagic degradation of virions, as virions and proteins of the Δ34.5 virus are degraded by autophagy (Talloczy et al., 2006). Recently, cytomegalovirus (CMV), a member of the β-herpesvirus family, was shown to inhibit autophagy through an as-of-yet unidentified mechanism (Chaumorcel et al., 2008).

γ-herpesviruses, including Kaposi's Sarcoma-associated herpesevirus (KSHV) and murine γ-HV68 encode homologs of cellular Bcl-2 that inhibit autophagy through antagonism of Beclin 1 (Liang et al., 2006; Pattingre et al., 2005). Bcl-2-like proteins seem to have evolved mechanisms to antagonize the autophagy function of Beclin 1 more effectively than their cellular counterparts;

viral Bcl-2 proteins have a higher binding affinity than cellular Bcl-2 family members for Beclin 1 (Ku et al., 2008), and escape physiological regulation of binding to Beclin 1 by JNK1-mediated phosphorylation (Wei et al., 2008). As Beclin 1 is a tumor suppressor gene (Levine, 2007), it will be important to determine whether viral Bcl-2 antagonism of Beclin 1 function contributes to the oncogenic potential of the γ-herpesviruses.

In addition to viral evasion of autophagy, some viruses may have acquired mechanisms to subvert the autophagy pathway for their own benefit. The best-characterized example is poliovirus, a member of the non-enveloped single-stranded RNA picornavirus family. Poliovirus replication occurs on LC3-positive double-membrane vesicles and is decreased by siRNA against components of the autophagic machinery (Jackson et al., 2005). Additionally, expression of poliovirus protein 2BC is sufficient to induce LC3-II conversion, although it is unclear if this is a direct effect of the viral protein on LC3 or perhaps a more indirect effect (Taylor and Kirkegaard, 2007). Autophagy also facilitates replication of another member of the picornavirus family, Coxsackievirus B3; pharmacological inhibition of autophagy with 3-MA or siRNA against *Atg7*, *beclin 1*, or *VPS34* decreases viral replication, whereas autophagy stimulation with rapamycin treatment or starvation increases viral replication (Wong et al., 2008). A recent study suggests that dengue virus 2, a member of the flavivirus family, also utilizes the autophagy machinery for replication (Lee et al., 2008). A second flavivirus, hepatitis C virus (HCV), induces autophagy in immortalized

hepatocytes (Ait-Goughoulte et al., 2008), and autophagy genes are required for HCV replication initiation (Dreux et al., 2009). A second study indicates that autophagy genes are not required for early steps, but are required for HCV virion production (Tanida et al., 2009). It is possible that differences in virus strains or cell lines account for these discrepancies. Another hepatitis virus, a hepadnavirus, HBV, may also used its X protein to hijack early steps in the autophagy pathway to promote its own replication, through PI3K activation (Sir et al., 2010), and/or by induction of Beclin 1 expression (Tang et al., 2009).

Increasing evidence suggests cross-talk between the HIV virus and the autophagy pathway. One recent report suggests that HIV can inhibit autophagy in macrophages (Zhou and Spector, 2008). HIV possesses complex interactions with the autophagy pathway, where early steps in the pathway facilitate viral replication and late autolysosomal degradation reduces yields (Kyei et al., 2009). These functions are skewed in favor of the virus by the HIV Nef protein that inhibits later stages of the pathway (Kyei et al., 2009). In support of a positive function of autophagy in HIV infection (or at least the protein conjugation systems involved in autophagosomal membrane formation), a recent genome-wide siRNA screen identified several autophagy genes that function in this step of autophagy (e.g., ATG7, ATG8 (GABARAPL2), ATG12, and Atg16L2), as host factors required for HIV replication (Brass et al., 2008).

The replication of some other viruses seems not to be affected either positively or negatively by autophagy. In contrast to poliovirus and

Coxsackievirus B3, studies with Drosophila C virus (Cherry et al., 2006) and human rhinovirus 2 (Brabec-Zaruba et al., 2007) suggest that autophagy subversion may not be a universal requirement for picornavirus replication. Further, Atg5 and Beclin 1 are dispensable for the replication of vaccinia virus, a member of the poxvirus family, at least in MEFs and embryonic stem cells, respectively (Zhang et al., 2006). Mouse coronavirus replication does not require Atg5 in low passage MEFs or primary bone marrow-derived macrophages (Zhao et al., 2007). Thus, the relative importance of autophagy and the nature of its function may vary considerably in different types of virus infections.

Aims of this Study

The general aim of this study is to characterize the role of autophagy in innate defense against viral infection. While autophagy clearly plays a role in protecting against viral disease (a role that is underscored by the presence of viral evasion and subversion strategies), the precise mechanism(s) that underlie this protective role *in vivo* remain unclear. Further, while studies *in vitro* have demonstrated that viruses can counteract the autophagy pathway, the role of viral antagonism of autophagy in animals has not been characterized. Investigating mechanisms of viral evasion *in vivo* should provide insight into how viruses have evolved to cause disease, and should help clarify the role of autophagy in mammalian antiviral immunity. Although overexpression studies in mice and knockdown experiments in plants and flies provided genetic evidence for the role

of autophagy in host defense, direct study an endogenous mammalian autophagy gene during viral infection has not been reported. Detailed characterization of an endogenous autophagy gene should verify the antiviral role of autophagy in mammals, and may reveal insight into the cellular and molecular mechanisms of this protection. Lastly, mechanisms for sequestering selective autophagy substrates have only recently been uncovered, yet relatively little is known about how microbes are selectively targeted, and especially so for viruses. Defining host factors involved in this process should further our understanding of the ways in which cells target viruses by autophagy, and may unveil general insight into targeting of other important cellular autophagy substrates.

CHAPTER TWO
HSV-1 ICP34.5 Confers Neurovirulence by Targeting the Beclin 1 Autophagy Protein.

INTRODUCTION

HSV-1 is an enveloped, double-stranded DNA virus (with a genome encoding approximately 84 open reading frames (Rajcani et al., 2004)), of the Alphaherpesvirinae subfamily. HSV-1 is transmitted horizontally, infects mucocutaneous sites initially, and then spreads via neurons to dorsal root ganglia (primarily the trigeminal ganglion) where it establishes latency. In addition to causing mild cutaneous ulcers during primary infection and reactivation, HSV-1 infection can result in severe encephalitis in neonates and adults. Even with treatment, 30% of infected adults do not survive HSV-1 encephalitis, and only a small percentage of survivors regain normal neuronal functioning (Kimberlin, 2007; Tyler, 2004).

The mouse model of HSV-1 encephalitis has provided important clues regarding the molecular determinants of HSV-1 neurologic disease. Most notably, Chou et al. first demonstrated that the virally-encoded protein ICP34.5 is required for neurovirulence in mice (Chou et al., 1990). ICP34.5 is also required for neurologic disease in humans, since an ICP34.5-deleted virus can be used safely as an oncolytic agent to treat high-grade gliomas (Harrow et al., 2004). ICP34.5 contains a GADD34 homology region (Chou and Roizman, 1994) that reverses eIF2α phosphorylation by recruiting protein phosphatase-1α (He et al., 1997). This observation has led to the proposal that ICP34.5 may function in

neurovirulence by blocking eIF2α kinase signaling-dependent host translational arrest (Chou and Roizman, 1994). However, substitution of the corresponding domain from the murine homolog of GADD34 into ICP34.5 maintains the ability of HSV-1 to reverse eIF2α phosphorylation and prolong viral protein synthesis *in vitro*, but results in a virus that is attenuated *in vivo* (He et al., 1996; Markovitz et al., 1997). Moreover, a second-site mutation in an ICP34.5-disrupted virus resulting in immediate early expression of the US11 gene product restores the ability of the virus to reverse eIF2α phosphorylation and host cell shutoff (Mulvey et al., 1999) but fails to restore neurovirulence (Mohr et al., 2001). Therefore, factors in addition to inhibition of host cell translational shutoff likely contribute to ICP34.5-mediated neurovirulence.

The first link between infection and autophagy, described in 1978, was the electron microscopic (EM) visualization of HSV-1 and CMV inside autophagosomes (Smith and de Harven, 1978). Tallóczy et al. demonstrated that the antiviral, interferon-inducible PKR signaling pathway promotes autophagy in response to HSV-1 infection, and the HSV-1 neurovirulence protein ICP34.5 antagonizes this response (Tallóczy et al., 2002). These latter findings raise the possibilities that autophagy may also protect against HSV-1 infection and that HSV-1 ICP34.5-mediated blockade of autophagy may contribute to viral neurovirulence. However, the role of HSV-1 or other viral antagonism of autophagy in viral pathogenesis is not yet known.

In this study, we found that the HSV-1 ICP34.5 neurovirulence protein directly interacts with the mammalian autophagy protein, Beclin 1. To investigate the functional significance of the HSV-1-ICP34.5/ Beclin 1 interaction, we examined the ability of wild-type and Beclin 1-binding deficient ICP34.5 mutants to antagonize Beclin 1-mediated autophagy in yeast and mammalian cells. Our results show that ICP34.5 can specifically antagonize Beclin 1-mediated autophagy and that the Beclin 1-binding domain, but not the GADD34 domain, is essential for this function. Furthermore, we show that a Beclin 1-binding deficient ICP34.5 mutant virus is neuroattenuated in mice, suggesting that the ICP34.5-Beclin 1 interaction plays an important role in the pathogenesis of fatal HSV-1 encephalitis. The neurovirulence of this virus is restored in *pkr*$^{-/-}$ mice, providing genetic evidence for PKR-mediated autophagy in protection against HSV-1 disease. Our findings identify an as-of-yet undefined mechanism of virulence: targeting of the autophagic machinery by a virally-encoded protein.

EXPERIMENTAL PROCEDURES

Yeast strains, expression vectors, and assays. The *atg6*-disruped *S. cerevisiae* strain, JCY3000, and wild type strain SFY526 have been previously described (Seaman et al., 1997; Liang et al., 1998). For yeast two-hybrid studies, previously described plasmids were used including full-length human *beclin 1* (1-1350bp), a C-terminal-truncation mutant of human *beclin 1* (1-708bp) or yeast *ATG6* cloned into the GAL4 activation domain plasmid pGAD424 (Liang et al.,

1998; Liang et al., 1999). The full length open reading frame of HSV-1 strain F ICP34.5 cloned into pGBT9 ß-galactosidase domain plasmid was provided by Bernard Roizman. Yeast two hybrid analyses of these plasmids was performed in SFY526 cells as described (Liang et al., 1998). For autophagy studies, yeast expression vector constructs included empty vector pMS424, pMS424 encoding human *beclin 1* (Liang et al., 1999), pMS424 encoding *S. cerevisiae ATG6* (Seaman et al., 1997), empty vector pGPD426, and pGPD426 encoding HSV-1 strain 17 ICP34.5. Yeast autophagy was measured in JCY3000 cells during nitrogen starvation conditions by quantitative DIC microscopy as previously described (Liang et al., 1999, Tallóczy et al., 2002).

Mammalian cell lines. HEK293, MCF7, and SK-N-SH cell lines were obtained from ATCC (American Type Culture Collection) and maintained according to ATCC instructions. The construction and maintenance of MCF7 cell lines stably transfected with tetracycline-repressible flag-*beclin 1* has been previously described (Liang et al., 2001). Mouse *beclin 1*$^{-/-}$ and *beclin 1*$^{+/+}$ ES cells were provided by Nathaniel Heintz and cultured as described (Yue et al., 2003). ES cells were cultured without MEF feeder layers before experiments to ensure homogenous ES cell populations. Primary sympathetic neuron cultures were prepared from superior cervical ganglia of postnatal day 2 129 Ev/Sv mice using a modification of a previously described protocol (Easton et al., 1997).

Virus strains. The HSV-1 ICP34.5 deletion mutant (17termA) and its marker-rescued virus (17termAR) were made in the background of strain 17 of

HSV-1 and have been previously described (Bolovan et al., 1994; Leib et al., 2000). To construct an HSV-1 virus lacking the nucleotides encoding amino acids 68-87 of HSV-1 (termed HSV-1 ICP34.5Δ68-87) and its marker rescue control (HSV-1 ICP34.5Δ68-87R), we used our previously published BAC method (Gierasch et al., 2006). Please refer to Figure S1 for a schematic diagram of the construction of these viruses and to Supplementary Experimental Procedures for details of the construction of these viruses.

Viral growth curves. Viral growth in SK-N-SH neuroblastoma cells was measured during infection with HSV-1 34.5Δ68-87 or HSV-1 34.5Δ68-87R at an MOI of 0.01 pfu/cell by performing plaque assay titration of freeze-thawed lysates on Vero cells. For *in vivo* viral replication studies, mice were sacrificed at the indicated time points after infection and frozen brain tissue homogenates were used for plaque assay titration on Vero cells.

Coimmunoprecipitation and western blot analyses. For coimmunoprecipitation studies of mammalian cells, HEK293 cells transiently transfected with N'-terminal flag-tagged human Beclin 1 or stably transfected MCF7.*beclin 1* cells were co-transfected with pCR3.1 plasmids expressing untagged or C'-terminal myc-tagged HSV-1 strain 17 ICP34.5 full length or deletion mutants using Lipofectamine 2000^{TM} (Invitrogen) according to the manufacturer's instructions. Cells were trypsinized two days post-transfection, washed three times in ice cold PBS and lysed in 375 µl of ice cold lysis buffer containing 50mM TrisHCl (pH7.4), 150mM NaCl, 1 mM EDTA, 1% TritonX-

100, 1x protease inhibitor cocktail. Beclin 1 was immunoprecipitated with anti-Flag antibody (Sigma F3165) and ICP34.5 was immunoprecipitated with either anti-ICP34.5 (generously provided by Ian Mohr) or anti-Myc (Novus ab9106) on Protein A sepharose beads (Amersham Biosciences). Coimmunoprecipitation of virally-expressed ICP34.5 and endogenous Beclin 1 was performed on SK-N-SH and ES cells infected with the indicated virus at an MOI of 5. ES cells were lysed 18-24 hrs post-infection with buffer containing 20mM HEPES (pH7.4), 150mM NaCl, 1 mM EDTA, 1% TritonX-100, 1x protease inhibitor cocktail and SK-N-SH cells were lysed with buffer containing 50mM Tris (pH8.0). ES cell lysates were cross-linked with 20mg DSTP dissolved in 200µl DMSO. Cross-linking was stopped by addition of 50mM Tris (pH8.0). Lysates were pre-cleared for 1hr with 40µl protein G-beads (Amersham Biosciences) and the supernatant immunoprecipitated with anti-Beclin 1 antibody (Santa Cruz Biotechnology) and protein G-beads. Immunoprecipitated proteins were separated on 7.5 to 12% TrisHCl-SDS-PAGE gel and blotted onto PVDF membrane for immunodetection of Beclin 1 and ICP34.5. Beclin 1 was immunoprecipitated and detected in Western blot analyses using either anti-Flag (HEK293 cells, MCF7 cells) (Sigma F3165, 1:100 dilution) or anti-Beclin 1 (Novus Biologicals or Santa Cruz, 1:100 dilution) and ICP34.5 was detected in cell lysates and co-immunoprecipitates using either anti-Myc (MCF7 cells) (Novus ab9106, 1:10,000 dilution) or a rabbit polyclonal anti-ICP34.5 antibody raised against GST-purified N-terminal 69 amino acids of the Patton strain 34.5 protein (HEK293 cells, MCF7 cells, ES

cells, SK-N-SH cells) (generously provided by I. Mohr; 1:1000 dilution). EIF2α phosphorylation in SK-N-SH was detected by Western blot analysis as described previously (Tallóczy et al., 2002) using anti-phosphospecific eIF2α Ab (1:100 dilution) (Research Genetics).

Mammalian cell autophagy assays. Quantitative GFP-LC3 light microscopy autophagy assays were performed in MCF7.*beclin 1* cells cotransfected with a GFP-LC3-expressing plasmid, pEGFP-C1 (Kabeya et al., 2000) and a pCR3.1 construct expressing full length or deletion mutants of C-terminal Myc-tagged HSV-1 strain 17 ICP34.5 as described (Pattingre et al., 2005). Quantitative EM autophagy assays were performed as previously described (Tallóczy et al., 2002) in primary sympathetic neurons pretreated with 100 IU/ml recombinant mouse IFN-α (Sigma) for 18 hours, infected with HSV-1 17termA, HSV-1 34.5Δ68-87, or HSV-1 34.5Δ68-87R at an MOI of 5, and fixed 24 hours after infection.

Host cell shutoff assays. Host cell shutoff assays were performed as previously described (Chou and Roizman, 1992), using SK-N-SH cells infected at an MOI of 5 and incubated at 16 hours after infection with [^{35}S]methionine (specific activity 1175 Ci/mmol; 1Ci = 43.5 TBq; MP Biomedicals, Inc) for 1.5 hours in media lacking methionine.

Animal experiments. Four to eight week-old C57BL/6J mice (Jackson Laboratory), and *pkr*$^{-/-}$ or wild type 129 Ev/Sv backcrossed control mice (Leib et al., 2000) of either sex were used in all studies. For HSV-1 encephalitis mortality

studies, mice were anesthetized, injected intracerebrally with 1-5 x 10^5 pfu of virus in 30 μl HBSS, and followed daily for 3 weeks for survival. All animal procedures were performed in accordance with Institutional Animal Use and Care Committee policies.

Histopathological analyses. At serial time points after infection, mice were euthanized, and the left cerebral hemispheres were fixed by immersion in 4% paraformaldehyde. Serial paraffin-embedded sections were stained with H&E and subjected to immunohistochemical analysis using a rabbit polyclonal antibody to HSV-1 (1:6000 dilution) in conjunction with a MACH 4® Universal HRP-polymer detection system (Dako).

RESULTS

HSV-1 ICP34.5 Inhibits Beclin 1-Dependent Autophagy in Yeast

In a yeast two-hybrid screen using HSV-1 ICP34.5 as a bait, one of the ICP34.5- interacting proteins identified was the mammalian autophagy protein, Beclin 1 (personal communication, Bernard Roizman). Our laboratory confirmed that HSV-1 ICP34.5 interacts with human Beclin 1 in a yeast two-hybrid assay (Z. Tallóczy, Figure 1A). Unlike the interaction between Beclin 1 and cellular and viral Bcl-2 proteins (Pattingre et al., 2005; Liang et al., 2006), the N' terminal half of Beclin 1 is not sufficient for the interaction between Beclin 1 and ICP34.5. Full-length human Beclin 1, but not a truncation mutant encoded by nucleotides 1-708, binds to HSV-1 ICP34.5. Thus, the alphaherpesvirus-encoded protein,

ICP34.5, binds to a region of Beclin 1 that is distinct from the region of Beclin 1 targeted by viral Bcl-2 proteins encoded by gammaherpesviruses.

Although mammalian Beclin 1 interacts with ICP34.5 in yeast, the yeast ortholog of Beclin 1, Atg6, does not interact with HSV-1 ICP34.5 (Figure 1A). Therefore, we used yeast disrupted of *ATG6* to examine the effects of ICP34.5 on Beclin 1-dependent autophagy. We measured autophagy by quantitative DIC microscopy of yeast following nitrogen starvation (Z. Tallóczy, Figure 1B-C). As reported previously (Liang et al., 1999; Melendez et al., 2003; Pattingre et al.,

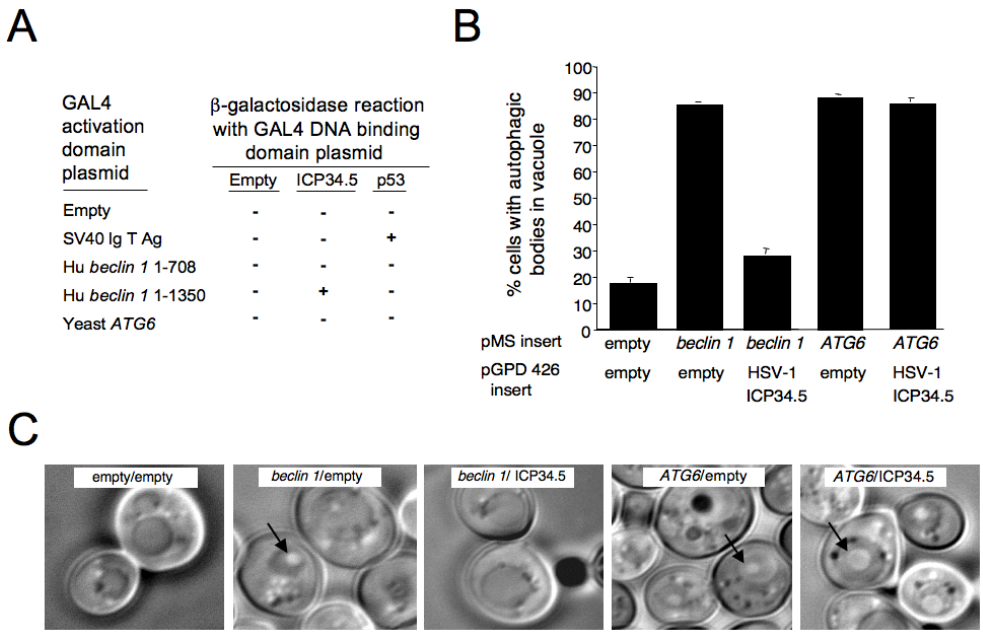

Figure 1. ICP34.5 Inhibits Beclin 1-Dependent Autophagy in Yeast. (A) Yeast two-hybrid interactions of ICP34.5 and Beclin 1. +, positive reaction within 8 hours; -, lack of positive reaction at 24 hours. Nucleotide position of genes fused to plasmid is indicated next to human *beclin 1* constructs. (B) Quantitation of starvation-induced autophagy in *atg6*Δ yeast transformed with plasmids indicated below X-axis. Results represent mean ± SEM for triplicate samples. For each sample, a minimum of one hundred cell profiles was analyzed, and cell profiles with one or more autophagosome within the vacuole were scored as positive. Similar results were obtained in five independent experiments. (C) Representative DIC photomicrographs of *atg6*Δ yeast transformed with indicated plasmids following starvation for four hours. Arrows denote representative autophagosomes.

2005), human *beclin 1* transformation restores starvation-induced autophagy in autophagy-defective *atg6* null yeast. However, co-transformation of ICP34.5 with *beclin 1* abrogates the ability of Beclin 1 to rescue starvation-induced autophagy, decreasing levels to those observed in autophagy-deficient *atg6*Δ yeast (Figure 1B, $p<0.0001$, t-test). ICP34.5 has no effect on the ability of *ATG6* transformation to rescue autophagy in *atg6*Δ yeast. Taken together, these results indicate that ICP34.5 is likely to inhibit autophagy by binding to Beclin 1.

ICP34.5 Inhibits Beclin 1-Dependent Autophagy in Mammalian Cells

Next, we sought to confirm the interaction between HSV-1 ICP34.5 and Beclin 1 in mammalian cells. In HEK293 cells transiently transfected with plasmids expressing flag epitope-tagged Beclin 1 and HSV-1 ICP34.5, we found that flag-Beclin 1 coimmunoprecipitated with ICP34.5 and that ICP34.5 coimmunoprecipitated with flag-Beclin 1 (Y. Wei, Figure 2A), indicating that Beclin 1 and ICP34.5 can interact in mammalian cells. To determine whether ICP34.5 does interact with endogenous Beclin 1 in virally-infected cells, we performed coimmunoprecipitation studies of HSV-1-infected wild-type (*beclin*

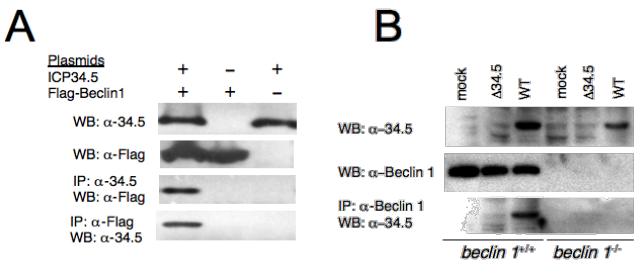

Figure 2. ICP34.5 Binds to Beclin 1 in Mammalian Cells. (A) Coimmunoprecipitation of Flag-tagged Beclin 1 with ICP34.5 in HEK293 cells transfected with the indicated plasmids. (B) Coimmunoprecipitation of endogenous Beclin 1 with ICP34.5 in *beclin 1*$^{+/+}$ or *beclin 1*$^{-/-}$ mouse ES cells infected with the indicated virus.

1$^{+/+}$) embryonic stem (ES) cells and HSV-1-infected ES cells containing a homozygous null mutation in *beclin 1* (*beclin 1*$^{-/-}$) (Figure 2B). We found that ICP34.5 coimmunoprecipitates with Beclin 1 in HSV-1-infected *beclin 1*$^{+/+}$ ES cells. No specific bands were observed in HSV-infected *beclin 1*$^{-/-}$ ES cells or in wild-type, *beclin 1*$^{+/+}$ ES cells infected with a previously characterized mutant strain of HSV-1 (17termA) (Bolovan et al., 1994) deleted of the entire ICP34.5 gene (Figure 2B). Thus, ICP34.5 interacts with endogenous Beclin 1 in virally-infected mammalian cells.

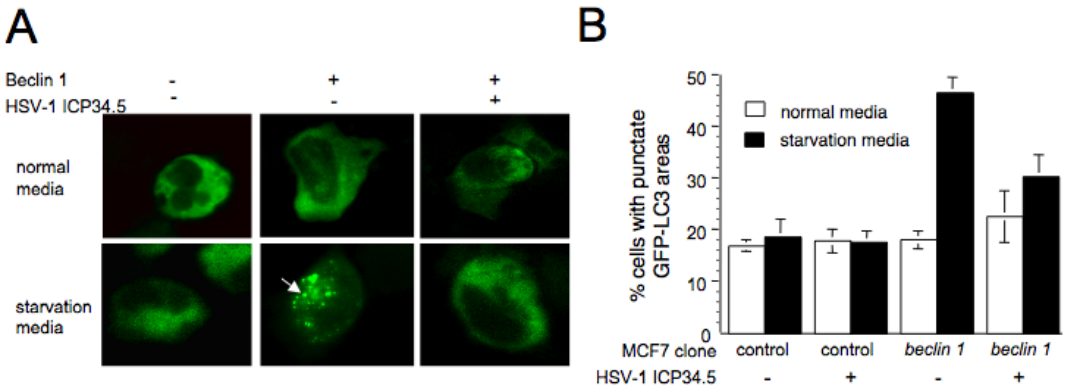

Figure 3. ICP34.5 Inhibits Beclin 1-Mediated Autophagy in Mammalian Cells. (A) Representative photomicrographs of images used for quantitative analyses in (B). Arrow denotes representative punctate GFP-LC3 dot corresponding to an autophagosome. (B) Quantitation of autophagy, as measured by GFP-LC3 punctations, in MCF7 cells transfected with plasmids expressing Beclin 1 and/or ICP34.5 during growth in normal media (open bars) or starvation media (filled bars). Results represent mean ± SEM for triplicate samples. For each sample, a minimum of 100 cells was analyzed. Similar results were obtained in five independent experiments.

To examine whether ICP34.5 antagonizes the autophagy function of Beclin 1 in mammalian cells, we used MCF7 human breast carcinoma cells stably transfected with human *beclin 1* (MCF7.*beclin 1* cells) or MCF7 cells stably transfected with empty vector (MCF7.control cells) (Liang et al., 2001). MCF7 cells express low levels of endogenous Beclin 1 and fail to increase autophagic

activity in response to starvation unless Beclin 1 is ectopically expressed (Liang et al., 1999; Liang et al., 2001; Pattingre et al., 2005; Furuya et al., 2005). Therefore, we assessed the effects of HSV-1 ICP34.5 on the ability of *beclin 1* to rescue autophagy in MCF7 cells (Z. Talloczy, Figure 3A-B).

To measure autophagy, we used the fluorescent autophagy marker, GFP-LC3, which forms punctate dots upon proteolytic processing and lipidation during autophagy (Kabeya et al., 2000) (Figure 3A). Similar to previous reports, we found that MCF7.control cells fail to increase their autophagy activity in response to amino acid starvation, whereas MCF7.*beclin 1* cells undergo a significant increase in autophagic activity following starvation ($p=0.003$ for MCF7.*beclin 1* cells in normal media vs. starvation media, t-test) (Figure 3B). Transfection of an ICP34.5 expression plasmid significantly decreased starvation-induced autophagy in MCF7.*beclin 1* cells ($p= 0.008$, t-test) (Figure 3B). These data demonstrate that ICP34.5 can inhibit Beclin 1-dependent autophagy in mammalian cells.

Amino Acids 68-87 of ICP34.5 are Required for Beclin 1 Binding and Inhibition of Beclin 1-Dependent Autophagy

Next, we performed a structure-function analysis to map the domain of ICP34.5 responsible for binding to Beclin 1 and inhibition of Beclin 1-dependent autophagy. To accomplish this, we performed coimmunoprecipitations of MCF7.*beclin 1* cells transfected with different myc-tagged ICP34.5 constructs

and also assessed the ability of the ICP34.5 constructs to inhibit starvation-induced autophagy in MCF7.*beclin 1* cells.

ICP34.5 contains an N' terminal region, followed by a tripeptide repeat, and a C' terminal GADD34 homology domain (Figure 4A). Previous studies have shown that the GADD34 domain binds protein phosphatase-1α to dephosphorylate eIF2α and block eIF2α kinase signaling-dependent host cell shutoff during HSV-1 infection (He B, 1997). We found that wild-type ICP34.5 and ICP34.5 lacking the GADD34 domain (ICP34.5ΔGADD34) both immunoprecipitated with flag-Beclin 1 in MCF7.*beclin 1* cells (Z. Talloczy, Figure 4B). The lower levels of ICP34.5ΔGADD34 that coimmunoprecipitate with Beclin 1 are likely due to lower levels of expression of the ICP34.5ΔGADD34 protein (Figure 4B, see upper panel) rather than actual differences in binding affinity. Thus, the GADD34 domain of ICP34.5 that is required for antagonism of eIF2α phosphorylation is dispensable for Beclin 1 binding.

To further characterize the GADD34-independent interaction between ICP34.5 with Beclin 1, we constructed ICP34.5 mutants containing 20 amino acid deletions in the N' terminal half of the protein. Three ICP34.5 deletion mutants resulted in stable protein expression and could be used for further analyses, including mutants deleted of amino acids 48-67, 68-87, or 88-107 (herein referred to as ICP34.5Δ48-67, ICP34.5Δ68-87, and ICP34.5Δ88-107, respectively) (Figure

4B, and data not shown). Of these three deletion mutants, ICP34.5Δ48-67 and ICP34.5Δ88-107. but not ICP34.5Δ68-87, coimmuno-precipitated with Beclin 1 (Figure 4B, and data not shown). This indicates that deletion of the region spanning amino acids 68-87 (but not deletions of similar length in nearby flanking regions) abolishes the interaction between ICP34.5 and Beclin 1.

To evaluate the effect of ICP34.5 binding to Beclin 1 on Beclin 1-dependent starvation-induced autophagy, we co-transfected MCF7.*beclin 1* cells with plasmids expressing HSV-1 ICP34.5 mutants and the autophagosome marker, GFP-LC3 (Z. Talloczy, Figure 4C). Consistent with the ability of ICP34.5ΔGADD34 to coimmunoprecipitate with Beclin 1 in MCF7.*beclin 1* cells, HSV-1 ICP34.5ΔGADD34 inhibits autophagy in these cells as effectively as wild-type ICP34.5 ($p = 0.3364$, t-test). Similarly, the 20 amino acid deletion mutants that retain the ability to interact with Beclin 1 (ICP34.5Δ48-67 and ICP34.5Δ88-107) also inhibit starvation-induced autophagy ($p=0.4833$, t-test). In contrast, the mutant ICP34.5Δ68-87, which is unable to co-immunoprecipitate with Beclin 1, fails to inhibit starvation-induced autophagy in *MCF7.beclin 1* cells ($p = 0.0028$, t-test). This demonstrates that amino acids 68-87 are required not only for binding to Beclin 1 but also for inhibition of Beclin 1-dependent autophagy. The GADD34 domain of ICP34.5 is dispensable for this autophagy-inhibitory activity, suggesting that ICP34.5 can modulate host cell functions

through its interactions with Beclin 1 in a protein phosphatase-1α-independent manner.

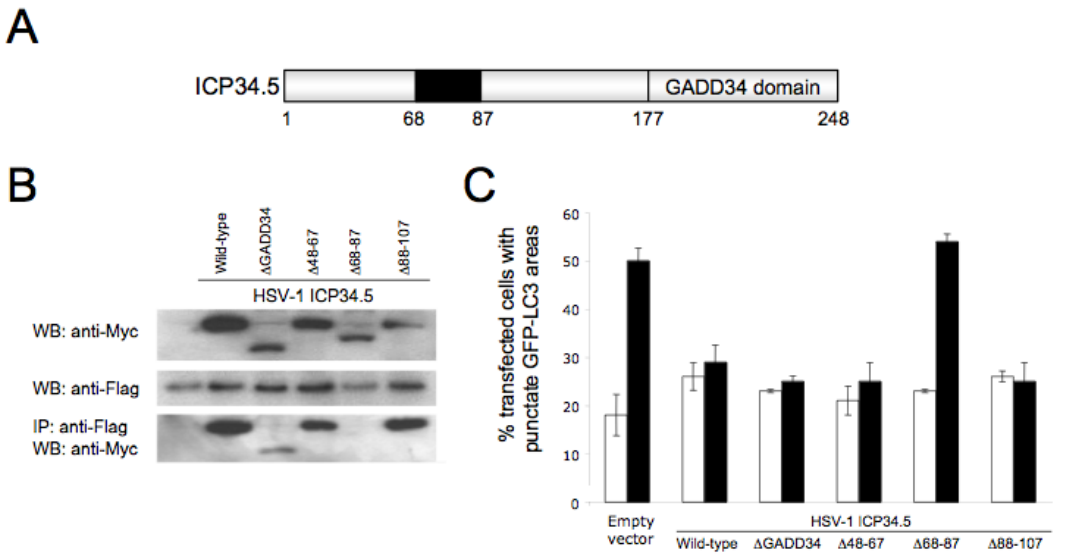

Figure 4. A Twenty Amino Acid Region of ICP34.5 is Required for Beclin 1 Binding and Inhibition of Autophagy. (A) Schematic representation of ICP34.5 showing position of Beclin 1 binding region (amino acids 68-87) and GADD34 homology region. (B) Coimmunoprecipitation of Myc-tagged wild-type or indicated mutant ICP34.5 and Flag-tagged Beclin 1 in MCF7.*beclin 1* cells. (C) Quantitation of autophagy, as measured by GFP-LC3 punctate regions in MCF7.*beclin 1* cells transfected with the indicated HSV-1 ICP34.5 plasmids during growth in normal media (open bars) or starvation media (filled bars). Results represent mean ± SEM for triplicate samples. For each sample, a minimum of 100 cells was analyzed. Similar results were obtained in three independent experiments.

Amino Acids 68-87 of ICP34.5 are not Required for Viral Growth *in vitro*, Viral Blockade of eIF2α Phosphorylation, or Viral Blockade of Host Cell Shutoff

To assess the functional significance of ICP34.5 inhibition of Beclin 1-mediated autophagy during viral infection, we constructed a mutant HSV-1 virus containing a deletion of amino acids 68-87 in ICP34.5 (referred to as HSV-1 34.5Δ68-87) and a marker rescue control (referred to as HSV-1 34.5Δ68-87R) (D.

Alexander, data not shown). HSV-1 34.5Δ68-87 expresses a protein of the predicted molecular weight (24.5 kDa) that reacts with a polyclonal anti-ICP34.5 antibody (Y. Wei, Figure 5A). However, no ICP34.5Δ68-87 mutant protein coimmunoprecipitates with Beclin 1, indicating that deletion of amino acids 68-87 blocks the ability of ICP34.5 to bind to Beclin 1 in virally-infected cells. The ICP34.5 protein expressed by the marker rescue virus HSV-1 34.5Δ68-87R coimmunoprecipitates with Beclin 1, confirming that the lack of interaction between ICP34.5Δ68-87 and Beclin 1 is not due to extragenic mutations. In contrast to a mutant HSV-1 virus lacking the entire ICP34.5 gene (HSV-1 17termA), which displays a growth defect (Chou et al., 1990), HSV-1 34.5Δ68-87 replicates to the same levels as the wild-type marker rescue HSV-1 strain (HSV-1 34.5Δ68-87R) in human SK-N-SH neuroblastoma cells (Figure 5B). In previous studies, it has been proposed that ICP34.5 is required for growth in SK-N-SH cells because of its ability to block virus-induced host cell shutoff by

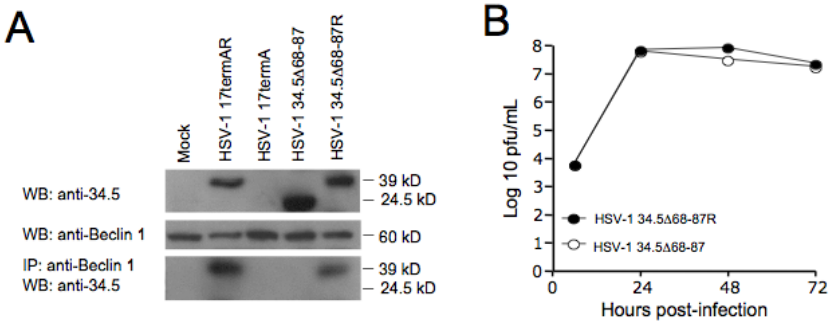

Figure 5. The Beclin 1 Binding Domain of ICP34.5 is Dispensable for HSV-1 replication *in vitro*. (A) Coimmunoprecipitation of endogenous Beclin 1 with ICP34.5 in SK-N-SH cells infected with HSV-1 ΔICP34.5 (17termA) or it marker rescue virus (17termAR), or HSV-1 34.5Δ68-87 or its marker rescue (HSV-1 34.5Δ68-87R). (B) Viral replication of HSV-1 34.5Δ68-87 and HSV-1 34.5Δ68-87R in SK-N-SH neuroblastoma cells.

dephosphorylating eIF2α. The mapping of this function of ICP34.5 to the GADD34 domain (which is not required for Beclin 1 binding), together with the wild-type levels of viral growth in HSV-1 34.5Δ68-87-infected SK-N-SH cells, suggested that HSV-1 34.5Δ68-87 should behave similarly to wild-type HSV-1 with respect to blockade of eIF2α phosphorylation and host cell shutoff. Indeed, we found that HSV-1 34.5Δ68-87 blocked eIF2α serine-51 phosphorylation as effectively as its marker rescue control virus (HSV-1 34.5Δ68-87R) whereas significant eIF2α serine-51 phosphorylation was observed in SK-N-SH cells infected with HSV-1 17termA (Figure 6A). Furthermore, this blockade of

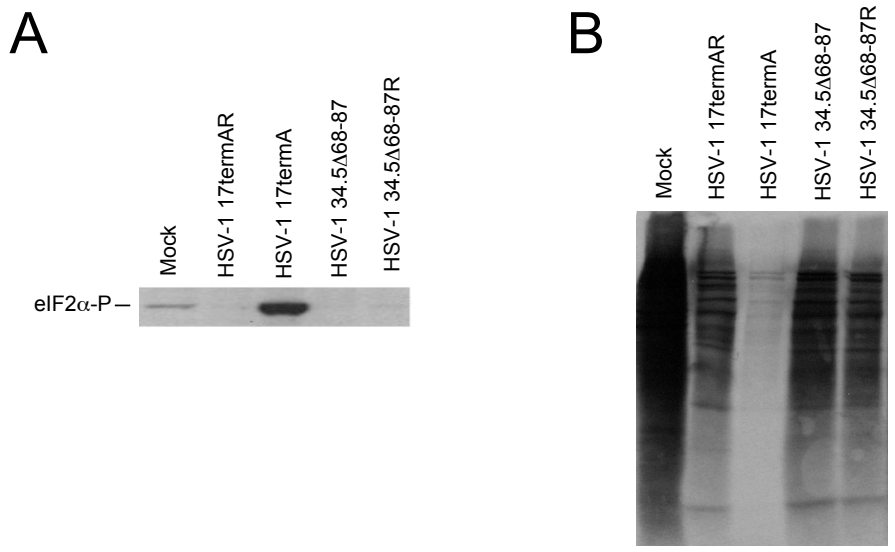

Figure 6. The Beclin 1 Binding Domain of ICP34.5 is Dispensable for ICP34.5-Mediated Blockade of Host Cell Shutoff. (A) Western blot detection of the serine-51 phosphorylated form of eIF2α in SK-N-SH neuroblastoma cells 16 hrs after infection with the indicated virus. (B) ^{35}S-labeled cellular proteins in SK-N-SH cells 16 hrs after infection with the indicated virus.

eIF2α phosphorylation correlated with the ability of HSV-1 34.5Δ68-87 to maintain protein synthesis in virally infected SK-N-SH cells at levels similar to those observed in cells infected with wild-type marker rescue viruses (e.g. HSV-1 17termAR (Bolovan et al., 1994), or HSV-1 34.5Δ68-87R) in contrast to the marked host cell shutoff observed in cells infected with HSV-1 17termA (Figure 6B). Together, these results demonstrate that amino acids 68-87 of ICP34.5 are dispensable for productive viral replication and inhibition of eIF2α phosphorylation and host cell shutoff in SK-N-SH cells.

The Beclin 1-Binding Deficient ICP34.5 Mutant Virus is Defective in Autophagy Inhibition in Neurons

To evaluate whether HSV-1 34.5Δ68-87 can inhibit autophagy, we performed EM analyses of primary sympathetic neurons infected with HSV-1 34.5Δ68-87, HSV-1 34.5Δ68-87R, and HSV-1 17termA. We chose to use neurons because they are a natural target for HSV-1 infection *in vivo* and previously we showed that HSV-1 lacking the entire ICP34.5 gene (HSV-1 17termA) but not wild-type HSV-1, induces autophagy in primary sympathetic neurons (Tallóczy et al., 2006). We found that HSV-1 34.5Δ68-87R-infected neurons (Figure 7A, upper right panel) exhibit levels of autophagy indistinguishable from mock-infected neurons (Figure 7A, upper left panel) (Figure 7B). In contrast, neurons infected with either the full ICP34.5 deletion mutant virus (HSV-1 17termA, Figure 7A, lower left panel) or the Beclin 1 binding-deficient ICP34.5 deletion

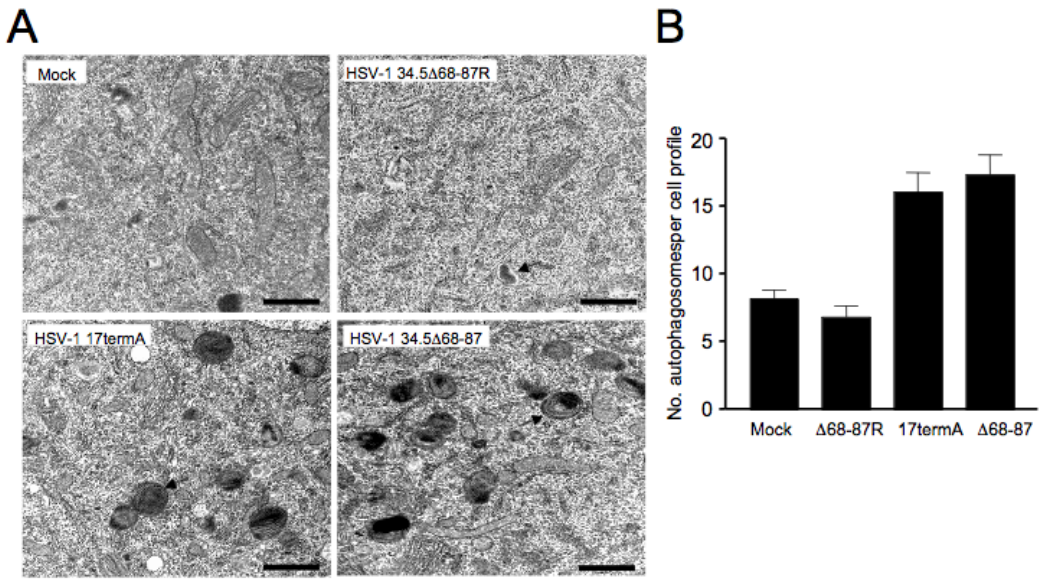

Figure 7. The Beclin 1 Binding Domain of ICP34.5 is Required for Inhibition of Autophagy in Neurons. (A) Representative electron micrographs of primary sympathetic neurons infected with the indicated virus. Arrows denote representative autophagosomes that would be scored as positive in (B). Scale bars, 1 μm. (B) Quantitation of the number of autophagosomes per cell profile in primary sympathetic neurons infected with the indicated virus. Results shown represent mean value ± SEM for 50 cells per experimental condition.

mutant virus (HSV-1 34.5Δ68-87, Figure 7A, lower right panel) have significantly higher levels of autophagosome accumulation ($p<0.0001$ for both mutants vs. HSV-1 34.5Δ68-87R; t-test) (Figure 7B). These results, together with our results in neuroblastoma cells, demonstrate that ICP34.5 binds Beclin 1 and inhibits autophagy in neurons *in vitro*, and that this activity is independent from its role in antagonizing host cell shutoff.

The Beclin 1-Binding Deficient ICP34.5 Mutant Virus is Neuroattenuated *in vivo.*

Together, our data with HSV-1 34.5Δ68-87 indicate that the Beclin 1-binding region of ICP34.5 is necessary for autophagy inhibition but not for ICP34.5-mediated blockade of host cell translational arrest. To evaluate the significance of ICP34.5 antagonism of Beclin 1 function in viral neuropathogenesis, we compared the mortality of C57/BL6 mice infected intracerebrally with $5x10^5$ pfu of either HSV-1 34.5Δ68-87 or HSV-1 34.5Δ68-87R (Figure 8A). Nearly 80% of mice succumbed to lethal HSV-1 34.5Δ68-87R infection within 10 days, whereas 85% of mice infected with HSV-1 34.5Δ68-87 were still alive 21 days after infection ($p<0.0001$, log-rank test). Consistent with the reduced mortality, we observed a striking defect in viral replication in the

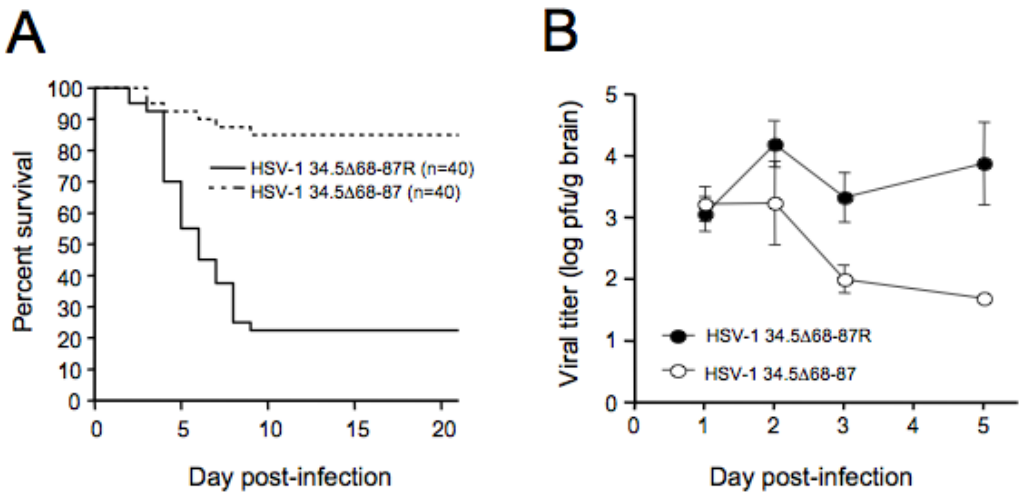

Figure 8. An HSV-1 Recombinant Virus Containing a Mutation in ICP34.5 that Abrogrates Binding to Beclin 1 is Neuroattenuated *in vivo*. (A) Survival of C57BL/6J mice infected intracerebrally with $5x10^5$ pfu with either HSV-1 34.5Δ68-87, or its marker rescue (HSV-1 34.5Δ68-87R). Results shown represent survival data combined from four independent infections. Similar results were observed in each experiment. (B) Viral replication of HSV-1 34.5Δ68-87 and HSV-1 34.5Δ68-87R in brain tissue of infected mice at indicated time after infection. Data shown represent mean ± SEM geometric titer for 7-10 mice per experimental group per time point.

brains of mice infected with HSV-1 34.5Δ68-87 (Figure 8B). Viral titers were similar in the brains of mice infected with HSV-1 34.5Δ68-87 and HSV-1 34.5Δ68-87R at day 1 after infection. However, levels of infectious virus declined below the limit of detection within five days after infection in the brains of mice infected with HSV-1 34.5Δ68-87. In contrast, significant levels of infectious virus were recovered in the brains of mice infected with HSV-1 34.5Δ68-87R for at least 5 days, after which time the majority of mice succumbed to lethal disease.

Histopathological analyses of the brains of mice at days 1, 3, and 5 after infection revealed leptomeningeal, perivascular and parenchymal inflammation (especially in the basal ganglia, brainstem, and hippocampus) in mice infected with both the HSV-1 34.5Δ68-87 and HSV-1 34.5Δ68-87R viruses, but the degree of parenchymal inflammation was more severe in mice infected with HSV-1 34.5Δ68-87R (Figure 9 left panels, data not shown). Very few HSV-1 immunoreactive neurons were observed in the brains of HSV-1 34.5Δ68-87-infected mice, whereas large regions of HSV-1 immunoreactive neurons were

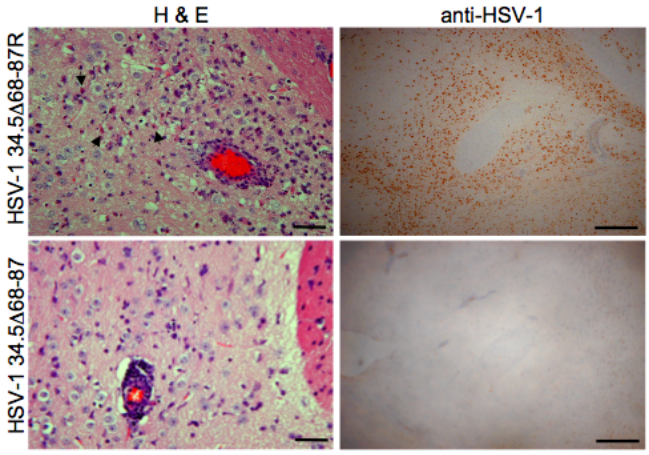

Figure 9. Infection with HSV-1 34.5Δ68-87 Results in Decreased Neuropathology. Representative images of H&E staining (left panels) and HSV-1 antigen staining (right panels) in basal ganglia from mice infected with HSV-1 34.5Δ68-87R (upper panels) or HSV-1 34.5Δ68-87 (bottom panels) on day 5 post-infection. Arrows in upper left panel indicate eosinophilic, necrotic neurons with pyknotic

observed in the brains of HSV-1 34.5Δ68-87R-infected mice (Figure 9, right panels). Furthermore, in HSV-1 34.5Δ68-87R-infected brains, there were numerous neurons with pyknotic nuclei and eosinophilic cytoplasm whereas neuronal pathology was rarely observed in HSV-1 34.5Δ68-87-infected mice (Figure 9, left panels). Thus, the brains of mice infected with HSV-1 34.5Δ68-87R demonstrate significantly more neuropathology than the brains of mice infected with HSV-1 34.5Δ68-87. Taken together, the mortality studies, CNS viral replication studies, and CNS histopathological analyses demonstrate that the Beclin 1-binding deficient mutant virus is highly neuroattenuated *in vivo*.

Restoration of Neurovirulence of the Beclin 1-binding Deficient ICP34.5 Mutant Virus in Mice with a Homozygous Deletion in *pkr*

Previously, we have shown that PKR signaling is required for autophagy induction and autophagy-dependent virion degradation in murine embryonic fibroblasts (MEFs) and sympathetic neurons (Tallóczy et al., 2002; Tallóczy et al., 2006). These findings raise the possibility that PKR signaling may lie genetically upstream of Beclin 1-dependent autophagy in HSV-1 antiviral host defense. To investigate this possibility, we evaluated whether the neurovirulence of the Beclin 1-binding ICP34.5 mutant virus is restored in 129 Ev/Sv mice containing a homozygous deletion in *pkr* (herein referred to as $pkr^{-/-}$ mice).

Consistent with previously described mouse strain differences in susceptibility to HSV-1 infection (Kirchner et al., 1978), we found that 129 Ev/Sv

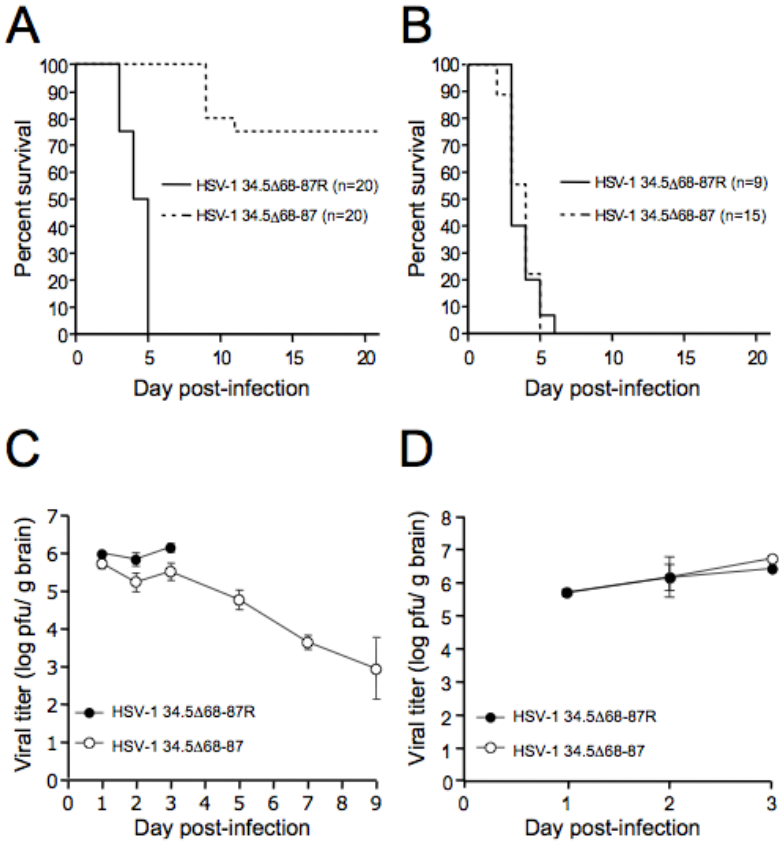

Figure 10. Restoration of Neurovirulence of a Beclin 1 Binding-Deficient Virus in *pkr*$^{-/-}$ mice. (A) Survival of wild-type 129 Ev/Sv mice infected intracerebrally with 1x10^5 pfu of either HSV-1 34.5Δ68-87, or its marker rescue (HSV-1 34.5Δ68-87R). (B) Survival of 129 Ev/Sv *pkr*$^{-/-}$ mice infected intracerebrally with 1x10^5 pfu of either HSV-1 34.5Δ68-87, or its marker rescue (HSV-1 34.5Δ68-87R). (A-B) Results shown represent survival data combined from 2-3 independent infections. Similar results were observed in each experiment. (C) Viral replication of HSV-1 34.5Δ68-87 and HSV-1 34.5Δ68-87R in brain tissue of infected 129 Ev/Sv mice at indicated time after infection. (D) Viral replication of HSV-1 34.5Δ68-87 and HSV-1 34.5Δ68-87R in brain tissue of infected 129 Ev/Sv *pkr*$^{-/-}$ mice at indicated time after infection. For C-D, data shown represent mean ± SEM geometric titer for 3-5 mice per experimental group per time point.

mice are more susceptible to fatal HSV-1 infection than C57BL/6J mice (D. Alexander, Figure 10A). However, similar to our findings in C57BL/6J mice, the HSV-1 34.5Δ68-87 mutant virus also results in significantly less mortality in wild-type 129 Ev/Sv mice as compared to the marker rescue control virus (Figure 10A; $p<0.0001$, log rank test). In contrast, in *pkr*$^{-/-}$ mice, the mortality of mice infected with HSV-1 34.5Δ68-87 was as high as the mortality of mice infected

with HSV-1 34.5Δ68-87R (Figure 10B). Furthermore, in wild-type mice, HSV-1 34.5Δ68-87 replication in brain is significantly lower than HSV-1 34.5Δ68-87R replication (and HSV-1 34.5Δ68-87 infectious virus is gradually cleared) (Figure 10C), whereas in *pkr*$^{-/-}$ mice, HSV-1 34.5Δ68-87 replicates in brain to levels similar to those observed during infection with HSV-1 34.5Δ68-87R (Figure 10D). Together, these findings demonstrate that *pkr* deletion *in vivo* restores the virulence of the Beclin 1-binding deficient ICP34.5 mutant virus. These findings suggest that PKR induction of Beclin 1-dependent autophagy is important for protection against HSV-1 encephalitis.

DISCUSSION

Here we provide evidence that an essential HSV-1 neurovirulence factor, ICP34.5, confers pathogenicity by binding to the mammalian autophagy protein, Beclin 1, and antagonizing the host autophagy response. To the best of our knowledge, these findings represent the first description of a microbial virulence factor directly antagonizing the host autophagy machinery to elicit disease. Previous studies have demonstrated that certain bacterial and viral gene products can antagonize host autophagy *in vitro*. During *Shigella* infection, the bacterial encoded virulence factor *IcsB* blocks the induction of autophagy by *VirG* (Ogawa et al., 2005). In addition, viral Bcl-2 proteins encoded by the oncogenic gammaherpesviruses block autophagy induction by binding to Beclin 1 (Pattingre et al., 2005; Liang et al., 2006). However, in these examples, the significance of

microbial antagonism of host autophagy in disease pathogenesis is not yet known. Our finding that the Beclin 1-binding domain of the HSV-1 encoded neurovirulence protein, ICP34.5, is essential for lethal HSV-1 encephalitis demonstrates the importance of microbial evasion of autophagy in disease pathogenesis.

The requirement for HSV-1-mediated inhibition of autophagy in the pathogenesis of viral encephalitis provides strong evidence that autophagy is an important mechanism of innate immunity *in vivo*. Several studies have shown that autophagy genes restrict intracellular bacterial growth in cultured cells (Levine, 2005; Deretic, 2006; Amano et al., 2006); however the role of autophagy in host defense against intracellular bacterial infections *in vivo* is not yet known. A previous study showed that enforced neuronal expression of Beclin 1 decreases Sindbis virus CNS replication, decreases Sindbis virus-induced neuronal apoptosis, and protects mice against lethal Sindbis virus encephalitis (Liang et al., 1998), raising the possibility that Beclin 1-dependent autophagy may play a role in innate antiviral immunity. In this study, we demonstrate that the Beclin 1-binding and autophagy-inhibitory domain of HSV-1 ICP34.5 is essential for neurological disease. This observation strongly suggests that autophagy is an important mechanism of innate immunity that must be successfully countered for certain viruses to be pathogenic.

As a corollary, viral evasion of autophagy likely represents an important strategy that viruses use to outsmart host antiviral defense. Previous studies have

shown that HSV-1 ICP34.5 is required for neurovirulence (Chou et al., 1990; Harrow et al., 2004), that ICP34.5 blocks PKR-dependent autophagy (Tallóczy et al., 2002; Tallóczy et al., 2006), and that blockade of PKR-dependent functions *in vivo* is essential for HSV-1 neurovirulence (Leib et al., 2000). However, since PKR activation also results in translational arrest in virally-infected cells, the significance of the autophagy-inhibitory effects of ICP34.5 in viral virulence has been unclear. Our studies permitted us to genetically dissect the role of ICP34.5-mediated inhibition of autophagy in viral virulence from ICP34.5-mediated antagonism of other PKR-dependent functions by constructing a recombinant mutant virus that retains its GADD34 domain and ability to block PKR-dependent translational arrest, but is defective in Beclin 1 binding and inhibition of autophagy in virally-infected neurons. This mutant virus is highly neuroattenuated *in vivo*, suggesting that ICP34.5-mediated blockade of host cell shutoff is not sufficient to confer neurovirulence but rather, that ICP34.5-mediated blockade of Beclin 1-dependent autophagy is required for neurovirulence. Moreover, our findings in mice lacking *pkr*$^{-/-}$, demonstrating restoration of neurovirulence of a mutant strain of HSV-1 that is specifically impaired in Beclin 1 binding and autophagy inhibitory activity, indicate that PKR lies genetically upstream of Beclin 1 in antiviral host defense *in vivo*. Since PKR is targeted by virulence factors encoded by many different viruses including other medically important pathogens such as hepatitis C virus and influenza virus (Katze et al., 2002), it will

be of interest to determine the role of autophagy evasion in the pathogenesis of diseases caused by such viruses.

One important question that arises is why ICP34.5 possesses two separate mechanisms for blocking host cell autophagy, including blockade of PKR-dependent signaling and blockade of Beclin 1 function. Although we have previously shown that cells require *pkr* and the serine-51 phosphorylation site of eIF2α to undergo virus-induced autophagy (Tallóczy et al., 2002), it is possible that very low levels of phosphorylated eIF2α are sufficient to trigger autophagy in HSV-1-infected wild-type cells. If so, successful inhibition of autophagy may require a second mechanism, such as blocking a downstream autophagy effector protein. Indeed, we found that the GADD34 domain of ICP34.5 which is sufficient to antagonize PKR-dependent translational arrest is not required to block autophagy in mammalian cells whereas the Beclin 1 binding domain of ICP34.5 is required for autophagy inhibition. Thus, antagonism of PKR signaling, in the absence of antagonism of Beclin 1 function, is not sufficient to block host cell autophagy (even though PKR and eIF2α serine-51 phosphorylation are required for autophagy induction).

The mechanism by which ICP34.5 inhibits Beclin 1-dependent autophagy is not yet known. Two major lines of evidence suggest that the binding of ICP34.5, either directly or indirectly, to Beclin 1 is required for its autophagy inhibitory function. First, ICP34.5 fails to interact with the yeast ortholog, Atg6, and has no inhibitory effect on the ability of *ATG6* transformation to rescue

autophagy in *atg6* null yeast. In contrast, ICP34.5 binds to Beclin 1 in yeast and blocks the ability of *beclin 1* to rescue autophagy in *atg6* null yeast. Second, in mammalian cells, we observed a direct correlation between the ability of different mutants of ICP34.5 to coimmunoprecipitate with Beclin 1 and to inhibit Beclin 1-dependent autophagy. Interestingly, the domain of Beclin 1 required for interacting with ICP34.5 appears to be distinct from that involved in binding to cellular and viral Bcl-2-like proteins or in binding to the Class III PI3 kinase, Vps34 (Liang et al., 1999; Pattingre et al., 2005; Furuya et al., 2005 and data not shown). Therefore, it is unlikely that ICP34.5 directly competes with Vps34 for binding to Beclin 1. Moreover, the lack of any structural similarity between HSV-1 ICP34.5 and gammaherpesvirus-encoded Bcl-2 proteins, coupled with the lack of conservation in regions of Beclin 1 required for binding to these proteins, indicates that different families of herpesviruses may have evolved diverse strategies to antagonize Beclin 1 activity in virally-infected cells. The utilization of diverse strategies by different virus families to target the same host autophagy protein underscores the likely importance of Beclin 1 antagonism in viral pathogenesis and the likely importance of Beclin 1-dependent autophagy in antiviral host defense.

Beclin 1-dependent autophagy may function in antiviral host defense by several different mechanisms. There is now increasing evidence that cytoplasmic bacteria are targeted for lysosomal degradation by an autophagy gene-dependent pathway (Levine, 2004; Amano et al., 2006), and it seems likely that a similar

pathway is involved in the degradation of intracytoplasmic virions. Indeed, we previously found that HSV-1 virions are degraded inside autophagosomes in MEFs and in primary cultured neurons (Tallóczy et al., 2006). Based upon our CNS replication studies with the Beclin 1 binding-deficient ICP34.5 mutant virus, we speculate that xenophagy may also function to restrict HSV-1 replication in virally-infected neurons *in vivo*. Autophagy may also play a direct role in promoting neuronal survival during viral infection. In support of this hypothesis, autophagy genes protect against programmed cell death in plant cells infected with tobacco mosaic virus (Liu et al., 2005), in mouse neurons infected with Sindbis virus (Liang et al., 1999), and in neurons subjected to non-infectious forms of cellular stress (Levine and Yuan, 2005).

It is interesting to note that basal autophagy in the mouse nervous system is critical to ensure protein quality control and the prevention of neurodegenerative diseases. Conditional deletion of either *atg5* or *atg7* in the central nervous system results in progressive accumulation of intraneuronal inclusion bodies, leading to neurodegeneration and motor deficits (Hara et al., 2006; Komatsu et al., 2006). Accordingly, it is possible that ICP34.5-mediated antagonism of autophagy may not only promote viral replication, increase neuronal death, and increase animal mortality during acute HSV-1 encephalitis, but also contribute to chronic cellular dysfunction in the neurons of survivors.

In conclusion, we have described a novel pathogen/ host interaction required to elicit fatal neurological disease. An essential function of the virulence

factor, HSV-1 ICP34.5 is to target the host autophagy machinery component, Beclin 1. Genetic disruption of PKR, an autophagy-inducing signaling molecule, completely restores the neurovirulence of an autophagy inhibitory-defective mutant virus. These findings provide evidence that autophagy plays an important role in protection against viral infection, and that successful viral evasion of autophagy plays a key role in disease pathogenesis.

CHAPTER THREE
Autophagy Protects Against Sindbis Virus Infection of the Central Nervous System

INTRODUCTION

The involvement of *ATG* genes in innate antiviral defense is phylogenetically conserved. In plants, the *ATG* genes *BECLIN 1*, *ATG7, ATG3,* and *VPS34* are essential for controlling tobacco mosaic virus replication and limiting the spread of programmed cell death during the hypersensitive response (Liu et al., 2005). In *Drosophila*, *ATG* genes protect against vesicular stomatitis virus (VSV) infection (Shelly et al., 2009); the disruption of *Atg5*, *Atg8* and *Atg18* is associated with increased VSV replication both in cultured cells and *in vivo*, resulting in increased animal lethality. Autophagy may also function in vertebrate antiviral host defense. Overexpression of Beclin 1 (the mammalian Atg6 ortholog) in neurons protects neonatal mice against lethal Sindbis virus (SIN) infection (Liang et al., 1998). The herpes simplex virus type 1 (HSV-1) protein ICP34.5 inhibits autophagy by binding to Beclin 1 and an HSV-1 mutant virus lacking the Beclin 1 binding domain of ICP34.5 has decreased neurovirulence (See Section II, (Orvedahl et al., 2007). Additionally, in mouse models of peripheral HSV-1 infection, the Beclin 1-binding deficient mutant virus has been shown to be cleared more rapidly and fails to counteract the adaptive immune response as efficiently as wild-type virus (Leib et al., 2009).

The *ATG* gene *Atg5* encodes an essential component of the Atg5-Atg12-Atg16 conjugation system, is required for the formation of autophagosomes in

mammalian cells (Mizushima et al., 2001), and has been shown to play diverse roles in immunity (Deretic and Levine, 2009). In addition to increased susceptibility to VSV infection, RNAi-mediated knockdown of *Atg5* in *Drosophila* results in increased lethality following infection with the intracellular bacterium, *Listeria monocytogenes* (Yano et al., 2008). Targeted deletion of *Atg5* in phagocytic cells renders mice more susceptible to infection with *L. monocytogenes* and with the parasite, *Toxoplasma gondii* (Zhao et al., 2008). Furthermore, *Atg5* may either positively or negatively regulate type I interferon (IFN) production in a cell type-dependent manner during mammalian VSV infection (Deretic and Levine, 2009). Despite these findings, the role of endogenous *ATG* genes in general, and *Atg5* in particular, in the host antiviral response in vertebrates has not yet been examined *in vivo*. Therefore, we examined the role of *Atg5* in protection against lethal SIN CNS infection in mice.

SIN is a positive-sense enveloped RNA virus in the alphavirus genus, with a genome encoding 8 proteins, including 4 non-structural, and 4 structural proteins. SIN is transmitted between mosquitoes and birds in nature, and infects humans as incidental hosts. SIN infection in humans results in a mild self-limiting febrile illness that can include a rash, myalgias, and arthralgias. However, SIN provides a unique mouse model system for studying virus-host interactions in neurons, and serves as a model for serious human encephalitides caused by alphaviruses, including Eastern, Western, and Venezualan equine encephalitis viruses. We chose to examine role of an endogenous autophagy gene with the

Sindbis virus system because: (1) neurons, as post-mitotic cells, may be more likely than dividing cells to be dependent on non-cytolytic mechanisms (such as autophagy) for antiviral defense (Orvedahl and Levine, 2008); and (2) SIN can be used simultaneously as a CNS pathogen and a vector for neuronal gene delivery *in vivo*, which is useful to probe the effects of host cell genetic manipulation on viral pathogenesis (Hardwick and Levine, 2000; Levine et al., 1996). Following intracerebral inoculation, SIN predominantly infects neurons (Jackson et al., 1988; Johnson, 1965; Levine et al., 1996) and exhibits age-dependent neurovirulence (Johnson et al., 1972). In neonatal mice, inflammatory infiltrates and classical signs of encephalitis are not observed (Johnson, 1965). Rather, lethal CNS infection is thought to be due to cell-autonomous virus-induced neuronal cell death, since using the SIN vector system, our laboratory and others have shown that virally-expressed inhibitors of apoptosis reduce the mortality of neonatal mice with CNS Sindbis virus infection (Griffin, 2005; Johnston et al., 2001).

In this study, we used the SIN vector system to inactivate Atg5 in virally-infected neurons, and also used neuron-specific *Atg5* knockout mice. Our results demonstrate that loss of neuronal Atg5 function results in increased susceptibility of neonatal mice to lethal SIN CNS infection. *Atg5* disruption does not affect viral replication, but does result in increased neuronal death that is associated with the accumulation of SIN proteins and cellular p62, an adaptor protein that binds to the autophagosomal membrane protein LC3 and is degraded by the autophagy

pathway (Bjorkoy et al., 2005; Klionsky et al., 2008). *In vitro*, we found that p62 interacts with SIN capsid and targets it to the autophagosome. The genetic knockdown of p62, or the essential autophagy protein, Atg7, results in increased SIN capsid accumulation and increased virus-induced cell death but not increased viral replication. Together, our *in vivo and in vitro* results suggest that autophagy protects against SIN pathogenesis by a cell-autonomous mechanism that facilitates viral protein clearance and prevents virus-induced cell death, without directly controlling viral replication.

EXPERIMENTAL PROCEDURES

Mammalian cell lines. Primary MEFs were established from GFP-LC3, *Atg5*$^{+/flox}$, and *Atg5*$^{flox/flox}$ mice (Hara et al., 2006; Mizushima et al., 2004) at day e13.5 and cultured as described (Su et al., 2003). *Atg5*$^{+/+}$ and *Atg5*$^{-/-}$ immortalized MEFs, were described previously (Hosokawa et al., 2006; Kuma et al., 2004; Mizushima et al., 2001). Primary MEFs and immortalized MEFs were cultured in 15% FBS media (high glucose DMEM, 15% fetal bovine serum, 1x penicillin/streptomycin, 118μM β-mercaptoethanol, and 1x MEM non-essential amino acids). Primary MEFs were passaged no more than five times. HeLa cells (provided by V. Stollar, (Li et al., 1997)) stably-expressing GFP-LC3 (HeLa/GFP-LC3 cells) were generated by subcloning the GFP-LC3 fragment from pEGFP-LC3 (provided by T. Yoshimori) into the NheI and EcoRI sites of the pIRESneo3 vector (Clontech) to generate the plasmid, pGFP-LC3-neo, and using G418 (100 μg/ml) selection to

isolate HeLa clones stably transfected with pGFP-LC3-neo. HeLa/GFP-LC3 cells were cultured in DMEM with 10% FBS containing 1x penicillin/streptomycin and 10 μg/ml G418.

Mouse strains. One to two day-old outbred CD1 mouse litters were obtained from Charles River. *Atg5*$^{flox/+}$ mice (provided by N. Mizushima) were crossed with *Atg5*$^{flox/+}$ mice to obtain *Atg5*$^{+/+}$, *Atg5*$^{flox/+}$, and *Atg5*$^{flox/flox}$ mice (Hara et al., 2006). *Atg5*$^{flox/flox}$ mice were crossed with B6.Cg-Tg(nestin-Cre)1Kln/J mice (Jackson Laboratories; stock#003771) to produce *Atg5*$^{+/flox}$; nestin-*Cre* mice described previously (Hara et al., 2006). *Atg5*$^{+/flox}$; nestin-*Cre* mice were crossed with *Atg5*$^{flox/flox}$ mice to obtain *Atg5*$^{+/flox}$; nestin-*Cre* control and CNS-specific *Atg5*-deficient mice (*Atg5*$^{flox/flox}$; nestin-*Cre* mice). *Atg5*$^{flox/flox}$ and *Atg5*$^{flox/flox}$; nestin-*Cre* mice were genotyped as described (Hara et al., 2006).

Wild-type and recombinant chimeric SIN strains. The SIN strain SVIA (ATCC) is derived from a low-passage isolate of the wild-type AR339 SIN strain (Taylor et al., 1955). To construct UV-inactivated SVIA, SVIA was treated for 5 minutes with a Stratalinker® UV Crosslinker 1800 (Stratagene), and the lack of infectious virus after UV irradiation was confirmed by plaque assay titration. The construction of the recombinant viruses, SIN/Atg5, SIN/Atg5K130R, SIN/Atg5.Stop, SIN/Cre, SIN/Cre.Stop, SIN-mCherry.capsid, and SIN-mCherry.capsid/GFP-LC3 was performed using the recombinant SIN vector

dsTE12Q as a backbone (Liang et al., 1998). To construct the Sindbis (SIN) recombinant chimeric viruses, SIN/Atg5 and SIN/Atg5K130R, the murine *Atg5* and *Atg5K130R* genes (Mizushima et al., 2001) were amplified by PCR using mAPG5/pClneo and mAPG5K130R/pClneo (provided by N. Mizushima) as templates. The PCR products were subcloned into pZeroBlunt (Invitrogen) and ligated into the *Bst*EII site of the Sindbis virus recombinant vector dsTE12Q (Liang et al., 1998) to yield the SIN/Atg5 and SIN/Atg5K130R plasmids. To construct SIN/Atg5.Stop, the same strategy was employed; however, two-step PCR was used to amplify the *Atg5* gene without the ATG start codon and a possible false ATG codon 177 base pairs from the start codon. The SIN/Cre virus was constructed by amplifying the bacterial *Cre* recombinase gene using pCreHyg (provided by D. Leib) as a template. The SIN/Cre.Stop virus was constructed by amplifying the *Cre* gene without the ATG start codon using the same strategy. The SIN-mCherry.capsid virus was generated by overlap-extension PCR using pRSETB-mCherry (provided by R. Tsien) to amplify mCherry, and dsTE12Q/Cre to amplify Sindbis virus capsid regions. The SIN-mCherry.capsid/GFP-LC3 virus was generated by amplifying GFP-LC3 from pEGFP-LC3 (provided by T. Yoshimori) subcloned into pZeroBlunt and then into the *BstE*II site of SIN-mCherry.capsid. The SIN/Atg5.Stop virus insert was amplified using two-step PCR with the following primer combinations GGGGTCACCACAGATGACAAAGATGTGCT and AACATCTTCTTGTCTAACCTTCTGAAAGTG, as well as

CACTTTCAGAAGGTTAGACAAGAAGATGTT and AAGGTCACCTCAATCTGTTGGCTGGGGGA. The SIN/Cre virus was constructed with the primers GGGGTCACCATG TCCAATTTACTGACCG and GGGGTCACCCTAATCGCCATCTTCCAGCA using pCreHyg as a template. The SIN-mCherry.capsid virus was generated using the primers CAGAGTACTA GAAGAGCGGCTTAAAACG (containing an endogenous *Sap*I site), and CGCCCTTGCTCACCATGGTGGTGGTGTTGTAGTATTAG (the first 16 nucleotides corresponding to antisense 5' start of mCherry, and last 22 nucleotides corresponding to the antisense Sindbis virus genome immediately 5' to capsid start), and ATGAATAGAGGATTCTTTAACATGC (corresponding to the first 25 bp of capsid) and CGTTCTTGACGTCGAACAATCTGTCG (containing an endogenous *Aat*II site within the capsid gene), were used to amplify the region 5' upstream of capsid and the first 361 nucleotides of the capsid gene, respectively, using the dsTE12Q plasmid as a template. The primers CTACAACACCACCACCATGGTGAGCAAGGGCGAGGAG (the first 16 nucleotides corresponding to the 5' region upstream of capsid, and last 21 nucleotides corresponding to the 5' start of mCherry) and GTTAAAGAATCCTCTATTCATCTTGTACAGCTCGTCCATGCC (the first 21 nucleotides corresponding to the antisense 5' start of capsid, and last 21 nucleotides corresponding the antisense 3' end of mCherry lacking the stop codon) were used to amplify mCherry from pRSETB-mCherry. The three PCR products were linked in two steps using the flanking primers to generate a ~1.6kb

fragment that was subcloned into pZeroBlunt, and then into the endogenous *Sap*I and *Aat*II sites of dsTE12Q. The SIN-mCherry.capsid/GFP-LC3 virus was generated using the primers TACAACGGTCAC CATGGTGAGCAAGGGCGAGGAGC and CGATCAGGTGACCTCACAAGCATGG CTCTCTTCC. Infectious virus was produced from all SIN recombinant chimeric vectors as described (Hardwick and Levine, 2000; Levine et al., 1996; Liang et al., 1998), and recombinant viruses were titered by plaque assays on BHK-21 cells.

***In vitro* virus infections.** All infections (virus and mock) were performed in reduced serum (1% FBS)-containing media. For comparison of viral replication in Atg5-expressing and Atg5-deficient cells (MEFs, ES cells, M5-7 cells), infections were performed at a multiplicity of infection (MOI) of 0.1 plaque-forming unit (PFU) per cell. MEFs and Neuro-2A cells were infected at an MOI of 5 for EM, fluorescent microscopy and biochemical studies. HeLa/GFP-LC3 cells were infected at an MOI of 5 for coimmunoprecipitation and radioimmunoprecipitation experiments; at an MOI of 20 for colocalization studies; and at an MOI of 1 for viability assays and replication studies.

Animal studies. All infections were performed by intracerebral (i.c.) inoculation of the designated number of PFUs of virus diluted in 30µl Hanks balanced salt solution (HBSS) into the right cerebral hemisphere. One to two day-old

randomized CD1 litters were infected with 5000 PFUs i.c. of recombinant SIN constructs, SIN/Atg5, SIN/Atg5K130R, and SIN/Atg5.Stop. One day-old litters resulting from an *Atg5*$^{+/flox}$ x *Atg5*$^{+/flox}$ cross were infected with 1000 PFUs i.c. of SIN/Cre and SIN/Cre.Stop. One week-old *Atg5*$^{flox/flox}$; nestin-*Cre* and *Atg5*$^{+/flox}$; nestin-*Cre* litters were infected with 1000 PFUs i.c. of dsTE12Q. For mortality studies, mice were monitored daily for 21 days. For measurement of CNS viral titers, freeze-thawed 10% (weight/volume) homogenates of the right hemispheres were used for plaque assay titration. For histopathology studies, the left hemispheres were fixed in 4% paraformaldehyde, embedded in paraffin, and cut sagitally from the medial surface into 5 μM adjacent sections. For *in vivo* autophagy assessment, one day-old GFP-LC3 litters (Mizushima et al., 2004) were infected with 1000 PFUs i.c. of SVIA, then euthanized 24 h later by perfusion with 4% paraformaldehyde, and frozen brain sections were prepared. See Supplemental Experimental Procedures for additional details on tissue sample preparations. All animal procedures were performed in accordance with institutional guidelines and with approval from the Institutional Animal Care and Use Committee.

Immunohistochemical and immunofluorescence studies. TUNEL staining of brain sections was performed according to manufacturers' instructions (Apoptag® peroxidase *In Situ* Apoptosis Detection Kit; Chemicon International), using Sigma *FAST*™ 3, 3'-diaminobenzidine (DAB) tablets as the peroxidase substrate.

Immunohistochemical staining of paraffin-embedded brain sections was performed using a rabbit polycl polyclonal anti-SIN antibody (provided by D. Griffin) (1:500 dilution) (Jackson et al., 1988), a rabbit polyclonal anti-SIN capsid antibody (provided by M. MacDonald) (1:2000) (Rice and Strauss, 1982), and a polyclonal guinea pig anti-cellular p62 antibody (Progen, 1:1000 dilution). Primary antibodies were detected with the ABC Elite kit (Vector Laboratories) according to the manufacturer's instructions. The number of SIN antigen-positive cells per mouse brain sagittal section and the number of TUNEL-positive cells per virus-infected area per mouse brain sagittal section was quantified as described in the Supplemental Experimental Procedures. Immunofluorescence staining of SVIA-infected GFP-LC3 MEFs and SVIA-infected GFP-LC3 neonatal mouse brains was performed using a rabbit polyclonal anti-SIN antibody as described in the Supplemental Experimental Procedures.

siRNA treatment. *p62*, *Atg7*, and non-silencing negative control siRNA's were purchased from Dharmacon. All siRNA experiments were performed using reverse transfection at a final concentration of 53 nM siRNA, Lipofectamine 2000 (Invitrogen) at a dilution of 1:1500, and otherwise according to manufacturer's instructions. At 48 hours after siRNA transfection, protein knockdown was assessed by Western blot analysis and viral infections were performed. The following sequences were used for siRNA knockdown of p62: p62-1, GAAAUGGGUCCACCAGGAA; p62-2, GAUCUGCGAUGGCUGCAAU; p62-

3, GCAUUGAAGUUGAUAUCGA; and for Atg7: GGGUUAUUACUACAAUGGUG.

Fluorescence, light, and electron microscopy and quantitation. GFP-LC3 MEFs were imaged and punctae were quantified with a Zeiss Axioplan2 microscope using a Zeiss PLAN-APOCHROMAT 63x objective by an observer blinded to experimental condition. For live cell imaging and colocalization studies, *Atg5*$^{+/+}$ or *Atg5*$^{-/-}$ MEFs were imaged in an environmentally-controlled chamber with an Olympus 40x objective on a personal DeltaVision microscope with softWoRx software (Applied Precision). Images were captured at 10-minute intervals with 8 z-sections per time point with 2 μm spacing. Images were deconvolved using softWoRx software. Movie generation and image manipulations were performed with ImageJ (NIH). For colocalization studies, HeLa/GFP-LC3 cells and were imaged similarly to live cells but with an oil-immersion 40x objective and with 10 z-sections obtained per sample. Colocalization was quantitated using Imaris software (Bitplane). siRNA identities were blinded to experimenter until after statistical analysis. For quantitation of pathology in infected brain sections, the number of Sindbis virus antigen-positive cells per unit area of midline brain sagittal sections was quantitated using Zeiss Axioplan2 Imaging software using a 20x objective. To quantify the number of TUNEL positive-cells per virus-infected focus, the areas of virus-infected foci

were measured for each brain sagittal section, and the number of TUNEL-positive cells in each virus-infected focus was counted using a 20x objective. EM studies were performed as described previously (Liang et al., 1999).

Coimmunoprecipitation and radioimmunoprecipitation. For coimmunoprecipitation studies, HeLa/GFP-LC3 cells were mock treated or infected with SVIA at an MOI of 5 in 60mm dishes for 11 hours and lysed in 600 μl TNT lysis buffer (50mM Tris-Cl pH 7.4, 150mM NaCl, 1mM EDTA, 1% TritonX-100, and protease inhibitors). Forty μl of lysates were reserved for Western blots as loading controls. Samples were pre-cleared using 40 μl protein G-agarose beads (Santa Cruz) and 6 μl normal guinea pig IgG (Santa Cruz) for 30 minutes to 1 hour, immunoprecipitated overnight with 6 μl anti-p62 antibody (Progen), or IgG control, and boiled for 5 minutes with Laemmli buffer containing 2.5% β-mercaptoethanol. For radioimmunoprecipitation, cells were treated with negative control or p62-2 siRNA for 48 hrs, infected at an MOI of 5 with SVIA, or pelleted and lysed as described below to assess siRNA knockdown. At 3 hours post-infection, cells were depleted of Met/Cys by washing three times with 2 ml Met/Cys-free media (Gibco) containing 2% dialyzed FBS (Gibco), and then incubated with the same media for 2 hours. Cells were then labeled for 1 hour with 21 μCi Trans-35S LABEL, Metabolic Labeling Reagent (MP Biomedicals), and washed 5 times with 1 ml 2% media supplemented with Met and Cys at 2 mM each. Cells were scraped and pelleted at 2.4k RCF, and stored at

-80° C until lysis. Cells were first lysed in 100 μl TNT lysis buffer, and TritonX-100-insoluble material was then pelleted at 16k RCF. The insoluble pellet was then solublized in 50 μl TSD buffer (50mM Tris-Cl pH 7.4, 1% SDS, 5mM DTT) by boiling for 10 minutes. Soluble and insoluble lysates were added to a final volume of 600 μl TNT buffer, precleared with normal rabbit IgG (Santa Cruz), and immunoprecipitated with 6 μl anti-SIN polyclonal antibody. Immunoprecipitates were boiled for 5 minutes in Laemmli buffer containing 1.25% β-mercaptoethanol, separated by SDS-PAGE, dried, and exposed by autoradiography at -80° C. Western blot analyses were performed as described below. Autoradiographs were quantitated using ImageJ software (NIH).

Western blot analyses. Western blot analyses were performed with the following primary antibodies: anti-p62 (1:500 dilution) (Progen for MEFs and Neuro-2A cells, BD Biosciences for HeLa/GFP-LC3 cells), anti-Atg7 (1:500 dilution) (Sigma), anti-SIN virus capsid (1:10,000 dilution) (provided by M. McDonald), anti-Atg5 (1:2000) (Mizushima et al., 2001), and anti-actin (1:2000 dilution) (Santa Cruz). For Western blot analyses, cells were lysed for 30 min on ice in TNT lysis buffer and cleared samples were boiled in 1:1 Laemmli buffer, separated on SDS-PAGE denaturing gels, and transferred to PVDF membranes (Biorad). Membranes were blocked with 5% nonfat milk in PBS/0.1% Tween-20 (PBST). Signals were visualized with a Supersignal®West Pico Chemiluminescent Substrate kit (Pierce). For Sindbis virus capsid and Sindbis

virus antigen Western blots in co-immunoprecipitation studies, samples were analyzed using a One-Step Complete IP-Western Kit For Rabbit Primary Antibody (GenScript Corporation), according to the manufacturer's instructions. Specifically, 10 μl of Sindbis virus capsid or Sindbis virus antigen antibody was incubated with WB1 solution, and samples were transferred to PVDF membranes after SDS-PAGE analysis.

Cell viability assays. Cell viability of HeLa/GFP-LC3 cells at serial time points after infection with dsTE12Q was determined by a Trypan Blue exclusion assay. Triplicate samples with a minimum of 100 cells per sample were counted for each experimental group.

Genomic PCR for *Atg5*. Genomic PCR for the *Atg5*$^{flox/flox}$ allele was performed as described (Hara et al., 2006). For *in vitro* analysis of SIN/Cre-mediated excision, primary *Atg5*$^{flox/flox}$ MEFs were infected with SIN/Cre or SIN/Cre.Stop at an MOI of 30, and genomic DNA from cell lysates were prepared using the Genomic DNA Buffer Set (Qiagen). Samples were then analyzed as described for mouse genotyping (Hara et al., 2006).

Autophagy assays. Autophagosome accumulation was measured in GFP-LC3 MEFs by counting the percentage of cells with one or more green punctae and the number of punctae per positive cell by an observer blinded to experimental

condition. Autophagic flux was measured by p62 Western blot analysis in MEFs. The presence of autophagic structures in MEFs was also confirmed by EM analyses.

Statistical analyses. Log-rank tests were used to analyze all mortality studies, and student t-tests were performed for all other experiments using Prism software. A p value of < 0.05 was considered statistically significant.

RESULTS

Live, But Not UV-Inactivated, SIN Induces Autophagy *in vitro*

To determine whether SIN infection induces autophagy *in vitro*, we infected primary GFP-LC3 MEFs with SVIA or UV-inactivated SVIA (UV-SVIA). There was a significant increase in the percentage of cells with autophagosomes (GFF-LC3 dots) in MEFs infected with live SVIA as compared to mock-infected MEFs beginning at 9 h (S. MacPherson, Fig. 1A, $p < 0.05$); and more than 60% of SVIA-infected MEFs contained GFP-LC3 dots by 15 h post-infection ($p < 0.001$ vs. mock-infected controls). In contrast, there was no increase in the percentage of cells with autophagosomes in MEFs infected with UV-inactivated SVIA as compared to mock infection. These data indicate that SIN-induced autophagy requires viral replication, at least in MEFs. The lack of autophagy induction at 3 h post-infection (Fig. 1A), a time point when viral entry but not viral replication has occurred, is consistent with this conclusion.

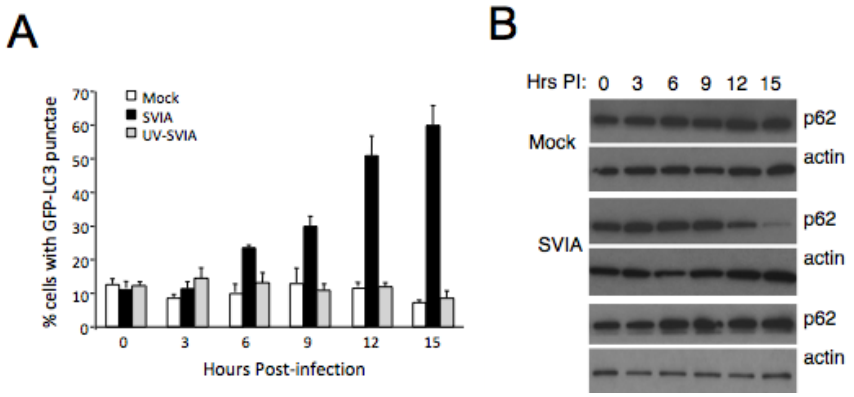

Figure 1. SIN Induces Autophagy *in vitro*. (A) Quantitation of the percentage of GFP-LC3 MEFs with GFP-LC3 punctae (autophagosomes) after infection with indicated virus. Data shown represent mean ± SEM for triplicate samples of at least 100 cells per sample. Similar results were observed in 3 independent experiments. (E) Measurement of autophagic protein degradation by p62 Western blot analysis in wild-type MEFs at serial time points after mock, SVIA, or UV-SVIA infection.

Since some pathogens induce early stages of autophagy, but block later stages (i.e. autophagolysosomal fusion), we investigated whether SIN induces a complete autophagic response (i.e. autophagic flux) by measuring levels of the autophagic substrate, p62. We found that in live SVIA, but not UV-SVIA-infected MEFs, there was a gradual decline in levels of p62 protein with barely detectable levels observed by 15 h post infection (Fig. 1B). Together with the GFP-LC3 assays, these data indicate that a complete autophagic response is induced in MEFs infected with replication-competent, but not UV-inactivated, replication-incompetent SIN.

At time points when increased autophagosomes were observed in SVIA-infected MEFs, but not earlier, we observed intracytoplasmic expression of SIN structural proteins, which strongly colocalized with GFP-LC3 punctae (S. MacPherson, Fig. 2A). Similar results were also observed with an antibody specific for SIN capsid protein (data not shown). These structures likely represent

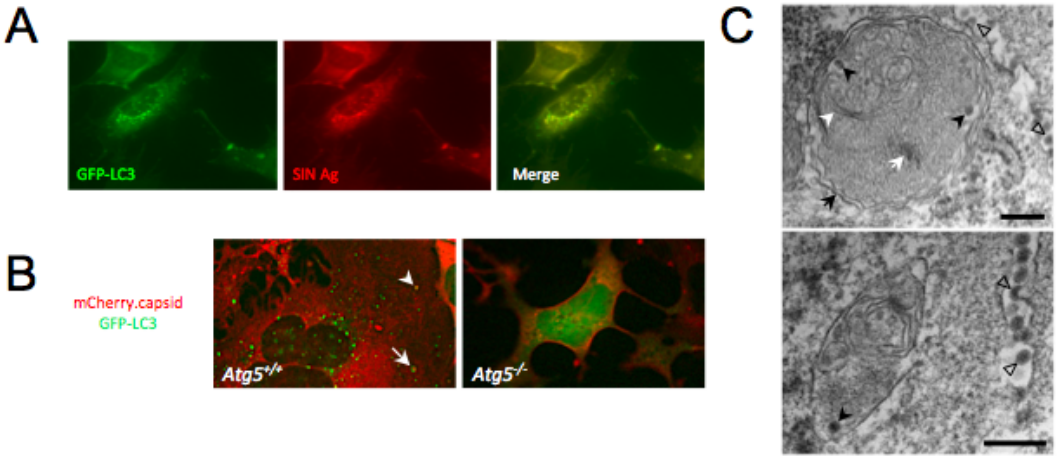

Figure 2. SIN proteins and virions localizae to autophagosomes. (A) Representative fluorescent microscopic image demonstrating colocalization of SIN structural proteins (red) with GFP-LC3 (green) in GFP-LC3 MEFs at 12 h post-infection (p.i.). (B) Representative fluorescent microscopic images showing colocalization in *Atg5*$^{+/+}$ MEFs or lack of colocalization in *Atg5*$^{-/-}$ MEFs of SIN capsid (red) and GFP-LC3 (green) in cells infected with SIN-mCherry.capsid/GFP-LC3. Images shown represent a single time point at 12 h p.i. from live cell imaging. Arrowhead denotes colocalized puncta; arrow denotes capsid-positive GFP-LC3 ring structure. See movie S1 for dynamic representation of mCherry.capsid and GFP-LC3 localization between 16 and 17 h p.i. in *Atg5*$^{+/+}$ MEFs. (C) Representative EMs of wild-type MEFs at 12 h p.i. with SVIA. Left panel demonstrates a double-membraned autophagosome (black arrow) containing SIN nucleocapsids (black arrowheads), cellular membranes (white arrowhead), and aggregates (white arrow). Right panel demonstrates a single-membraned autolysosome with SIN nucleocapsid (black arrowhead). Open arrowheads denote virions budding from the plasma membrane. Scale bars, 200 nm.

classical autophagosomes rather than non-specific GFP-LC3 aggregates, since GFP-LC3 punctate structures that colocalize with SIN capsid were observed in wild-type but not in *Atg5*$^{-/-}$ MEFs (Kuma et al., 2004) infected with a recombinant SIN strain, SIN-mCherry.capsid/GFP-LC3, that expresses mCherry fused to the endogenous capsid protein and that expresses GFP-LC3 from a double-subgenomic promoter (Fig. 2B).

Since SIN replicates on the cytoplasmic surface of single-membraned vesicles (not double-membraned vesicles) (Gil-Fernandez et al., 1973), this colocalization likely reflects the targeting of newly synthesized SIN proteins or

assembled SIN nucleocapsids to autophagosomes rather than an association of the SIN replication complex with LC3-positive membranes. Indeed, in live-cell time-lapse microscopy imaging of wild-type MEFs infected with SIN-mCherry.capsid/GFP-LC3, mCherry.capsid structures appear first and later are engulfed by GFP-LC3-positive membranes (Movie S1, available online at doi:10.1016/j.chom.2010.01.007), suggesting these structures are actively targeted by autophagy. Furthermore, electron microscopic (EM) analyses of SIN-infected MEFs revealed autophagosomes and autolysosomes that contained Sindbis virions (Fig. 2C and data not shown). The presence of virions in late autolysosomes supports the findings with p62 degradation that a complete autophagic response is occurring in infected cells. While autophagic structures contained Sindbis virions, there were also other cytoplasmic contents inside them, including cellular membranes and aggregates (Fig. 2C). Thus, the autophagic capture of SIN in MEFs is not entirely specific for viral contents.

SIN Infection Induces Autophagy *in vivo* and Viral Antigen Co-localizes With Autophagosomes in Neurons

To determine whether SIN induces autophagy in virally-infected neurons *in vivo*, we infected GFP-LC3 transgenic mice with SVIA and examined GFP-LC3 subcellular localization and SIN antigen expression. In uninfected mouse brains, as described previously (Mizushima et al., 2004), we did not detect GFP-LC3 punctae in neurons (S. MacPherson, Fig. 3, top). However, in the brains of

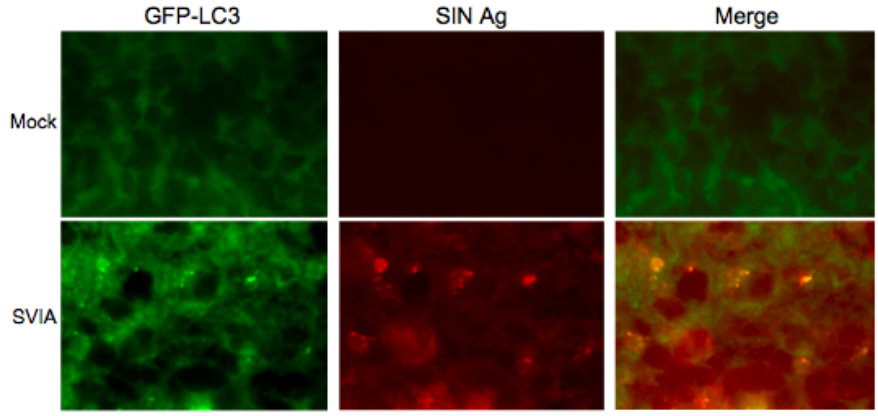

Figure 3. SIN-Induced autophagy in mouse hippocampal neurons.. Colocalization of SIN structural proteins (red) with GFP-LC3 in hippocampal neurons of GFP-LC3 transgenic mice 24 h after mock infection (top) or infection with SVIA (bottom). Similar hippocampal regions are shown for mock and SVIA-infected brains. No GFP-LC3 punctae were observed in any regions of the mock-infected brains.

SVIA-infected mice, we detected GFP-LC3 punctae specifically in neurons that also expressed SIN antigens (Fig. 3, bottom) and SIN antigens colocalized with GFP-LC3 punctae. Thus, SIN infection induces autophagy *in vivo* in mouse brain and, similar to *in vitro*, SIN proteins colocalize with autophagosomes.

Strategies for Investigating the Effects of Neuronal Atg5 on the Pathogenesis of SIN CNS Infection

To investigate the role of neuronal autophagy in the pathogenesis of SIN CNS infection, we used three complimentary strategies to inactivate the *ATG* gene, *Atg5*, in virally-infected neurons *in vivo* (Fig. 4A). In all three models, we used a backbone strain of SIN, dsTE12Q, that is relatively avirulent in neonatal mice to facilitate the detection of increased neurovirulence in the setting of *ATG* gene inactivation. In the first model (Fig. 4Ai), we used the recombinant chimeric SIN system (Hardwick and Levine, 2000; Liang et al., 1998) to express a

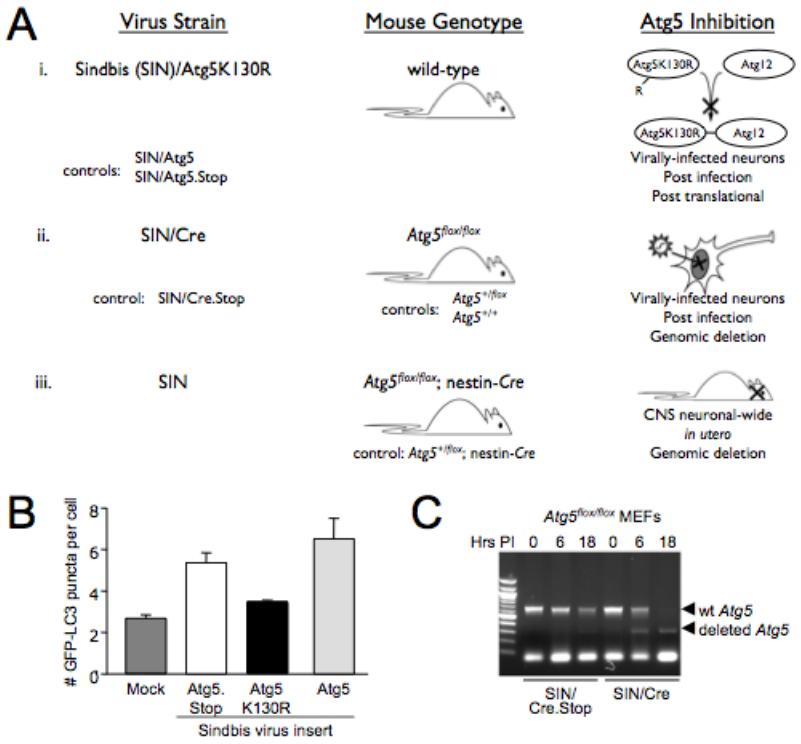

Figure 4. Scheme of experimental strategies to inhibit autophagy in neurons *in vivo*. (A) Conceptual overview of strategies to inhibit or knock out Atg5 specifically in neurons *in vivo*, and the relevant control viruses and mouse strains. (i) SIN expressing a dominant negative mutant Atg5 (Atg5K130R). (ii) SIN expressing Cre recombinase in *Atg5*$^{flox/flox}$ mice. (iii) nestin-*Cre* mice crossed to *Atg5*$^{flox/flox}$ mice. (B) Quantitation of the number of GFP-LC3 punctae (autophagosomes) per cell in GFP-LC3 MEFs at 12 h after infection with indicated virus below x axis. Data shown represent mean ± SEM for triplicate samples of at least 100 cells per sample. Similar results were obtained in 3 independent experiments. (C) Detection of genomic *Atg5* excision in primary MEFs obtained from *Atg5*$^{flox/flox}$ mice infected with SIN/Cre or SIN/Cre.Stop.

dominant-negative mutant of Atg5 (K130R, herein referred to as Atg5K130R). The K130R mutation inhibits a key step in the autophagic pathway by blocking covalent conjugation of Atg5 to Atg12 (Mizushima et al., 1998; Mizushima et al., 2001), resulting in impaired recruitment of LC3 to nascent autophagic isolation membranes and impaired autophagosome formation (Hamacher-Brady et al., 2006; Mizushima et al., 2001; Pyo et al., 2005). As controls, we constructed chimeric SIN constructs expressing wild-type Atg5 (SIN/Atg5) or a noncoding *Atg5* sequence devoid of ATG codons (SIN/Atg5.Stop). We confirmed that

SIN/Atg5K130R blocked virus-induced autophagy *in vitro* by counting the number of GFP-LC3 dots per cell in MEFs that were infected with SIN/Atg5K130R versus SIN/Atg5 or SIN/Atg5.Stop ($p < 0.05$, SIN/Atg5K130R vs. control viruses) (Fig. 4B). In the second model (Fig. 4Bii), we infected $Atg5^{flox/flox}$, $Atg5^{+/flox}$, or $Atg5^{+/+}$ mice with recombinant chimeric SIN constructs that express either Cre recombinase (SIN/Cre) or a noncoding Cre sequence (SIN/Cre.Stop). After infection with SIN/Cre (but not with SIN/Cre.Stop), *Atg5* is deleted only in infected neurons of $Atg5^{flox/flox}$ mice, whereas infected neurons from $Atg5^{+/flox}$ mice are rendered haploinsufficient, and there is no effect on *Atg5* in wild-type ($Atg5^{+/+}$) animals. We used PCR to confirm the excision of floxed *Atg5* alleles in $Atg5^{flox/flox}$ MEFs after infection with SIN/Cre (Fig. 4C). In the third model (Fig. 4Biii), we assessed the effect of pre-existing deletion of *Atg5* in both infected and uninfected neurons on SIN pathogenesis, using $Atg5^{flox/flox}$; nestin-*Cre* mice, which undergo neuron-specific deletion of *Atg5 in utero* (Hara et al., 2006). These mice are normal at birth, and do not display signs of progressive neurodegenerative defects until after 3 weeks of age.

Inhibition of Neuronal Atg5 Results in Increased Mortality from CNS SIN Infection

We assessed the effect of disruption of neuronal *Atg5* function on mortality due to CNS SIN infection in neonatal mice. In each model, increased mortality was observed in the setting of neuronal Atg5 inactivation (S.

MacPherson, Fig. 5). Wild-type mice infected with SIN/Atg5 and SIN/Atg5.Stop viruses had higher survival rates (73% and 76%, respectively) than those infected with SIN/Atg5K130R (41%; $p < 0.001$) (Fig. 5A). SIN/Cre-infected *Atg5*$^{flox/flox}$ mice were less likely to survive (52%; $p < 0.001$) than their *Atg5*$^{+/+}$ (75%) or *Atg5*$^{+/flox}$ (85%) littermates (Fig. 5B). However, mice infected with the control virus, SIN/Cre.Stop, exhibited the same mortality (90%) across all genotypes (Fig. 5C). Finally, *Atg5*$^{flox/flox}$; nestin-*Cre* mice were less likely to survive (71%; $p < 0.001$) than their control *Atg5*$^{+/flox}$; nestin-*Cre* littermates (100%) (Fig. 5D). No mortality was seen in mock-infected *Atg5*$^{flox/flox}$; nestin-*Cre* animals (Fig. 5E),

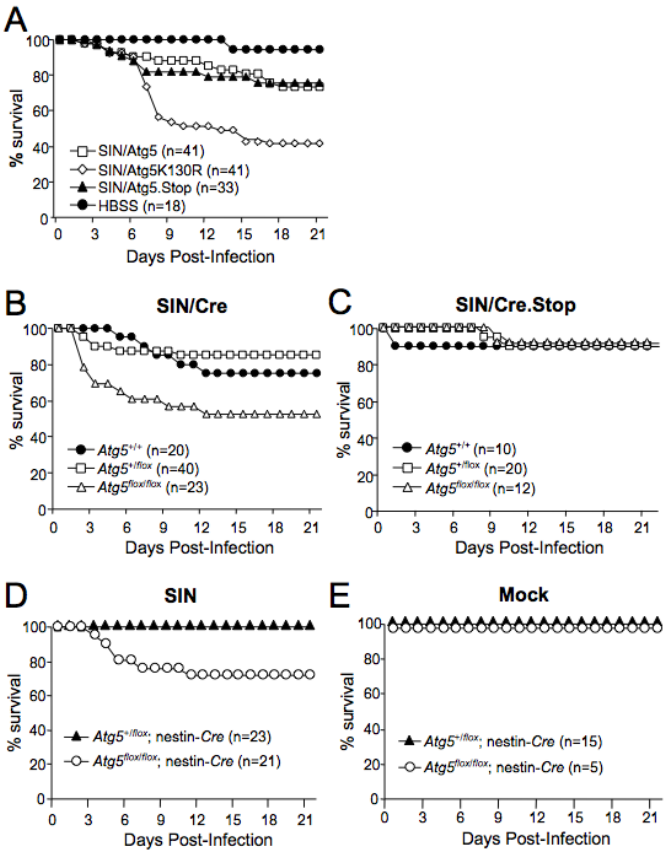

Figure 5. Increased SIN neurovirulence in mice with inactivation of neuronal Atg5. (A) Mortality of CD1 littermates infected with the indicated recombinant SIN strains or mock-infected with HBSS. Data shown represent combined mortality from 4 independent infections of 8-12 mice per group. Similar results were observed in each independent experiment. (B-C) Mortality of *Atg5*$^{flox/flox}$ or littermate controls (*Atg5*$^{+/flox}$ and *Atg5*$^{+/+}$) infected with recombinant SIN expressing Cre recombinase or SIN expressing non-coding Cre gene. Data shown in (B-C) represent combined mortality from infection of 22 and 8 separate litters, respectively. (D-E) Mortality of littermates from *Atg5*$^{+/flox}$; nestin-*Cre* transgenic mice crossed with *Atg5*$^{flox/flox}$ mice and infected with the dsTE12Q strain of SIN (D) or mock-infected (E). Data shown in (D-E) represent combined mortality from infection of 21 and 8 separate litters, respectively.

indicating that this increased mortality was due to increased susceptibility to lethal SIN infection, rather than constitutive neuronal deletion of *Atg5*.

Neuronal Atg5 Inactivation Alters Viral Antigen Clearance and Neuronal Cell Death Without Affecting CNS Viral Replication or Type I IFN Production

To gain insight into the mechanism of increased lethality in mice with neuronal *Atg5* inactivation, we examined levels of CNS viral replication, type I IFN production, and brain histopathology at serial time points after infection. We observed no differences in any of the three model systems in the levels of infectious virus in the brains of control animals versus mice with disrupted neuronal Atg5 function (S. MacPherson, Fig. 6A-C). Thus, *Atg5* does not seem to be required for the control of levels of infectious virus *in vivo* in virally-infected mouse brains. We also observed no differences in the levels of type I IFN in the brains of mice with intact neuronal Atg5 versus those with disrupted neuronal Atg5 function (data not shown). Also, as previously well-characterized in neonatal SIN infection (Johnson, 1965), perivascular and intraparenchymal inflammatory infiltrates were lacking in all experimental groups (data not shown). Thus, increased SIN-induced mortality in mice with neuronal Atg5 inactivation is unlikely due to alterations in viral replication, levels of innate immune signaling, or inflammation. Although no differences were observed in CNS viral titers, we observed marked differences in the numbers of viral antigen-positive cells in mice

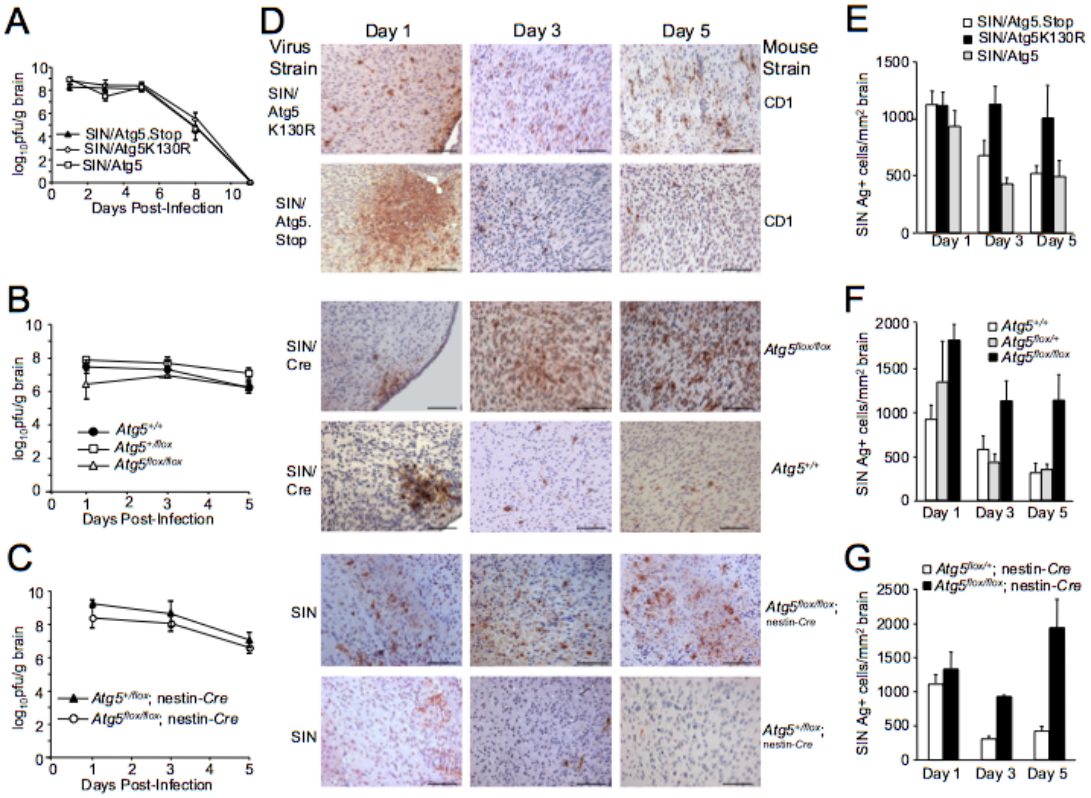

Figure 6. Atg5 Inhibition Delays Viral Antigen Clearance from Neurons Without Affecting SIN CNS Titers. (A-C) SIN titers in mouse brains. Data shown represent geometric mean titers ± SEM for groups of 4-8 mice per time point. (D) SIN antigen staining of brains of mice of the indicated genotype (right labels) infected with the indicated virus (left labels). All micrographs in (D) are from the superior colliculus of the mouse brain, a region that is infected by SIN in all mice in this study. The images shown are representative of the data quantitated in (E-G) for the total mouse brain, with the exception that there is high degree of inter-mouse variability in the level of colliculus staining at day one. Scale bars, 100 μm. (E-G) Quantitation of SIN antigen staining in the brains of mice treated as in (A-C), respectively. Data in (E-G) represent mean number of antigen-positive cells per unit area of mouse brain for 4-8 mice per experimental group.

with intact versus disrupted neuronal Atg5 function (S. MacPherson, Fig. 6D-G). At day one after infection, no significant differences were observed in the number of viral antigen-positive cells between mice with intact Atg5 function versus disrupted neuronal Atg5 function. However, after day one, in all three models, the numbers of viral antigen-positive cells declined in mice with intact neuronal Atg5 function but remained persistently elevated in mice with disrupted neuronal Atg5

function. At days 3 and 5 after infection, a significant increase was observed in the numbers of viral antigen-positive neurons in mice with disrupted neuronal Atg5 compared to the control group(s) in each model ($p < 0.05$). These data indicate that, while intact neuronal Atg5 function is not essential for the control of

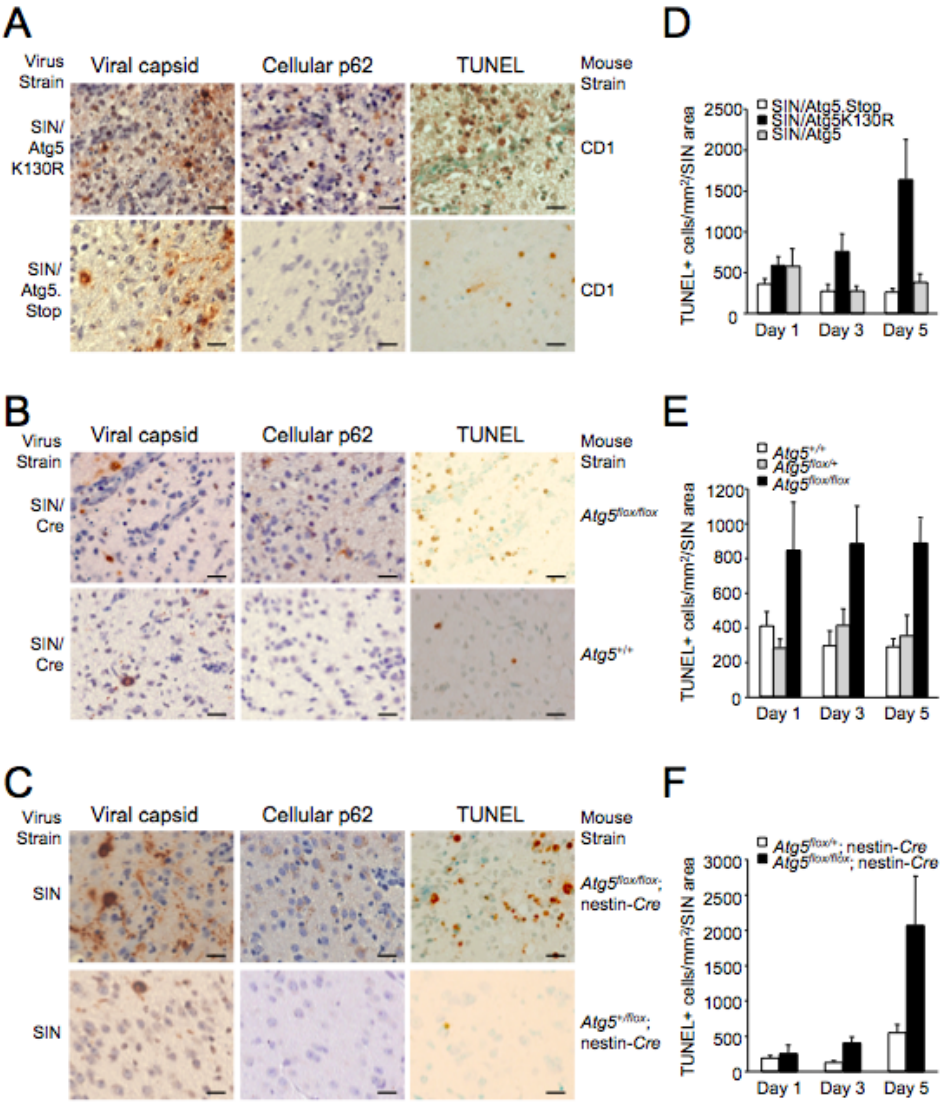

Figure 7. Increased SIN capsid staining, cellular p62 staining, and cell death in the brains of mice with neuronal Atg5 inactivation. (A-C) Detection of SIN capsid (left column), cellular p62 (middle column), and cell death by TUNEL staining (right column) in mouse brain. Shown are representative photomicrographs for each experimental group of the superior colliculus at day 5 p.i. For (A-C) similar results were observed in 4-8 mice per group. Scale bars, 20 μm. (D-F) Quantitation of number of TUNEL-positive cells per unit area of virus-infected region of brain at days 1, 3, and 5 p.i.. Data in (D-F) represent mean ± SEM for each brain from 4-8 mice per experimental group.

replication-competent SIN, it is essential for the clearance of SIN antigen from neurons.

We further confirmed the delayed clearance of SIN antigen from neurons by performing immunohistochemical staining of SIN capsid protein (S. MacPherson, Fig. 7A-C left panels). Additionally, we found that in regions of SIN antigen and capsid staining, there was an accumulation of cellular p62 protein in mice with disrupted neuronal Atg5 function, but not in infected mice with intact Atg5 function (Fig. 7A-C, center panels). Higher power analysis of adjacent sections showed that identical cells displayed capsid and p62 immunoreactivity in each mouse model of neuronal Atg5 inactivation (Fig. 8). No increases in cellular ubiquitin immunostaining were observed among any of the groups of virus-infected mice (data not shown).

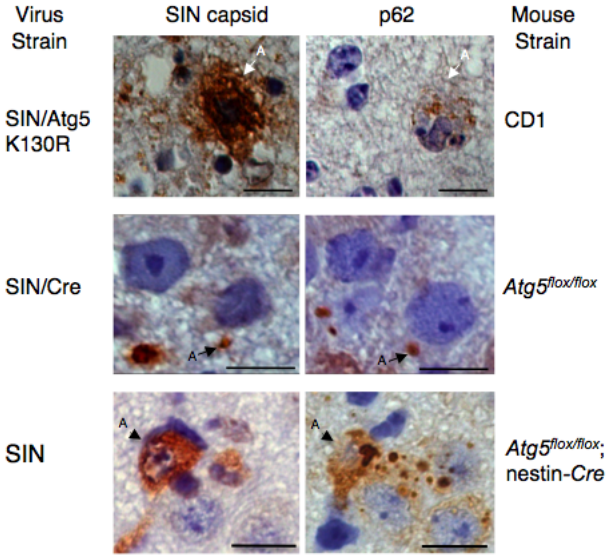

Figure 8. p62 Accumulates in Neurons that Express Sindbis Virus Capsid. Representative high-power micrographs showing adjacent sections of mouse brain stained for Sindbis virus capsid and cellular p62. Left labels indicate virus strain used for infection and right labels indicate mouse strain. Each row depicts precisely the same region of the brain in adjacent sections confirmed by coordinates in lower power micrographs. Representative cells that display both Sindbis virus capsid immunoreactivity and cellular p62 immunoreactivity are labeled with corresponding letters in each image. Scale bars, 10 μm.

Brain regions that exhibited increased capsid and p62 staining also contained increased TUNEL-positive cells (Fig. 7A-C, right panels). We quantitated the

number of TUNEL-positive cells per virus-infected region of the brain and found that in each model of neuronal Atg5 inactivation, significant increases in the numbers of TUNEL-positive cells were observed at day 3 post infection, and more strikingly, at day 5 post infection (Fig. 7D-F; $p < 0.05$ vs. controls). Higher power analysis of adjacent sections showed that identical cells displayed TUNEL and SIN antigen positivity (Fig. 9). Thus, in three different model systems in which neuronal Atg5 function is disrupted, SIN infection results in increased neuronal cell death.

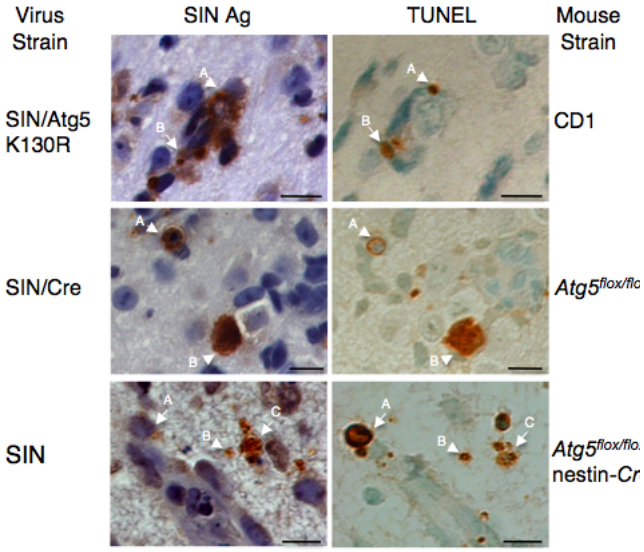

Figure 9. Sindbis virus-infected neurons are TUNEL-positive. Representative high-power micrographs showing adjacent sections of mouse brain stained for Sindbis virus antigen and TUNEL. Left labels indicate virus strain used for infection and right labels indicate mouse strain. Each row depicts precisely the same region of the brain in adjacent sections confirmed by coordinates in lower power micrographs. Representative cells that display both Sindbis virus antigen immunoreactivity and TUNEL-positivity are labeled with corresponding letters in each image. Scale bars, 10 μm.

p62 is Involved in SIN Capsid Targeting to Autophagosomes

Our findings above indicate that: (1) Atg5 may perform a protective cellular housekeeping role during viral infection of post-mitotic cells such as neurons; and (2) p62 may serve as an adaptor protein, not only for the autophagic clearance of ubiquitinated cellular proteins, but also for the autophagic clearance of viral proteins. To investigate this latter possibility, we used an *in vitro* system

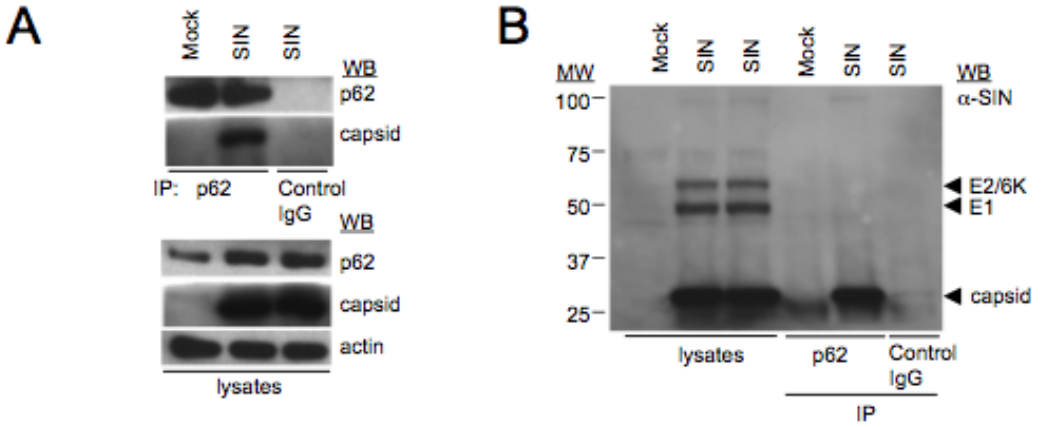

Figure 10. p62 interacts with SIN capsid. (A-B) Coimmunoprecipitation of SIN capsid with p62 in HeLa/GFP-LC3 cells mock-infected or infected with SVIA (labeled SIN) either by Western blotting with a polyclonal anti-SIN virus capsid antibody (A) or a polyclonal anti-SIN antibody that detects E2/6K, E1, and capsid protein (B).

that is amenable to biochemical and genetic knockdown studies. We found that in virally-infected HeLa cells, p62 coimmunoprecipitates with SIN capsid protein (Fig. 10A, B), but not with SIN E1 or E2 envelope glycoproteins (Fig. 10B). Furthermore, siRNA knockdown of p62 in HeLa cells (Fig. 11A) significantly decreases the colocalization of SIN capsid protein and GFP-LC3 punctae ($p < 0.05$) (Fig. 11B, C). Consistent with the degradative function of autophagy and our observations that SIN antigens persist in autophagy-deficient infected mouse brains *in vivo*, we found that siRNA knockdown of p62 delayed the degradation of SIN capsid (but not the E1 or E2 envelope glycoproteins) in HeLa/GFP-LC3 cells using a pulse-chase labeling radioimmunoprecipitation assay (Fig. 11D-F). This delayed clearance was most evident in the detergent-insoluble protein fraction, which was previously demonstrated to be cleared through p62-mediated autophagy (Komatsu et al., 2007). Thus, *in vitro*, p62 interacts with SIN capsid and is required for its targeting to autophagosomes. This interaction, if conserved

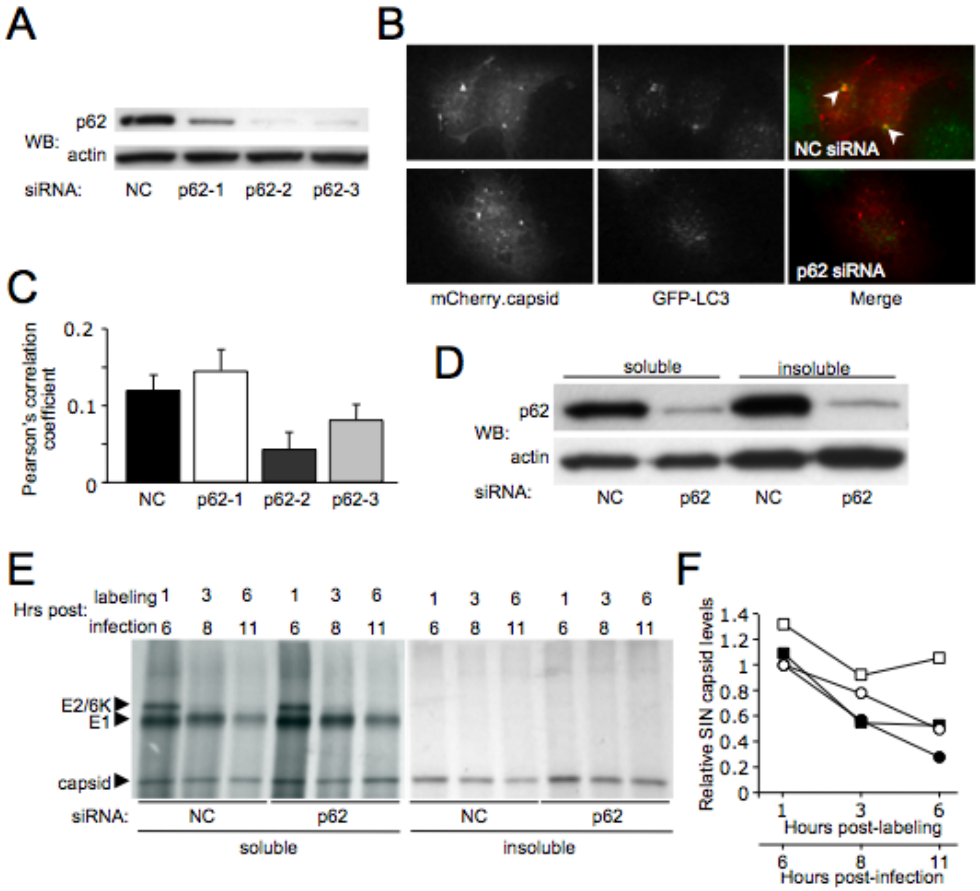

Figure 11. p62 targets capsid for autophagy. (A-C) Detection of SIN capsid colocalization with GFP-LC3 after p62 knockdown. Western blot analysis of p62 expression in HeLa/GFP-LC3 cells treated with individual p62 siRNA oligos or non-silencing negative control oligos (NC) (A). Representative image of HeLa/GFP-LC3 cells treated with p62-2 siRNA (bottom) or NC (top), and infected with SIN-mCherry.capsid (B). Quantitation of mCherry.capsid colocalization with GFP-LC3 in cells treated with the indicated siRNA (C). Data shown represent the mean of at least 50 infected cells per condition ± SEM. Similar results were obtained in 3 independent experiments. (D-H) Analysis of SIN protein degradation after p62 knockdown. Western blot analysis of p62 expression in the fractions used in (E) for radioimmunoprecipitation (D). Radioimmunoprecipitation with an anti-SIN antibody of soluble and insoluble fractions from HeLa/GPF-LC3 cells treated with NC or p62 siRNA, infected with SVIA, and pulse-chased for the indicated times (E). Quantitation of capsid levels in (E) relative to 1 h control levels for each fraction (F). Closed circles, NC soluble; closed squares, p62 soluble; open circles, NC insoluble; open squares, p62 insoluble. Similar results were observed in 3 independent experiments.

in infected neurons *in vivo*, may potentially explain the accumulation of SIN capsid protein and cellular p62 in the brains of infected mice with disrupted neuronal autophagy.

p62 and Atg7 are Important for the Survival of SIN-Infected Cells *in vitro*

Our findings above indicate that p62 serves as an adaptor that targets SIN to the autophagosome. Next, we sought to evaluate the physiological consequences of p62 knockdown on SIN replication and SIN-induced cell death. Consistent with the delayed clearance of SIN capsid with p62 knockdown as measured by pulse-chase analysis (Fig. 11), we found that p62 siRNA results in an increase in steady-state levels of SIN capsid as compared to control siRNA at 12 and 24 h after infection (Fig. 12A). In these same conditions where p62 siRNA results in increased SIN capsid accumulation, we observed a significant increase in virus-induced cell death at 24 h after infection ($p < 0.001$ vs. non-coding siRNA

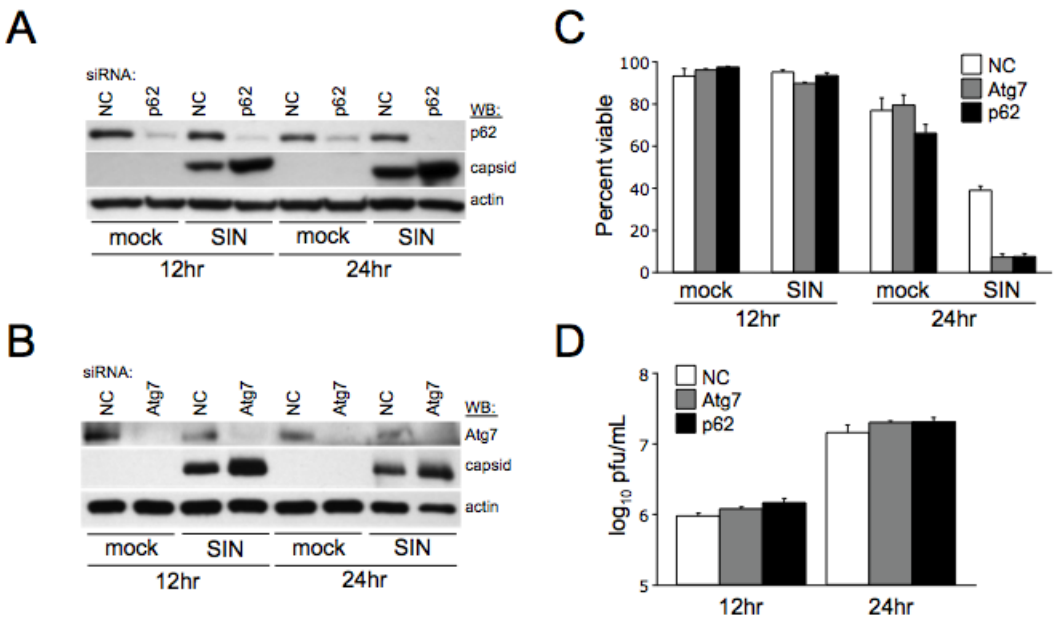

Figure 12. p62 and Atg7 promote the survival of SIN-infected cells. (A-B) Western blot analysis of p62 and capsid expression (A) or Atg7 and capsid expression (B) in HeLa/GFP-LC3 cells treated with the indicated siRNA and infected for the time indicated. (C) Cell death quantitation of cells treated as in (A) and (B) as measured by a trypan blue exclusion assay. Data shown represent mean ± SEM of at least 100 cells per sample for triplicate samples for each condition. (D) Levels of infectious SIN in supernatants of cells in (C). Data represent geometric mean titers ± SEM for triplicate samples. For (A-D), similar results were obtained in three independent experiments.

control) (Fig. 12C). However, we did not observe any alterations in levels of viral replication in p62 siRNA-treated cells at these time points (Fig. 12D) or in a 96 hour growth curve (data not shown). Thus, similar to neuronal Atg5 inactivation *in vivo*, we found that p62 inactivation *in vitro* results in SIN capsid accumulation, increased virus-induced cell death, and no effect on viral replication.

To further confirm that the p62 siRNA phenotype was a function of decreased autophagy, we performed similar experiments using siRNA against *Atg7*, another component of the protein conjugation system that is required for autophagosomal membrane expansion (Komatsu et al., 2005). Similar to siRNA against p62, siRNA targeted against *Atg7* results in an increase in steady-state levels of SIN capsid protein (Fig. 12B), an increase in virus-induced cell death at 24 h post infection ($p < 0.001$ vs. non-coding siRNA control) (Fig. 12C), and no changes in levels of infectious virus (Fig. 12D). Thus, genetic knockdown *in vitro* of either the p62-SIN capsid-interacting targeting factor or the Atg7 autophagy execution protein phenocopies *in vivo* disruption of neuronal Atg5 function with respect to increased virus-induced cell death in the absence of increased viral replication. Together, these data suggest that p62-mediated autophagic clearance of SIN capsid protein may be important for cell survival during viral infection.

DISCUSSION

Here we demonstrate that neuronal function of the *ATG* gene, *Atg5* is essential to protect mice against fatal CNS alphavirus infection. While previous genetic knockout or knockdown studies have suggested an important role for *ATG* genes in the protection of mice, *Drosophila*, worms, and slime molds against bacterial or protozoal pathogens (Jia et al., 2009; Yano et al., 2008; Zhao et al., 2008), and in the protection of *Drosophila* (Shelly et al., 2009) and plants (Liu et al., 2005) against viral infection, our results provide evidence for a protective role of an endogenous *ATG* gene in antiviral host defense in mammals. Thus, *ATG* genes play a conserved role in antiviral immunity – ranging from plants, to *Drosophila*, to mice.

Our findings suggest a unique mechanism by which *ATG* genes protect host organisms against viral infection, which involves the clearance of viral proteins. In previous studies, the knockdown or knockout of *ATG* genes in plants and *Drosophila* has been shown to increase viral replication and increase animal mortality (in *Drosophila*) (Shelly et al., 2009) or pathology (in plants) (Liu et al., 2005). In addition, mice with *Atg5*-deficient plasmacytoid dendritic cells have impaired type I IFN production following infection with VSV (Lee et al., 2007). Surprisingly, although we observed increased SIN replication *in vitro* in one clone of immortalized *Atg5*$^{-/-}$ MEFs, we did not observe increased SIN replication in other *Atg5*-deficient cell lines or in the brains of mice with neuronal inactivation of Atg5 (nor, did we observe any defects in type I IFN production *in vivo*). We therefore conclude that the increased SIN-induced animal mortality is not due to a

direct role of neuronal *Atg5* in the control of viral replication or regulation of innate immune signaling. Rather, mice with disruption of neuronal Atg5 function had increased neuronal death associated with impaired clearance of SIN proteins. Although it is difficult to conclude the precise cause of either neuronal or organismal death in the context of *in vivo* mouse studies, one plausible explanation is that, in post-mitotic cells such as neurons, the failure to properly clear viral proteins by autophagy results in cellular toxicity and increased animal lethality.

Our *in vitro* data provide support for the hypothesis that autophagy-mediated clearance of SIN proteins is cytoprotective and identify a mechanism by which the SIN capsid protein is targeted for autophagic degradation. We found that the p62 cellular adaptor protein interacts with SIN capsid and is required for SIN capsid targeting to the autophagosome. Moreover, genetic knockdown of p62 or Atg7 increases capsid accumulation and cell death, without increasing levels of SIN infectious virus. Thus, p62-mediated autophagic targeting of SIN capsid may function to promote cell survival during SIN infection. While cell death inhibits viral replication in many settings, virus-induced cell death is an established important factor in the pathogenesis of neuronotropic viral infections (Levine, 2002). Accordingly, we propose that the cytoprotective function of autophagic-mediated degradation of SIN capsid may contribute to the protective role of endogenous *ATG* genes against lethal CNS SIN infection.

Our findings present an example of p62 targeting a specific microbial protein for autophagic degradation. Recent studies have indicated a role for p62 in targeting ubiquitin-coated *Salmonella* for autophagic degradation (Zheng et al., 2009). However, a biochemical interaction between p62 and a viral or other microbial protein is unprecedented. p62 is believed to function as an adaptor that binds ubiquitin and polyubiquitin through its C-terminal UBA domain and binds LC3 through a more N-terminal LC3 interaction region (LIR) domain (Pankiv et al. 20077). It is not yet known which domain of p62 is required for its interaction with SIN capsid, whether this interaction is direct or indirect, and whether p62 targets other structural proteins from other viruses to autophagosomes. Interestingly, our data suggest that, unlike p62-dependent autophagic targeting of cellular proteins or ubiquitin-coated bacteria, the interaction between p62 and SIN capsid and the targeting of SIN capsid may be ubiquitin-independent. In contrast to the neurodegenerative phenotype in older neuron-specific *Atg5*- or *Atg7*-deficient mice where there is accumulation of both ubiquitin aggregates and p62 aggregates (Hara et al., 2006; Komatsu et al. 2006), we only observed p62, and not ubiquitin, aggregates in SIN-infected mice with neuronal *Atg5* inactivation. We were also unable to detect ubiquitination of SIN capsid *in vitro* in conditions where it interacts with p62. Thus, autophagy-dependent protein quality control in neurons may involve p62 in the clearance of both cellular and viral proteins, but other, as-of-yet undefined molecular tags besides ubiquitin may serve to link certain viral proteins to p62-dependent autophagy targeting pathways.

Unlike reports with *Listeria* or VSV infection in *Drosophila*, a pre-formed pathogen-associated molecular pattern in SIN does not appear to induce autophagy upon cellular entry, since UV-inactivated SIN does not induce autophagy in either MEFs or mouse neuronal cells. The requirement for viral replication in SIN-induced autophagy may suggest either (1) autophagy is induced through the delivery of viral nucleic acids to endosomal Toll-like-receptors (a process that in itself has been shown to require the autophagic machinery in VSV-infected pDCs (Lee et al. 2007); or (2) cytoplasmic sensors of viral RNA (i.e. retinoic acid-inducible gene I (RIG-I)-like receptors (RLRs)) may play a heretofore-undefined role in autophagy stimulation. An important area of future research will be to elucidate the precise cytoplasmic signaling events that link detection of viral replication to autophagy activation during SIN and potentially other viral infections.

Our studies suggest that neuronal Atg5 protects against lethal SIN infection in a cell-autonomous manner. We used three complimentary models to inactivate neuronal *Atg5*; in the first two, *Atg5* was specifically inactivated in virally-infected neurons exclusively after viral replication whereas in the third model, *Atg5* was deleted *in utero* in neurons. The observation of a similar phenotype in all three models provides strong support that the observed increased neurovirulence, impaired viral protein clearance, and increased neuronal death is a direct consequence of neuronal Atg5 inactivation. These models have the advantage that they permit us to assess the direct effects of neuronal Atg5

inactivation on virus-host interactions in neurons, without confounding variables introduced by Atg5 deficiency in other cell types or on other stages of viral pathogenesis, such as peripheral replication and CNS invasion. However, the role of Atg5 deficiency in these other stages of pathogenesis that occur in the natural route of mosquito-borne arboviral infections is not yet known. Similarly, our experimental design does not permit us to definitively rule out a role for neuronal Atg5 deficiency in shaping innate immune responses other than type I IFN production or adaptive immune responses that may contribute to SIN pathogenesis.

Other groups have reported potential autophagy-independent functions of the *ATG* gene, *Atg5*, including a pro-apoptotic function by a calpain-mediated cleavage fragment (Yousefi et al., 2006) and autophagy-independent recruitment of Irga6 GTPase recruitment to *T. gondii* parasitophorous vacuoles (Zhao et al., 2008). Our findings are most consistent with an autophagy-dependent function of Atg5, as: (1) we observed increased, not decreased, cell death, in the setting of Atg5 disruption, suggesting that Atg5 is not acting as a cell death factor; (2) we confirmed that SIN nucleocapsids were captured inside classical double-membraned autophagosomes in wild-type MEFs and found that SIN capsid protein could not be targeted to autophagosomes in *Atg5*-deficient MEFs; and (3) we observed impaired clearance of viral proteins and an accumulation of p62 aggregates in virally-infected neurons lacking Atg5 function. While this phenotype is strongly consistent with a defect in the classical lysosomal

degradative role of autophagy, we cannot exclude a contribution of autophagy-independent functions of *Atg5* in protecting neurons against SIN infection. Further studies of SIN pathogenesis in mice with neuronal inactivation of other *ATG* genes will be important to confirm the role of the autophagy pathway in neuronal protection against SIN infection. However, our findings with *Atg7* siRNA in HeLa cells provide *in vitro* evidence that other components of the autophagy pathway promote SIN capsid protein clearance and cell survival during virus infection.

In summary, our findings provide strong evidence for an important cell-autonomous role for neuronal Atg5 in *in vivo* protection against SIN infection. Based on our characterization of mouse brain titers and histopathology, this protection is associated with neuronal Atg5-dependent control of viral protein clearance and neuronal Atg5-dependent protection against cell death, but not neuronal Atg5-dependent control of virus replication. Moreover, our *in vitro* studies provide strong evidence that p62 functions to promote the survival of infected cells through autophagic targeting and clearance of viral proteins. Although further studies are required to definitively prove a direct cause and effect relationship between impaired viral protein (and/or cellular protein) p62-mediated clearance and increased cell death in SIN-infected mice with disrupted neuronal Atg5 function, our studies raise the intriguing hypothesis that autophagy-dependent protein quality control may be a previously unappreciated function in the vast repertoire of host antiviral immune responses.

CHAPTER FOUR
High Content Screening for Host Factors Required for Targeting Viral Proteins to Autophagosomes

INTRODUCTION

Macroautophagy (herein referred to as autophagy) is an evolutionarily conserved process in which damaged or superfluous proteins and organelles are targeted for lysosomal degradation through sequestration in a double-membraned autophagosome. Autophagy can also target foreign invading microbes for degradation and immune modulation (Deretic and Levine, 2009; Sumpter and Levine, 2010). While autophagic targeting of cytoplasmic microbes plays an integral role in host immunity, the mechanisms by which pathogens are targeted by autophagy remain relatively poorly understood. We previously demonstrated that the autophagy gene *Atg5* protects against Sindbis virus encephalitis, and the autophagosome adaptor protein p62 may target Sindbis virus capsid protein for autophagic degradation to promote cellular survival (See Section III, (Orvedahl et al., 2010)). This study suggests that host factors involved in targeting viral proteins may be essential components of autophagy response to infection.

In contrast to the traditional view that it is an indiscriminate cytoplasmic recycling pathway, autophagy is emerging as a pathway that is highly specialized to selectively sequester substrates. These substrates include mitochondria (Geisler et al., 2010; Kanki et al., 2009; Kawajiri et al., 2010; Kim et al., 2007; Lee et al., 2010c; Narendra et al., 2008; Okamoto et al., 2009), protein aggregates (Gal et al., 2009; Iwata et al., 2005; Jeong et al., 2009; Komatsu et al., 2006; Lee et al.,

2010c; Pandey et al., 2007; Ravikumar et al., 2005), organelles (Farre et al., 2008; Kim et al., 2008; Nazarko et al., 2009; Yorimitsu and Klionsky, 2007), specific proteins and protein complexes (Kraft et al., 2008; Li, 2006; Massey et al., 2006; Pohl and Jentsch, 2009; Qing et al., 2007; Qing et al., 2006; Yu et al., 2006), and pathogens (Dupont et al., 2009; Gutierrez et al., 2007; Huett et al., 2009; Kyei et al., 2009; Ogawa et al., 2005; Talloczy et al., 2006; Thurston et al., 2009; Yoshikawa et al., 2009; Zheng et al., 2009). Targeting for at least some of these substrates is mediated through adaptor molecules that link the ubiquitinated substrates to LC3 in the growing autophagosome membrane (Noda et al., 2010; Pankiv et al., 2007; Shvets et al., 2008). These adaptors include the most well characterized member, p62/SQSTM1 (Bjorkoy et al., 2005), as well as NBR1 (Kirkin et al., 2009; Lamark et al., 2009), and NDP52 for bacteria (Thurston et al., 2009).

A number of proteins have been identified and characterized in mediating selective autophagy, though several key questions remain. These include but are not limited to: the identity of signals that regulate this process; precise cytoplasmic rearrangements that occur during substrate sequestration; identity of enzymes that mark cargo with ubiquitin and/ or other tags; and whether these processes function redundantly for diverse autophagy substrates or if mechanisms are specifically tailored for individual classes of substrates. Viral proteins and viruses can be targeted by autophagy, but the questions posed above also apply to viral sequestration. We sought to investigate autophagic targeting of viral proteins

in an unbiased genome-wide screen. We used Sindbis virus to assay viral targeting, which we have shown can be targeting by the autophagy pathway (Orvedahl et al., 2010). Our studies reveal that diverse cellular pathways and processes are involved in viral targeting, and provide further insight into general mechanisms of autophagic targeting.

EXPERIMENTAL PROCEDURES

Mammalian cell lines. HeLa/GFP-LC3 cells have been described (Orvedahl, et al, 2010), and were cultured in DMEM containing 10% heat-inactivated FBS, 1x Penicillin/Streptomycin, and 10μg/mL G418. HeLa/GFP-LC3 cells were passaged no more than 20 times from stable clone generation for all experiments. HeLa cells (ATCC) were cultured in 10% FBS, and 1x Pen/Strep.

Virus strains. Generation and amplification of the recombinant Sindbis virus strain, SIN-mCherry.capsid, has been described (See Section III, and (Orvedahl et al., 2010)). Briefly, viral RNA was *in vitro* transcribed from the recombinant dsTE12Q-mCherry.capsid plasmid and transfected into BHK-21 cells using well-established methods (Hardwick and Levine, 2000). Viral stocks were titered on BHK-21 cells.

siRNA screening. A genome-wide siRNA library (Dharmacon) containing 21,125 SMARTpools (each containing 4 siRNAs targeting an individual gene)

was seeded in triplicate glass-bottom 96-well plates (Greiner) (in 30μL Optimem (Gibco), final concentration of 53nM) using a BioMek liquid handler. Lipofectamine 2000 (Invitrogen) was added (in 20μL Optimem, final concentration of 1:200) with a Biotek dispenser, followed by addition of 6.4 x 10^3 HeLa/GFP-LC3 cells in 100μL normal culture media using a MultiDrop dispenser for reverse transfection. After 48 hours to allow knockdown, supernatant was removed by low speed centrifugation. Control wells in column 1 were mock infected with 30 μL Optimem, and control wells in column 12 and all sample wells (columns 2-11) were infected with SIN-mCherry.capsid virus in 30μL at a multiplicity of infection (MOI) of 5 using a Biotek dispenser. After 1 hr incubation, 120 μL of media containing 2% FBS was added to all wells. After 11 hours of infection, 10 μL of 2% media containing Hoechst 33342 (Invitrogen) (5μg/mL final) was added to the wells, plates were incubated for 40 minutes at 37°, followed by supernatant removal by low speed centrifugation, followed immediately by addition of 75 μL pre-warmed 2% PFA (Electron Microscopy Sciences) in 1x PBS containing Ca^{++} and Mg^{++} (Sigma). Cells were fixed overnight at 4°, PFA was then replaced with 1x PBS (Gibco), and plates were sealed and then stored at 4° until imaging. Primary hits were confirmed with sets of 4 individual siRNAs, in triplicate, with plates prepared using the same methods as the primary screen.

High content imaging and statistical analysis. Images were captured with a Pathway 855 automated microscope (BD Biosciences) using a 40x objective in Hoechst, GFP, and mCherry channels, using epifluorescence. A 5 x 6 montage of adjacent fields were captured in each channel for each well. Raw images were segmented using the Imaging and Advanced Imaging packages in Pipeline Pilot software (Accelrys). Briefly, cell boundaries were identified using watershed segmentation with Hoechst nuclear regions as markers, and cytosolic Hoechst signal as background. mCherry intensity statistics were then calculated for each cell, and infected cells were classified as having cellular mCherry intensity 25th percentile above the top 1 percent of signal in cells from all mock-infected wells on each plate. GFP and mCherry punctae were segmented using a difference of Gaussian method on natural log transformed images to detect punctae in cells with varying expression intensities. XY coordinates and area for each punctum from infected cells that contained both green and red punctae were analyzed for colocalization. Colocalization coefficient measurements, Z-score determination, and all statistical analyses were performed with the open-source R software package (www.r-project.org). For colocalization analysis a colocalization event was defined when a green dot touches or overlaps with a red dot in the same cell. The number of colocalization events in each cell was modeled as a Poisson count distribution. Generalized linear models were used to determine whether a siRNA treatment significantly increased or decreased the number of green dots by comparing the siRNA treated well to the negative controls. The total possible

colocalization events (number of green dots multiplied by number red dots) was included in the generalized linear models to adjust for the potential confounding effects of number of dots in each cell. The Z scores for the generalized linear models were used as summary statistics for each siRNA treated well for hits selection. Z scores were analyzed as follows to determine hit cutoffs: 195 primary hits for siRNAs that decrease colocalization were defined as those with z-scores for all three replicates below 2 standard deviations (S.D.) from the mean of all replicates, and/or those whose median z-score (for those with values for at least 2 replicates) was below 3 S.D. from the mean of all median z-scores. Primary hits for siRNAs that increase colocalization were defined as those with z-scores for all three replicates above 1.5 standard deviations (S.D.) from the mean of all replicates. Primary hits were considered validated if at least 2 oligos from the set of 4 individual oligos had a combined p-value less than 0.05 compared to on-plate negative control siRNA.

Cell death screen. HeLa/GFP-LC3 cells were seeded in clear flat-bottom 96-well plates (Costar) at the same cell densities and transfection conditions as the high content screens described above, except that plates were seeded in sextuplet. After 48hrs knockdown, triplicate plates were mock treated or infected at an MOI of 5 with dsTE12Q strain of Sindbis virus in 30μL Optimem. After 1 hr incubation, 120 μL of media containing 2% FBS was added to all wells. After 24 hrs viral infection, media was removed from plates by low speed centrifugation, and 50 μL

CellTiter-Glo reagent (Promega) (diluted 3:1, 1x PBS/ 1% TX-100: CellTiter-Glo) was added to wells. Plates were incubated at room temperature on an orbital shaker for 5 minutes to allow cell lysis and ATP measurement, and luminescence values were read on an Envision plate reader. Raw data was normalized to on-plate negative control siRNAs, and each individual oligo was considered confirmed if triplicate normalized infected values were decreased from triplicate normalized uninfected values with a p-value < 0.05.

Bioinformatics. Bioinformatics analysis was performed as described (Brass et al., 2009).

Mitophagy assay. HeLa cells (ATCC) were reverse transfected in 4-chambered slides with 100 ng YFP-Parkin (kindly provided by R. Youle) and 50 nM of the indicated siRNA, and grown for 48hrs to allow siRNA knockdown. Cells were treated with DMSO or CCCP (Sigma) at 10 μM for 24 hrs, and Hoechst 33342 at 5 μg/mL for 40 minutes before fixation in 2% PFA.

Western blot (WB), co-immunoprecipitation (IP), and immunofluorescence (IF). The following antibodies were used: p62 (BD Biosciences, 1:500 (WB)), Atg7 (Sigma, 1:500 (WB)), SMURF1 (Novus, 1:200 (WB), 1:1000 (IP)), RFWD3 (Novus, 1:1000 (IP)), anti-SIN capsid (C. Rice, 1:1000 (WB)), actin-HRP (Santa Cruz, 1:2000), Tom20 (Santa Cruz, 1:500 (IF)), and AlexaFluor594-conjugated

donkey anti-mouse (Molecular Probes, 1:450 (IF)). Western Blot and Co-Immunopreciptation were performed as described (See Section III, and (Orvedahl et al., 2010)). For immunofluorescence studies, cells were fixed in 2% PFA, permeabilized in PBS containing 0.05% Triton X-100, washed 3 times with PBS, blocked for 30 minutes in PBS/1% BSA (PBSA), incubated with primary antibody diluted in PBSA for 2 hours, washed 2 times with PBSA, incubated with secondary antibody diluted in PBSA for 45 minutes, washed 2 times with PBSA, then mounted for microscopy. Images were captured with a Zeiss Axioplan2 microscope using a Zeiss PLAN-APOCHROMAT 63x objective.

RESULTS

To identify novel genes required to target Sindbis virus capsid proteins to autophagosomes we performed a genome-wide, high-content siRNA screen. To assay autophagic targeting of viral proteins, we developed a fluorescence reporter assay using recombinant Sindbis virus expressing mCherry fused to the endogenous capsid gene to infect HeLa/GFP-LC3 cells (Fig. 1A, and (Orvedahl et al., 2010)). While this assay could potentially identify host factors required for viral infection, or GFP-LC3 puncta formation, we focused on siRNA's that did not affect these parameters, but specifically disrupted the colocalization of mCherry.capsid and GFP-LC3 (termed here "targeting determinants") (Fig. 1B). We screened a human siGenome library, containing 21,125 siRNA pools (each targeting 4 unique sites per gene), in triplicate with an inverted automated

microscope, and used automated image segmentation software to identify subcellular mCherry.capsid and GFP-LC3 puncta (Fig 1C, see methods for a

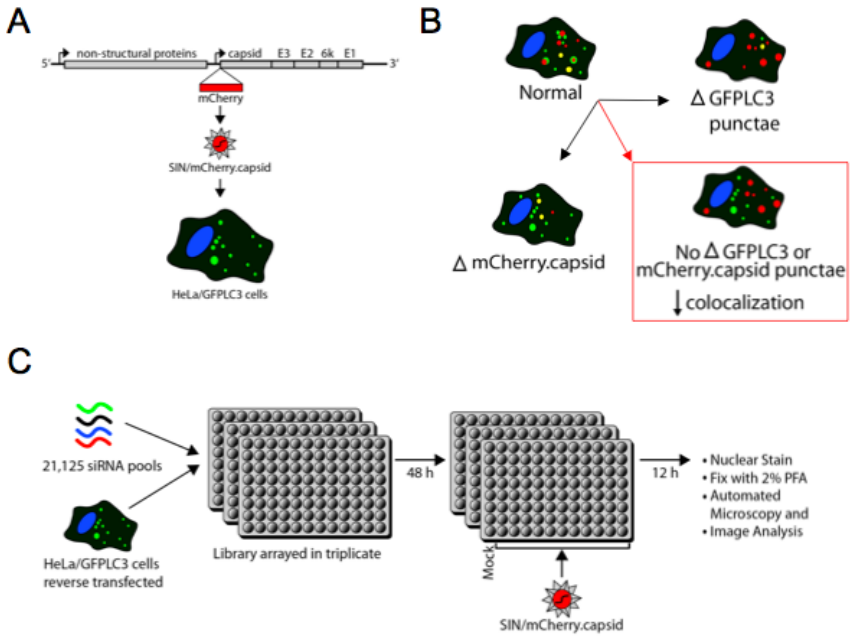

Figure 1. Assay and high-content screen overview. (A) Schematic of recombinant Sindbis virus genome used to generate SIN particles that were infected into HeLa/GFP-LC3 cells. (B) Representation of potential cellular phenotypes that can be identified in our screen. We focused on genes that did not affect mCherry.capsid or GFP-LC3 punctae levels in cells, but those siRNAs that specifically affected the ability for mCherry.capsid to localize to GFP-LC3 puncta. (C) Schematic of screening strategy for primary colocalization screen.

detailed description). 1428 pools could not be scored due to insufficient numbers of cells, insufficient numbers of infected cells, or insufficient numbers of punctae across triplicates. For the remaining 19,697 pools, when compared to on-plate negative controls, knockdown of 195 of genes resulted in decreased colocalization (Appendix A, Table 1), while siRNAs against 13 genes resulted in increased colocalization (Appendix A, Table 2). These genes were then re-screened with sets of 4 individual siRNA's to rule out potential off-target effects from individual siRNA's in the primary pools (Fig 2). In our confirmation screen, knockdown

with at least one oligo resulted in decreased colocalization for 182 (93%), while two or more oligos satisfied these criteria for 141 (72%) hits (Appendix A, Table

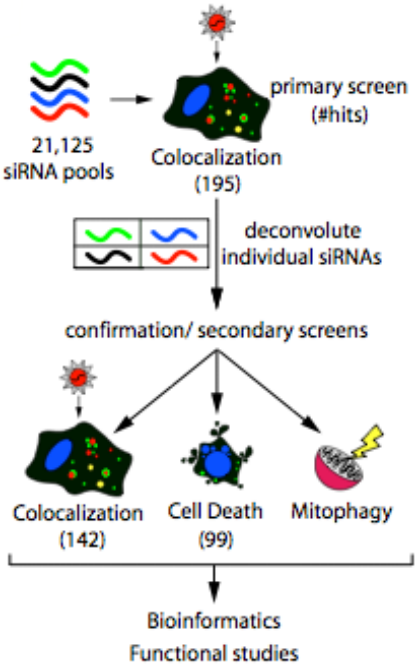

Figure 2. Confirmation screening and experimental strategy. Pools for primary hits were deconvolved into 4 individual oligos and arrayed in a confirmation library. This library was screened in the same microscopy-based assay as the primary screen to confirm this hits, as well as a cell survival assay and mitophagy assay. The numbers in parentheses correspond to the number of pools identified in the primary screen, or number of genes confirmed with > 1 oligo in the secondary screens, that decrease colocalization or cell survival. Mitophagy assays were performed on a candidate basis. Genes identified in the screens were subjected to bioinformatics and further functional studies with candidates.

3). We observed a low confirmation rate for siRNAs that increased colocalization, and constrained focus to only siRNAs that decreased colocalization for subsequent bioinformatics analysis, secondary screening, and mechanistic studies. We previously found that autophagy promotes survival of Sindbis virus-infected cells, potentially by preventing the accumulation of toxic viral proteins (Orvedahl et al., 2010). To determine if our hits from high content screening also functioned in this biological context, we screened our confirmation library of 4 individual oligos for genes that, when knocked down, resulted in increased cell death after SIN infection. We controlled for intrinsic cytotoxic effects of siRNAs by including an uninfected set of plates, and controlled for plate-to-plate variability

by normalizing samples to on-plate non-silencing control siRNAs. This secondary screen found 150 genes (77%) had at least 1 oligo that decreased survival during infection, and 99 (51%) genes had 2 or more oligos that resulted in increased susceptibility to Sindbis virus-induced cell death (Appendix A, Table 4, Column 6). The correlation between colocalization and cell death phenotype across the individual oligos was 0.63 (p-value = 5.8E-05, Fisher's exact test) (Appendix A, Table 4, Column 7). This correlation supports our previous findings that autophagic targeting of viral proteins promotes survival of infected cells (Orvedahl et al., 2010), and provides biological validation that the genes identified and confirmed in our image-based screen perform important cellular pro-survival functions during SIN infection.

We performed bioinformatics analysis on our primary hit list for genes that, when knocked down, decrease colocalization of SIN capsid with GFP-LC3. This analysis revealed that our list of genes are significantly enriched in pathways related to amino acid metabolism, mRNA processing, actin-myosin-troponin functions, p38-MAPK pathways, and IFN-γ signaling (Fig 3, Top). In agreement with actin/ myosin network enrichment, the biological processes associated with these hits were significantly enriched for transport process (Fig 3, Middle). Similarly, the annotated molecular functions for the primary hits include significant representation for kinases and cytoskeletal proteins (Fig 3, Bottom). These data suggest that our screen identified classes of genes that may act in a concerted manner to target viral proteins to autophagosomes, and provides

Pathway–associated networks

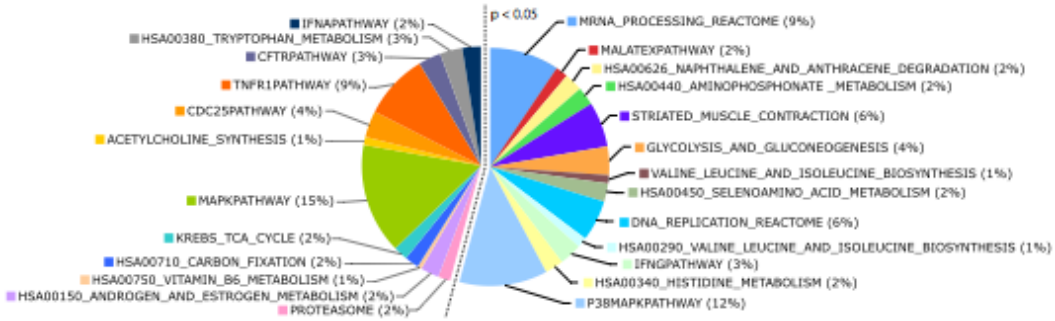

Biological Processes

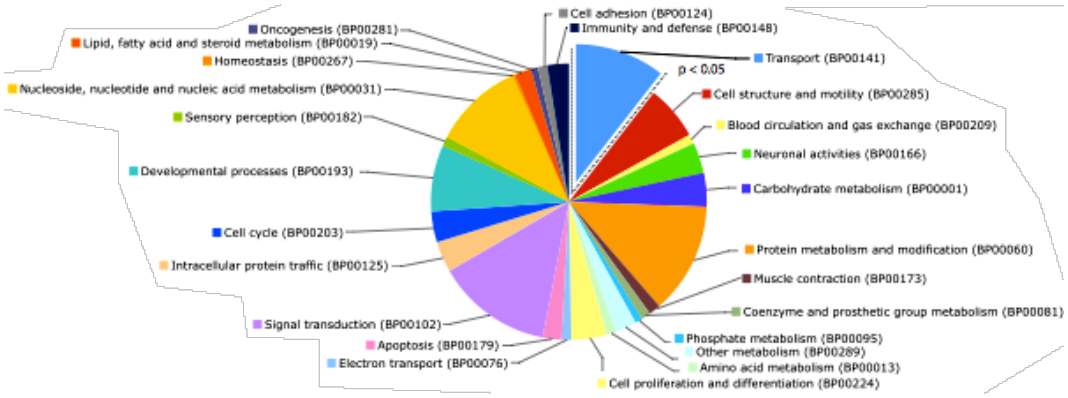

Molecular Functions

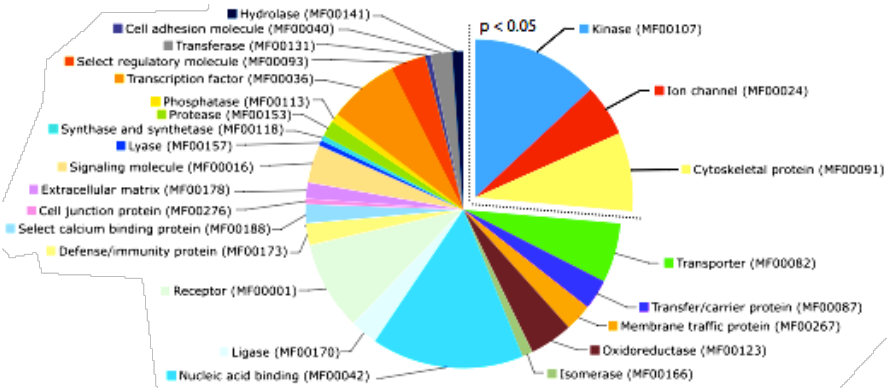

Figure 3. Top 25 molecular functions, biological processes, and pathway associated networks. Top: Pathway-associated networks represented by primary hits (percentage equals fraction of genes within set displayed.). Middle: Biological processes represented by primary hits. Bottom: Molecular functions of primary hits. For each diagram, significantly enriched classes are expanded and enclosed by dotted line.

potential links between previously unassociated processes and selective autophagy.

To identify novel interactions and further characterize our hits, we constructed protein-protein interaction maps within the framework of functional cellular pathways. As shown in Figure 3, Top, and Figure 4, our hits are significantly enriched in pathways related to mRNA processing, actin-myosin-troponin functions, p38-MAPK, and IFN-γ signaling. Many of our hits form peripheral connections with nodes, suggesting that they may act as modifiers for

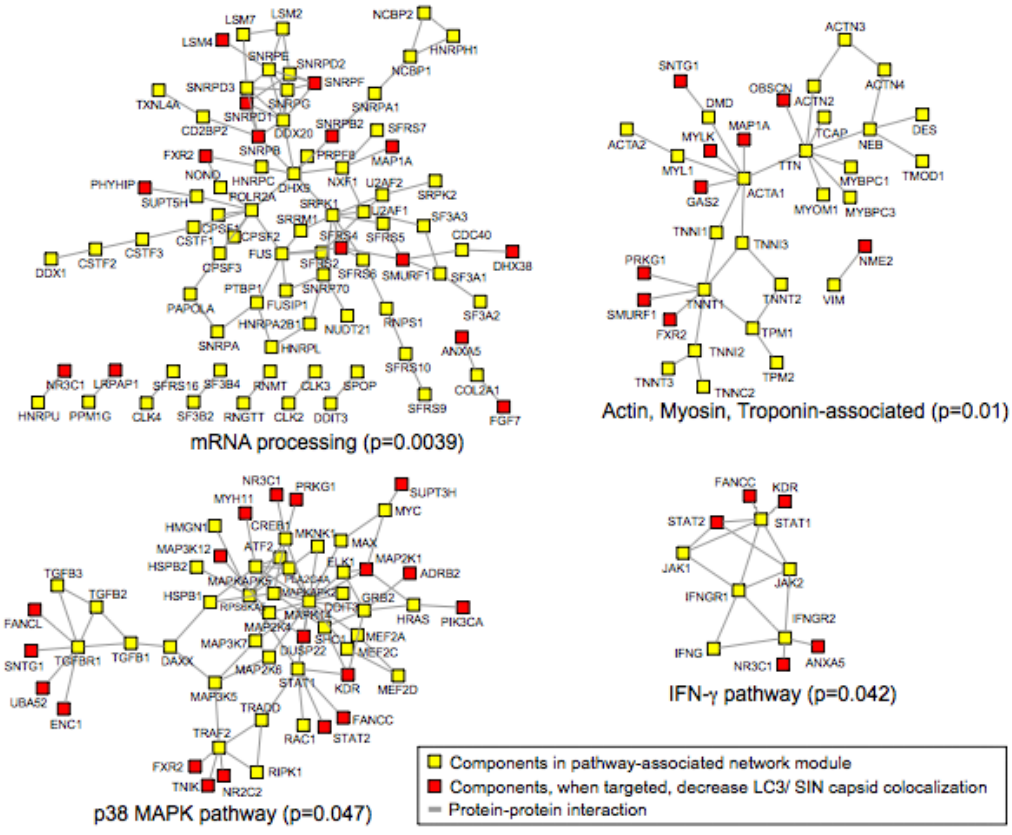

Figure 4. Significantly enriched pathway associated networks. Networks showing interactions within cellular pathways that contain significant enrichment for primary hits (red squares) that decrease colocalization.

these pathways or serve to connect these functions with other cellular processes. Of note, one of our hits, SMURF1, was identified in both mRNA processing, and actin-myosin networks, while a predicted interacting partner, UBA52, interacts with p38 MAPK pathway members (Fig 4). The findings that interaction partners are located within different networks supports the possibility that hits identified in our screen may link processes here-to-fore unassociated with one another, and with autophagic targeting.

Ubiquitination of some proteins and organelles is thought to tag these cytoplasmic components as substrates for autophagic degradation, but only a small number of E3 ligases have been implicated in this process (Kirkin et al., 2009). Interestingly, we identified 6 known and predicted E3 ligases and associated proteins in our screen, and confirmed all 6 in our colocalization screen, and 4 in our cell death screen (Table 4). We found that two of these, SMURF1 (Fig. 5A) and preliminarily RFWD3 (Fig. 5B), interacted with Sindbis capsid in infected cells (Fig. 5). As of this writing, the antibody used to immunoprecipitate RFWD3 was unable to detect RFWD3 on western blot after immunoprecipitation.

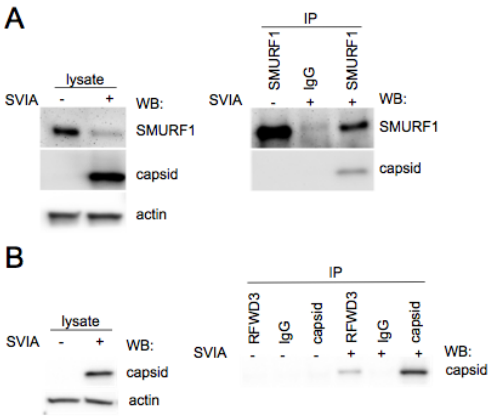

Figure 5. Coimmunoprecipitation of SIN capsid with E3 ligases. Capsid coimmunoprecipitation with SMURF1 (A) and RFWD3 (B) from GFP-LC3 HeLa cells infected with SIN. These experiments have been performed at least twice with similar results.

These two genes scored positive in our secondary cell survival screen, with individual oligos correlating between both assays (Table 4). Interestingly, we did not find ubiquitination of Sindbis capsid after immunoprecipitation and western blot (data not shown). These data are in agreement with our previous findings that ubiquitinated aggregates do not accumulate in neurons in mouse brains infected with Sindbis virus, in the setting of Atg5 inactivation (Orvedahl et al., 2010). It is therefore possible that these E3 ligases interact with and regulate cellular machinery required to target capsid for autophagy, but that capsid may not be a direct target for ubiquitination by E3 ligases.

We reasoned that host cells might possess mechanisms that are dedicated to specifying viral proteins for autophagic targeting, but that some components may also be conserved in other forms of selective autophagy. A well-characterized form of selective autophagy is the clearance of damaged or unneeded mitochondria, or 'mitophagy' (Kim et al., 2007), which is mediated by PINK1-Parkin interactions at damaged mitochondrial membranes (Geisler et al., 2010; Kawajiri et al., 2010; Lee et al., 2010c; Narendra et al., 2008; Narendra et al., 2010). To test whether genes identified in our screen functioned specifically in viral targeting, or if they also functioned as general targeting factors, we assayed for oligos that disrupted Parkin-mediated clearance of CCCP-damaged mitochondria. HeLa cells have been reported to express low levels of endogenous Parkin, and require exogenous expression for complete mitophagic clearance of damaged mitochondria (Narendra et al., 2008). As shown in Figure 6, treatment

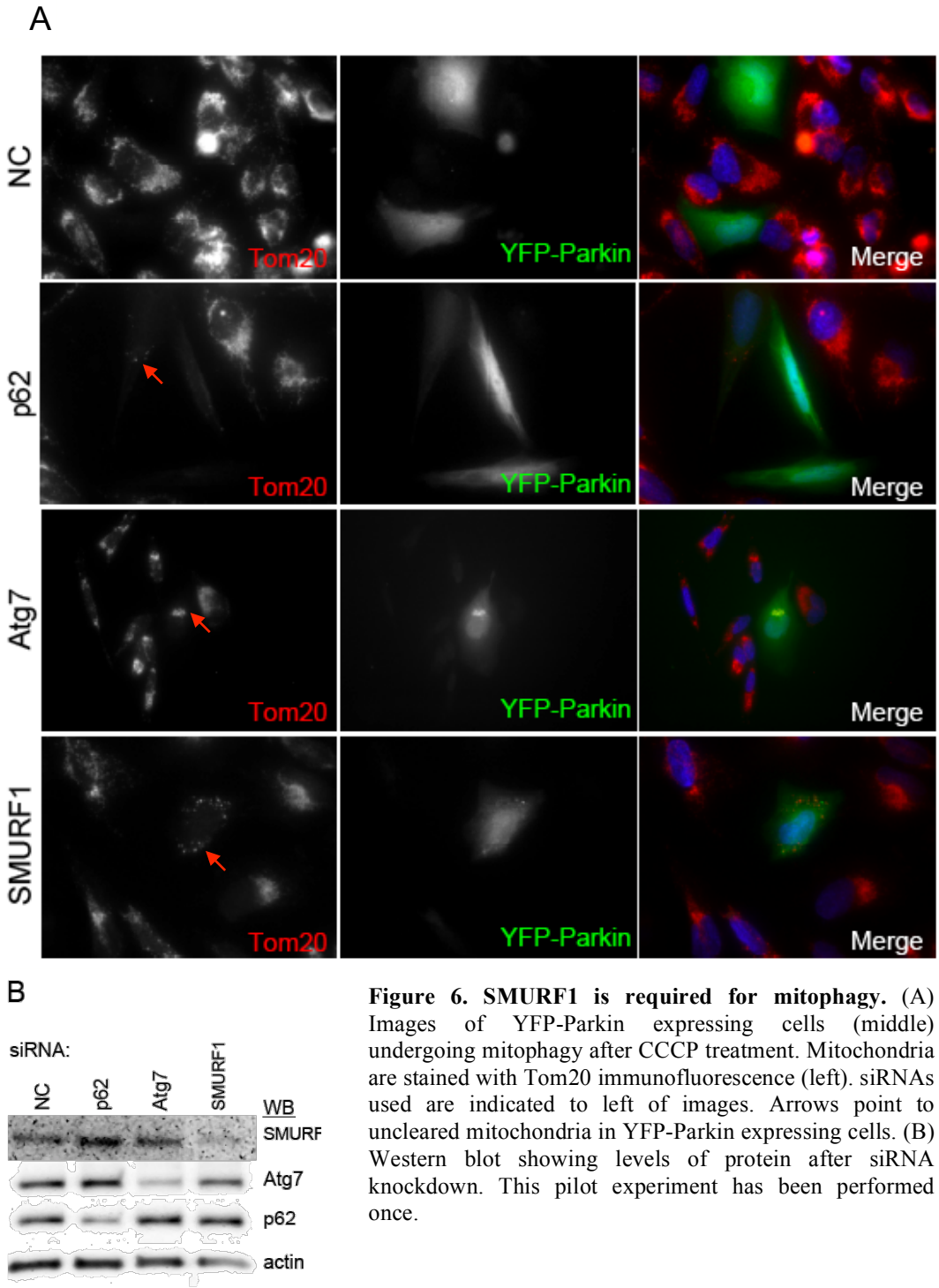

Figure 6. SMURF1 is required for mitophagy. (A) Images of YFP-Parkin expressing cells (middle) undergoing mitophagy after CCCP treatment. Mitochondria are stained with Tom20 immunofluorescence (left). siRNAs used are indicated to left of images. Arrows point to uncleared mitochondria in YFP-Parkin expressing cells. (B) Western blot showing levels of protein after siRNA knockdown. This pilot experiment has been performed once.

with negative control siRNA resulted in complete clearance of mitochondria in YFP-Parkin-expressing cells after 24 hrs CCCP treatment. Knockdown of p62 or Atg7 resulted in partial blockade of mitochondrial clearance (Fig 6A, B). However, knockdown of SMURF1 resulted in a striking defect in YFP-Parkin-mediated mitochondrial clearance (Fig 6A, B). Moreover, mitochondria in SMURF1 siRNA treated cells exhibited more punctate character, and partially colocalized with YFP-Parkin punctae. These findings suggest that host cells may use conserved machinery to target autophagic substrates (at least between viral proteins and mitochondria), and that SMURF1 is a novel component of this machinery.

DISCUSSION

While functions of autophagy in cellular and organismal homeostasis and disease are increasingly being recognized and characterized, the molecular mechanisms of how autophagy substrates are selectively targeted have remained relatively poorly understood. In this study we screened for genes that are required to target Sindbis capsid protein to autophagosomes in infected cells. The genes identified represent diverse functional classes and cellular processes, suggesting that autophagic targeting is complex and highly integral to cellular networks. In this work, we have identified molecules that have not here-to-fore been implicated in autophagy or targeting of substrate to autophagy. These findings provide new

insight and serve as a resource for further investigation into mechanisms of selective autophagy.

Our bioinformatics analysis revealed unexpected processes are involved in targeting SIN capsid to autophagosomes. mRNA processing was highly enriched in our pathway analysis, which could indicate that host RNA binding proteins are also involved in viral genome stability or interactions with the viral nucleocapsid. SIN virus genomes containing encapsidation signals are required for initiation and completion of nucleocapsid formation (Tellinghuisen and Kuhn, 2000). It is unlikely that knockdown of these factors simply results in decreased presence of capsid structures (thus giving a false positive result for decreased colocalization), as we specifically normalized colocalization measurements to account for relative levels of capsid punctae formation. Rather, these findings raise the possibility that the host mRNA processing machinery facilitates normal formation of nucleocapsids, and that knockdown of these factors result improperly formed nucleocapsids that are not recognized by the autophagy targeting machinery. By extension, this raises the possibility that host cells may recognize a fully formed epitope present in the quaternary structure to target SIN capsids to autophagy, in a model similar to HIV capsid recognition and restriction by Trim5-α (Forshey et al., 2005). In contrast to a pro-packaging role of mRNA binding proteins, it is possible that these host proteins recognize a forming viral RNA-capsid intermediate structure, that this interaction facilitates loading of these complexes to the autophagosome, with siRNA knockdown resulting in decreased

colocalization. A third, straightforward, possibility is that mRNA processing factors are required for expression of host specificity determinants for capsid targeting, thus affecting colocalization of capsid with autophagosomes through an indirect route.

SMURF1, an E3 ligase, was identified as a selectivity determinant for Sindbis virus capsid, and preliminary results suggest that it is also involved in autophagic clearance of mitochondria. These findings suggest that overlapping mechanisms exist for specifying substrates for targeting by autophagy. This concept is supported by our previous finding that the autophagy adaptor, p62, which mediates autophagic clearance of host and bacterial substrates (Kirkin et al., 2009), is also involved in capsid targeting (Orvedahl et al., 2010). The indication that SMURF1 may be involved in mitophagy, along with negative findings of capsid ubiquitination, also suggest that SMURF1 may not directly target capsid but may regulate proteins that are generally required for autophagy substrate targeting. SMURF1 was initially identified as an E3 for SMAD proteins (SMAD ubiquitin regulatory factor 1)(Zhu et al., 1999), but has been implicated in diverse cellular processes, including regulation of cytoskeletal dynamics (Bryan et al., 2005; Huang et al., 2009; Sahai et al., 2007; Wang et al., 2003; Yamaguchi et al., 2008). Our findings that screen hits are enriched for the actin-myosin-troponin pathway, the biological process of transport, and molecular functions of the cytoskeleton, point towards and essential role for cytoskeletal dynamics in selective autophagy. Further support for this hypothesis is findings in

yeast (Monastyrska et al., 2009; Reggiori et al., 2005), and mammalian cells (Lee et al., 2010b), that actin cytoskeleton is required for selective autophagy, but not starvation-induced autophagy.

Pathways identified in our screen are in concordance with known signaling pathways that regulate autophagy during immunity. p38 MAPK pathway was significantly enriched, and to date is the molecule identified most proximal to the autophagy machinery in the classical TLR-4 signaling pathway (Xu et al., 2007). While the mechanism of TLR-induced autophagy is not fully known, a recent study suggests that the TLR-4 receptor complex can directly activate Beclin 1 to induce autophagy (Shi and Kehrl, 2010). Another recent finding suggests p38 MAPK regulates starvation-induced and basal autophagy through mAtg9 regulation (Webber and Tooze, 2010). The role of p38 MAPK regulation of mAtg9 during infection remains to be determined, and it should be noted that our colocalization quantification normalized for levels of GFP-LC3 dots. Thus during viral infection, it is possible that p38 MAPK pathways are dispensable for autophagy induction, but may be involved in mediating substrate targeting for autophagy. Another immune pathway previously described in autophagy regulation and xenophagy is the IFN-γ pathway and IFN-γ–inducible GTPases (Al-Zeer et al., 2009; Cadwell et al., 2009; Feng et al., 2009; Gutierrez et al., 2004; Singh et al., 2006; Zhao et al., 2008). While a direct role has not been demonstrated for IFN-γ in autophagy during viral infection, a previous study found that non-cytolytic clearance of SIN from neurons requires IFN-γ signaling,

a process that we have postulated could be mediated by autophagy (Orvedahl and Levine, 2008).

Lastly, we identified Atg13 as a host specificity determinant for targeting SIN capsid to GFP-LC3 punctae. While previous reports demonstrated that Atg13 is required for autophagy induction in complex with ULK1 in mammals (Chan et al., 2009), our findings suggest that Atg13 may further play a role in specifying autophagy substrates for sequestration at the initiation step of autophagosome biogenesis. The study by Chan, et al. demonstrated a function for Atg13 in Atg9 trafficking (Chan et al., 2009), and it is important to note that Atg9 also functions in selective autophagy in yeast (He et al., 2006). Importantly, we did not isolate other known autophagy genes as host selectivity determinants. These negative results support our method for specifically identifying selectivity factors and not general autophagy regulatory factors that may arise as false positives for deceased colocalization by decreasing total number of GFP-LC3 punctae.

In summary, we have developed a novel assay that combines high-content microscopy with siRNA library screening to identify host molecules and pathways that are required for targeting SIN capsid proteins by autophagy. Our screen identified diverse cellular pathways and processes, including those previously linked to autophagy regulation, as well as previously unconnected pathways. Moreover, our study provides novel insight into these processes (such as p38 MAPK and IFN-γ signaling, and cytoskeletal functions) by linking them to selective autophagy of viral proteins. Identification of mRNA processing

pathways represents an as-of-yet uncharacterized pathway for selective autophagy, raising intriguing questions regarding the host autophagy response to RNA viruses and the nature of viral components that are targeted. The molecules identified here should serve as a guide for future studies of selective autophagy in health and disease.

CHAPTER FIVE
General Discussion and Future Directions

GENERAL DISCUSSION

Autophagy has emerged as an integral pathway in maintaining cellular homeostasis and adapting to stress. These functions also extend to the response to infection with diverse pathogens, including viruses. As a counter measure, viruses have evolved to antagonize this host response to promote disease. In the studies presented here we: 1) characterized the role of viral antagonism of autophagy as a virulence mechanism; 2) characterized the role of autophagy in protecting against viral disease; 3) and defined host factors required for host targeting of viral proteins. These studies provide insight into the host response to infection in general and the role of autophagy during this response, and provide molecular clues into how host cells target viruses to autophagy. These findings also raise a number of questions, and provide a foundation for further areas of study.

HSV-1 Evasion of Autophagy in Neurovirulence

A hallmark of essential host immune pathways is the evolution of microbial virulence factors that target these pathways, which is exemplified by the host IFN response (Garcia-Sastre and Biron, 2006). Autophagy has recently emerged as a common nexus for viral virulence factors, though roles for these factors in viral disease are only beginning to be uncovered. Given the multiple

roles of autophagy in protecting against viral infection, it is not surprising that multiple effects are being observed for these virulence factors (discussed below). It is also likely that additional novel functions of autophagy during viral infection may be discovered through the study of viral evasion mechanisms.

We found that antagonism of host autophagy by HSV-1 was essential for its ability to cause fatal encephalitis in mice (Orvedahl et al., 2007). Increased animal survival was associated with decreased CNS inflammation, decreased viral replication, and decreased neuronal death in mouse brains infected with the autophagy inhibition-defective mutant virus. These findings suggest that autophagy may function in a cell autonomous role to prevent HSV-1 growth and promote cellular survival. However, it is possible that autophagy also functions to promote the activation of innate or adaptive immunity during HSV-1 infection. In support of this hypothesis, a recent study has demonstrated that the mutant HSV-1 strain that fails to antagonize Beclin 1-mediated autophagy is also attenuated in its ability to counteract CD4+ T-cell responses in a mouse model of peripheral infection (Leib et al., 2009). Another recent study confirmed the role of viral antagonism of autophagy in viral disease. Though the precise mechanism remains unclear, E, *et al*. demonstrated that γ-HV-68 strains with mutations that render vBcl-2 incapable of antagonizing Beclin 1-mediated autophagy fail to maintain latency in spleens of infected mice (E et al., 2009). The author's suggest that autophagy may function to degrade viral proteins required for latency, promote adaptive or innate immune responses, and/ or other as-of-yet defined functions (E

et al., 2009). Together these studies confirm the essential role of viral antagonism of host autophagy in promoting viral disease, and suggest that viral virulence factors can counteract multiple protective roles of autophagy during viral infection.

Interplay between pathogens and host autophagy is complex, with some indications that viruses and other pathogens can co-opt the autophagy pathway or autophagy machinery to facilitate their replication (See Section I). It is important to note that all *in vivo* reports to date, in studies examining genetic disruption or microbial inactivation of autophagy, including studies presented here, have suggested that autophagy plays an essential anti-viral role (E et al., 2009; Leib et al., 2009; Liu et al., 2005; Orvedahl et al., 2007; Orvedahl et al., 2010; Shelly et al., 2009). However, some viruses that have been suggested to utilize autophagy for their replication, including HCV (Dreux et al., 2009; Tanida et al., 2009) and HIV (Brass et al., 2008; Kyei et al., 2009), lack readily available small rodent or other models. HIV has recently been demonstrated to disrupt autophagy-mediated antigen processing and presentation by dendritic cells *in vitro* (Blanchet et al., 2010). Concomitantly, the autophagy gene *Atg5* was demonstrated to be essential for antigen presentation by dendritic cells *in vivo* (Lee et al., 2010a). As HIV is thought to induce early steps of autophagy, and block later degradative steps, to promote viral yields (at least in macrophages *in vitro*) (Kyei et al., 2009), it is therefore possible that HIV promotes pro-viral aspects of autophagy and antagonizes anti-viral host functions of autophagy (including virion degradation

and adaptive immune activation). The relative contribution of autophagy in HIV (and HCV) infection and pathogenesis *in vivo* await future studies in humanized mice or primate models.

Autophagy in Host Defense Against Viral Infection

While studies with viruses ablated of their autophagy antagonism functions suggested that autophagy protected against infection (discussed above), the role of an endogenous autophagy gene in mammalian antiviral defense remained unclear. Additionally, the precise function(s) of autophagy in mediating anti-viral defense was unknown. Our studies using a model of fatal SIN CNS infection examined the endogenous autophagy gene *Atg5* in neurons *in vivo*, and the autophagy gene *Atg7* and autophagy adaptor p62 *in vitro*, and demonstrated an essential role for autophagy genes in antiviral defense (Orvedahl et al., 2010). Additionally, our results provided a model in which autophagy functions to degrade viral proteins and prevent their cytotoxic accumulation to prevent cell death (Orvedahl et al., 2010).

While we did not observe changes in levels of infectious Sindbis virus after autophagy gene inactivation (Orvedahl et al., 2010), it is possible that autophagic targeting of viral proteins underlies the inhibitory effects of autophagy on viral growth that is observed during other viral infections (HSV-1 in mammals (Orvedahl et al., 2007; Talloczy et al., 2006), VSV in Drosophila (Shelly et al., 2009), and TMV in plants(Liu et al., 2005)). It is possible that excess viral protein

production overwhelms the ability of autophagy to limit SIN replication, but that endogenous autophagy levels sufficiently maintain viral protein clearance at levels compatible with cell survival. Intriguingly, overexpression of the autophagy gene *Beclin 1* in Sindbis virus infected neurons does result in decreased viral growth (as well as increased neuronal survival), suggesting that endogenous autophagy levels may be enhanced in this system (Liang et al., 1998), and raise the exciting possibility that therapeutic upregulation of autophagy may also potentiate antiviral effects. It has been shown that p62-mediated autophagy of ubiquitinated proteins delivers them to lysosomes to generate anti-mycobacterial ubiquitin fragments (Alonso et al., 2007; Ponpuak et al., 2010). It is presently unknown whether autophagy and p62-mediated targeting of host proteins also functions in antiviral defense. Likewise, it is unknown is selective processes or adaptors are involved in autophagy of viral proteins and nucleic acids for adaptive (Lee et al., 2010a; Munz, 2010) and innate (Lee et al., 2007) immune activation, or if non-selective autophagy in infected cells loads compartments containing these receptors with their cognate ligands.

We found that autophagy prevented SIN antigen clearance, and the autophagy adaptor p62 interacted with Sindbis virus capsid protein to facilitate its removal *in vitro*. Mutations in p62 are associated with both inherited and sporadic forms of the Paget's disease of the bone, which is characterized by osteolytic bone lesions and bone fragility (Helfrich and Hocking, 2008; Ralston et al., 2008). As p62 functions as a signaling adaptor in inflammatory pathways (Moscat et al.,

2007), one model is that p62 mutations underly pathogenesis of Paget's disease by disregulating signaling through the RANK/ NF-κB axis and hyperactivation of osteoclasts (Layfield and Shaw, 2007). However, NF-κB signaling may not fully account for p62 mutations in Paget's, as overexpression of p62 mutants is not sufficient to activate NF-κB (Helfrich and Hocking, 2008), and environmental triggers (including viral infection) are thought to account for the incomplete penetrance of inherited mutations (Ralston et al., 2008). A role for protein quality control through p62-mediated autophagy is supported by observations of aggregate accumulation in cells from Paget's diseases patients, which have been postulated to be viral nucleocapsids (Helfrich and Hocking, 2008). The link between viral infection and p62 mutations as an etiology to Paget's (though controversial (Mee, 1999; Ralston and Helfrich, 1999)) is tantalizing given our findings that p62 mediates autophagic degradation of viral capsid protein. Indeed, mutations in another autophagy related gene, VCP/p97, underlie a related disorder of inclusion body myopathy, Paget disease of bone, and frontotemporal dementia (IBMPFD) (Ju et al., 2009; Tresse et al., 2010). Although the multisystem disorder IBMPFD is not thought to be of viral origin, these findings underscore a role for defective autophagy in development of Paget's disease. While a first observation of autophagosomes and viral infection occurred with HSV-1 (Smith and de Harven, 1978), an earlier report suggested that autophagosome isolation membranes might target measles virus inclusions in infected cells after disassembly (Raine et al., 1969). Together these findings raise the as-of-yet

untested possibility that p62-mediated autophagy may protect against paramyxovirus infection, and that mutations in p62 may increase susceptibility to infection and osteoclast disregulation in Paget's disease.

We observed that disruption of Atg5 in mouse brain neurons or p62 knockdown *in vitro* resulted in increased SIN-induced cell death. The associated accumulation of viral antigen and SIN capsid suggests that viral protein accumulation may be toxic to infected cells, and that an important function of autophagy is to promote cell survival by limiting accumulation. However, the precise role of viral protein accumulation and mechanisms of cell death in this context has not been defined. In other protein aggregopathies, that autophagy has been implicated in protecting against, the mechanism of cell death is currently a subject of intense investigation (Martinez-Vicente and Cuervo, 2007). In these settings, it is thought that disruption or gain of function of the endogenous aggregating proteins, or interference with normal cellular functioning may underlie cellular degeneration (Kubota, 2009). The precise cytotoxic form of mutant proteins (soluble monomers, aggregating oligomers, and/or large intracellular aggregate inclusions) remains unclear, but mounting evidence suggests that oligomeric forms may be toxic, while large aggregates may actually serve a cytoprotective function (Mizushima and Klionsky, 2007). The precise forms of viral proteins that may underlie cytotoxicity, and molecular mechanism of cell death during accumulation, also remain unclear, but their elucidation may

provide further insight into mechanisms of targeting by autophagy, and cytoprotective roles of autophagy during infection.

Host Mechanisms of Targeting Viral Proteins by Autophagy

In recent years, our studies, and others, have provided insight into the roles of autophagy in protecting against viral infection, and mechanisms of viral invasion in viral pathogenesis, yet the precise cellular and molecular mechanisms of targeting viruses to the autophagy pathway have remained unclear. Using an unbiased siRNA screen to interrogate the human genome for factors involved in viral targeting, we discovered the involvement of novel pathways and molecules in selective autophagy. These findings generate testable hypotheses of how cells orchestrate autophagic targeting of substrates, and help explain and confirm previous studies on selective autophagy.

The role of cytoskeleton in mediating SIN capsid targeting was suggested through bioinformatics analysis, and supported by functional studies with a candidate protein SMURF1. As mentioned, SMURF1 degrades RhoA to spatially direct actin cytoskeleton arrangements during dynamic cellular reorganization events (Bryan et al., 2005; Wang et al., 2003). While a role for Rho-mediated cytoskeleton reorganization in autophagy is unclear, a recent study suggest that autophagy, and the p62 ortholog Ref(2)P, in Drosophila cells (and mouse macrophages) is required for cell motility through regulation of Rho1 activity (Kadandale et al., 2010). A previous study linking Rho with selective autophagy

determined that inhibitors or siRNA knockdown of Rho kinases ROCK1 and ROCK2, which are effectors of Rho GTPases that modulate cytoskeleton dynamics, resulted in decrease huntingtin accumulation and associated toxicity (Bauer et al., 2009). Likewise, LC3 interacts with and inhibits a Rho GEF (responsible for Rho activation), AKAP-Lbc (Baisamy et al., 2009). Thus, evidence to date suggests that autophagy and autophagy proteins function inversely with Rho GTPase functions (in that they coordinately regulate the other). It is attractive to hypothesize that SMURF1 may be a central mediator of autophagic regulation of Rho GTPases these events. A potential model for this activity in selective autophagy is that SMURF1 interactions with autophagy substrates (and LC3 on the isolation membrane) inactivate Rho GTPases locally, and that Rho-mediated cytoskeletal rearrangements may drive autophagosome expansion and sequestration in regions surrounding substrate (Fig 1). In support of this model, multiple Rho regulatory molecules were identified in our screen for

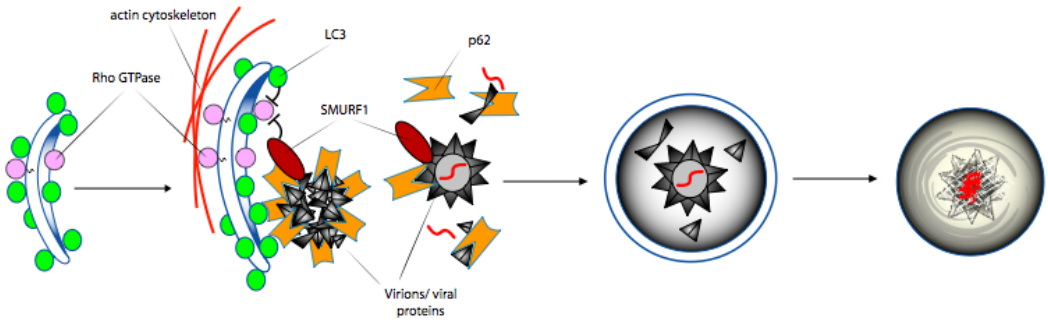

Figure 1. Hypothetical model of SMURF1 activity in selective autophagy. SMURF1 interacts with autophagy substrates and p62 (as reported (Barrios-Rodiles et al., 2005)). Asymmetric inactivation of Rho GTPase at the isolation membrane results in cytoskeletal rearrangements at the opposing surface, providing mechanical force for isolation membrane expansion and substrate engulfment.

specificity determinants: OBSCN, functions as a Rho GEF (Coisy-Quivy et al., 2009); DAAM2, mediates WNT-induced Rho activity (Nakaya et al., 2004); FAM13B, is a predicted RhoGAP; and GMIP, encodes a member of the ARHGAP family of Rho GTPase activating proteins (Aresta et al., 2002). Indeed, recent attention has focused on the exquisite spatiotemporal regulation surrounding Rho GTPases (Pertz, 2010). Additionally, many microbial virulence factors target Rho GTPases, positively or negatively (Shames et al., 2009), such that either activity may disrupt coordinated action during selective autophagosome biogenesis. This model, and the role of Rho in selective autophagy, awaits detailed experimentation.

FUTURE DIRECTIONS

Mechanism of ICP34.5 Inhibition of Beclin-mediated Autophagy

While we demonstrated that a region of ICP34.5 that is required for Beclin 1 binding and autophagy inhibition is also required for HSV-1 neurovirulence, it remains unclear how this interaction functions to inhibit the function of Beclin 1 in autophagy induction. Recent studies are defining a growing list of interaction partners for Beclin 1 (He and Levine, 2010), and detailed characterization of these factors during ICP34.5 expression and HSV-1 infection may provide insight into it's mechanism of action. Another recent study suggested that a region partially overlapping with the Beclin 1 binding region (68-87) of ICP34.5 is required to disrupt TBK1 interactions with IRF3 to dampen innate immune signaling

(Verpooten et al., 2009). However, infection of IRF3 knockout mice does not rescue neurovirulence of the Δ68-87 mutant HSV-1 virus, suggesting that functions of this region separate from IRF3 antagonism are important for 34.5-mediated neurovirulence (Leib et al., 2009). It will be interesting to determine if TBK1 also function in autophagy regulation, and if 34.5 targets a Beclin 1 complex containing TBK1 or other innate signaling molecules. As PKR knockout mice restore the neurovirulence of the Δ68-87 mutant virus (Orvedahl et al., 2007), it will be important to determine if neurovirulence of the mutant virus is restored in neuronal-specific Atg gene knockout mice. Preliminary data suggests an incomplete, but statistically significant restoration of the virulence in the mutant mice with neuronal deletion of Atg5 (Fig. 2). Only mice homozygous for *Atg5*$^{flox/flox}$ allele with the *nestin*-cre allele exhibited mortality (Fig. 2), and no mortality was observed with any genotype in mock infected mice (data not shown). It is possible that developmental compensation occurs in these tissue specific knockout mice, and virally-mediated gene excision or possibly neuron-specific Beclin 1 knockout mice may demonstrate more pronounced rescue of the mutant virus.

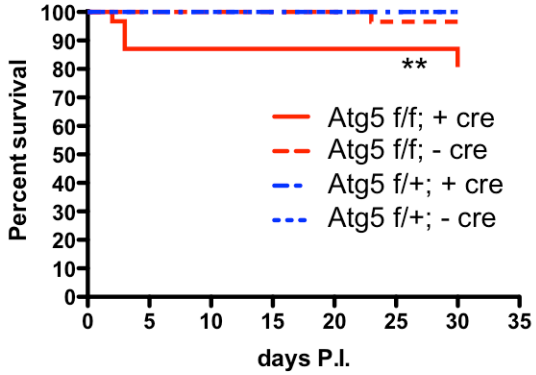

Figure 2. Partial restoration of neurovirulence of HSV-1Δ68-87 in *nestin*-cre; *Atg5*$^{flox/flox}$ mice. Survival of mice homozygous or heterozygous for *Atg5*$^{flox/flox}$ (f/f or f/+ respectively) and with or with out *nestin*-cre (+ or - , respectively), injected intracranially with HSV-1Δ68-87. **, $p < 0.005$. Number of infected mice is indicated in parentheses. This experiment was performed with at least 10 litters.

Mechanisms and Functions of Autophagic Targeting of Viral Proteins

We identified a potential mechanism of protection against Sindbis virus CNS disease – autophagic degradation of viral proteins – and generated a map of cellular networks that may orchestrate this response. However, a number of key questions remain, including: i) what form of viral nucleocapsids are targeted by autophagy (soluble monomers, forming nucleocapsid intermediates, fully formed nucleocapsids, or other mis-folded aggregates); ii) what is the mechanism of cytotoxicity during viral protein accumulation; iii) do pathways and functions identified in our screen act in a coordinated fashion or in parallel to facilitate capsid targeting; iv) what are the precise molecular events that govern isolation membrane initiation at the site of substrate sequestration during selective autophagy. The answers to these questions should provide further insight into functions of autophagy in protein quality control and potentially autophagosome biogenesis.

Sindbis virus nucleocapsids can be reconstituted *in vitro* from purified capsid monomers in the presence of viral genomes (Tellinghuisen et al., 1999), providing a system to address the structural determinants of autophagic targeting. We have shown that p62, SMURF1, and RFWD3 interact with capsid in infected cells, but an unanswered question is whether these host factors directly bind to capsid, or interact indirectly. In vitro pulldown experiments with soluble monomers, fully formed nucleocapsid, or intermediates (Tellinghuisen and Kuhn,

2000), would address the questions of direct interactions and the form of capsid targeted by these factors. It should be noted that intact virions can be detected in autophagosomes in infected cells, as well as the appearance of protein aggregates, suggesting that multiple forms of capsid may be targeted (Section III, Fig. 3) Additionally, *in vitro* ubiquitination assays are well established, which would address the outstanding question of whether SMURF1 and/ or RFWD3 ubiquitinate capsid, and if p62 binds capsid via this modification or through another mechanism. An alternative approach to address p62 interactions with capsid would be to perform structure function experiments with p62 deletion mutants in domains with known functions, such as its UBA (ubiquitin binding domain) (Seibenhener et al., 2004), PB1 (oligomerization domain) (Wilson et al., 2003), LIR (LC3 interacting region) (Ichimura et al., 2008; Pankiv et al., 2007), and Alfy interaction regions (Clausen et al., 2010). Requirement of the UBA domain, which binds ubiquitinated substrates, would also provide clues to the ubiquitination status of SIN capsid.

We found potentially pathways are involved in targeting virus capsid to autophagosomes, suggesting that these pathways may function together to coordinate substrate targeting. For example, p38 MAPK signaling may regulate substrate recognition by phosphorylating substrates or regulating targeting determinants. Experiments using p38 MAPK inhibitors or *in vitro* kinase assays to assess phosphorylation status of autophagy substrates may address these possibilities. Alternatively, many signaling pathways, including innate immune

signaling, are regulated with ubiquitinated chains serving as scaffolds. Determination of p38 MAPK activation status with siRNA knockdown for SMURF1 and other E3 ligase hits may address whether these proteins function upstream of p38 MAPK signaling.

It is unknown how capsid accumulation leads to death of infected cells. Our secondary screen found that many factors that are required for colocalization also function to promote cell survival during SIN infection. It is possible that some of these factors function in parallel with capsid targeting to promote other cell survival strategies, and detailed characterization of our screen hits may reveal these functions. For example, p62 has recently been identified as a regulator of the oxidative stress response by activation of stress-related transcriptional responses (Fan et al., 2010; Jain et al., 2010; Komatsu et al., 2010; Lau et al., 2010). As we only screened our confirmation library for cell survival factors (to confirm their function in capsid targeting), comparison of our screen results with genome wide cell survival screens may reveal host factors that are dispensable for capsid targeting (ie. not found in our genome wide screen), but function downstream of capsid targeting to promote cell survival. One scenario would be genes that are required for recycling of lysosomes after autophagic targeting of capsid, or lysosomal permeases that generate essential breakdown products that are required to promote survival.

We presented a speculative model of SMURF1 activity in specifying capsid (and mitochondrial) targeting by autophagy, by spatiotemporal regulation

of Rho GTPase. Studies to address this model would include overexpression studies of dominant active, dominant negative, or ubiquitination insensitive mutants of Rho GTPases (Ozdamar et al., 2005; Wang et al., 2006). In the model presented in Fig. 1, if spatial regulation of Rho GTPase is involved in orienting autophagosome sequestration towards substrates, global activation or ubiquitination insensitive mutants may disrupt polarization of the isolation membrane, resulting in non-selective autophagosome formation. Likewise, dominant negative forms of Rho GTPase may result in failure of selective autophagosome formation, but may have no effect on non-selective autophagy. Assaying for mitophagy, SIN capsid degradation, and other forms of selective autophagy with these constructs would provide mechanistic support for these findings. Another aspect of this model requiring investigation would be the cellular localization of Rho GTPases and the actin cytoskeleton at the initiation step and during isolation membrane formation and expansion during non-selective and selective autophagy. Detailed localization experiments with autophagy proteins known to involved in these steps may address this question. Fine structure immuno-EM studies of isolation membranes revealing Rho GTPase on the outer surface and SMURF1 or other targeting determinants on the inner face would further support this model. An alternative model for cytoskeletal involvement during selective autophagy would be the trafficking of vesicles or isolation membranes to substrates (or substrates to isolation membranes), or in the formation and/ or disassembly of aggresomes to regulate substrate availability for

sequestration. These possibilities could be addressed by live-cell imaging with markers of isolation membranes (ie. GFP-Atg5) and tagged substrates, with siRNA knockdown of SMURF1 or other targeting determinants.

We found that the targeting determinant SMURF1 was involved in both capsid targeting and mitochondrial targeting. An important area of further exploration will be the requirement of these targeting factors in the host response to other viruses, including those for which autophagy has been suggested to protect against (HSV-1 (Orvedahl et al., 2007), TMV (Liu et al., 2005), and VSV (Shelly et al., 2009)). Paramyxoviruses may be another family of viruses that are likely to be targets for autophagy, given the links discussed above between this family of viruses, p62, and Paget's disease of the bone. Further evidence for an involvement of autophagy during measles virus infection is provided by the finding that measles virus binding to the cell surface receptor CD86 activates autophagy through the adaptor GOPC that binds Beclin 1 (Joubert et al., 2009). It is interesting to note that one of our targeting determinants identified in our screen, CSPG5, is an interacting partner of GOPC (Hassel et al., 2003). Thus, the role of autophagy and targeting determinants in measles virus infection remains and attractive area for future investigations. Selective autophagy of viral proteins provides an advantage to the host that the molecules parasitized by viruses during replication and structural protein synthesis can be reclaimed. Likewise, this function provides evolutionary pressure for the emergence of viral mechanisms to evade targeting. It will be interesting to determine if viruses (and other) possess

mechanisms to specifically evade selective autophagy, while maintaining or increasing non-selective autophagy (given the importance of autophagy in normal cellular homeostasis).

In summary, our findings have helped define important host pathogen interactions in the evolutionary battle for survival. Viruses evade autophagy to promote disease, and the host deploys the autophagy machinery to degrade viral proteins and maintain survival. Future studies will undoubtedly reveal more complex interactions between microbes and the host autophagy pathway, and these studies will surely provide insight into the functions of autophagy during infection and during normal cellular homeostasis. Through these studies the development of small molecules that regulate both non-selective and selective autophagy and compounds that counteract microbial evasion strategies should provide clinical tools in the fight against infectious diseases.

Appendix A

Table 1. Primary Hits that Decrease Colocalization

Gene_Symbol	Locus_ID	Accession
AKR1CL2	83592	NM_031436
CA7	766	NM_005182
CCDC36	339834	NM_178173
FABP1	2168	NM_001443
GNE	10020	NM_005476
MDH1	4190	NM_005917
NADSYN1	55191	NM_018161
PDK1	5163	NM_002610
PDK4	5166	NM_002612
PFKP	5214	NM_002627
PGK2	5232	NM_138733
PNPO	55163	NM_018129
COX6B1	1340	NM_001863
COX8A	1351	NM_004074
MRPS10	55173	NM_018141
MRPS2	51116	NM_016034
NDUFA4L2	56901	NM_020142
NDUFB9	4715	NM_005005
ADRB2	154	NM_000024
BMP2KL	347359	XM_293293
BOC	91653	NM_033254
C20ORF12	55184	NM_018152
C5	727	NM_001735
C7orf68	29923	NM_013332
CD163L1	283316	NM_174941
CXCR7	57007	NM_020311
DKKL1	27120	NM_014419
DUSP22	56940	NM_020185
EIF2AK1	27102	NM_014413
FAM13B	51306	NM_016603
FCGR3B	2215	NM_000570
FGF14	2259	NM_004115
FGF7	2252	NM_002009
GDF5	8200	NM_000557
GPR81	27198	NM_032554
HBP17	9982	NM_005130
IL13RA1	3597	NM_001560
IPPK	64768	NM_022755
KDR	3791	NM_002253
MAP2K1	5604	NM_002755
MAP3K12	7786	NM_006301
MS4A4A	51338	NM_024021
MSTN	2660	NM_005259
NR2C2	7182	NM_003298
PI4K2A	55361	NM_018425
PIK3CA	5290	NM_006218
REEP2	51308	NM_016606

RGS17	26575	NM_012419
SFRP4	6424	NM_003014
STAT2	6773	NM_005419
TREM1	54210	NM_018643
LRPAP1	4043	NM_002337
REP15	387849	XM_370686
RIMS3	9783	NM_014747
SCRN1	9805	NM_014766
TXLNA	200081	NM_175852
ANXA5	308	NM_001154
CALCB	797	NM_000728
CAPS	828	NM_004058
CETN1	1068	NM_004066
P2RX5	5026	NM_002561
P2RY4	5030	NM_002565
TRPC5	7224	NM_012471
PLOD2	5352	NM_000935
ALKBH5	54890	NM_017758
CDK2AP1	8099	NM_004642
CHAF1B	8208	NM_005441
CRNKL1	51340	NM_016652
DPF3	8110	NM_012074
FANCC	2176	NM_000136
FANCF	2188	NM_022725
HIST1H3H	8357	NM_003536
HSF2BP	11077	NM_007031
MBD5	55777	NM_018328
MLLT3	4300	NM_004529
NME2	4831	NM_002512
NR3C1	2908	NM_000176
NTHL1	4913	NM_002528
SATB1	6304	NM_002971
SUPT3H	8464	NM_003599
TEAD4	7004	NM_003213
ZNF189	7743	NM_003452
ZNF593	51042	NM_015871
ZNF681	148213	NM_138286
C15ORF12	55272	NM_018285
DHX38	9785	NM_014003
LSM4	25804	NM_012321
RBM18	92400	NM_033117
SFRS4	6429	NM_005626
SNRPB	6628	NM_003091
SNRPB2	6629	NM_003092
SNRPD1	6632	NM_006938
SNRPF	6636	NM_003095
ZCCHC17	51538	NM_016505
BET1	10282	NM_005868
CHST3	9469	NM_004273
CLINT1	9685	NM_014666
CSPG5	10675	NM_006574
PRKD2	25865	NM_016457

STOM	2040	NM_004099
STX10	8677	NM_003765
TBC1D5	9779	NM_014744
KIAA0174	9798	NM_014761
YIPF1	54432	NM_018982
ZFYVE16	9765	NM_014733
BLOC1S1	2647	NM_001487
CLVS1	157807	NM_173519
NAGA	4668	NM_000262
PEX13	5194	NM_002618
PEX3	8504	NM_003630
PHYHIP	9796	NM_014759
ACTRT1	139741	NM_138289
C1QR1	22918	NM_012072
DAAM2	23500	NM_015345
ENC1	8507	NM_003633
GAS2	2620	NM_005256
GMIP	51291	NM_016573
KRT15	3866	NM_002275
KRT6A	140446	NM_058242
KRT73	319101	NM_175068
LAK	80216	NM_025144
MAP1A	4130	NM_002373
MTSS1	9788	NM_014751
MYOM1	8736	NM_003803
NEF3	4741	NM_005382
NF2	4771	NM_000268
NTN4	59277	NM_021229
OBSCN	57729	XM_290923
PRKG1	5592	NM_006258
SNTG1	54212	NM_018967
TNIK	23043	XM_039796
ATG13	9776	NM_014741
EIF2S1	1965	NM_004094
FXR2	9513	NM_004860
ITPKC	80271	NM_025194
NUP93	9688	NM_014669
ASB2	51676	NM_016150
FANCL	55120	NM_018062
MEX3C	51320	NM_016626
RFWD3	55159	NM_018124
SMURF1	57154	NM_020429
UBA52	7311	NM_003333
HPR	3250	NM_020995
KRCC1	51315	NM_016618
PPY	5539	NM_002722
SERPINB10	5273	NM_005024
C14ORF104	55172	NM_018139
MYH11	4629	NM_002474
MYLK	4638	NM_005965
MYLK3	91807	NM_182493
ACIN1	22985	NM_014977

CNOT7	29883	NM_013354
GPC1	2817	NM_002081
HEATR6	63897	NM_022070
C11orf41	25758	XM_039515
C1orf210	149466	NM_182517
C1orf223	374973	XM_371248
C3orf72	401089	XM_376269
C8orf59	401466	XM_376783
CHCHD8	51287	NM_016565
FAM131B	9715	NM_014690
FAM176B	55194	NM_018166
FLJ25363	401082	XM_376257
KIAA0232	9778	XM_291106
LARP1B	55132	NM_018078
LENG9	94059	NM_198988
LMCD1	29995	NM_014583
LOC729698	729698	XM_377887
NLRP14	338323	NM_176822
RCTPI1	729708	XM_371261
STK32A	202374	NM_145001
TMEM203	94107	NM_053045
TMEM39A	55254	NM_018266
TMEM39B	55116	NM_018056
ADAMTS7	11173	NM_014272
HAPLN1	1404	NM_001884
CLDN7	1366	NM_001307
ATP1B1	481	NM_001677
CPA3	1359	NM_001870
GABRA5	2558	NM_000810
KCNAB2	8514	NM_003636
KCNH3	23416	NM_012284
KCNK3	3777	NM_002246
KCNQ1	3784	NM_000218
SCN1A	6323	NM_006920
SLC1A3	6507	NM_004172
SLC1A4	6509	NM_003038
SLC22A3	6581	NM_021977
SLC25A19	60386	NM_021734
SLC25A36	55186	NM_018155
SLC35B3	51000	NM_015948
SLC35C1	55343	NM_018389
SLC37A4	2542	NM_001467
SLC6A1	6529	NM_003042
SLCO1A2	6579	NM_005075

Table 2. Primary hit that increase colocalization

Gene_Symbol	Locus_ID	Accession
AMY1A	276	NM_004038
DPM3	54344	NM_018973

EIF5	1983	NM_001969
ELL2	22936	NM_012081
ENSA	2029	NM_004436
HSPC152	51504	NM_016404
IFNB1	3456	NM_002176
INPPL1	3636	NM_001567
MYO3B	140469	NM_138995
SARA1	56681	NM_020150
SRP19	6728	NM_003135
STRN	6801	NM_003162
ZNF239	8187	NM_005674

Table 3. Confirmation screen for factors that decrease colocalization.

id	# oligos with pv 0.05	Gene_Symbol	Accession
22985	4	ACIN1	NM_014977
54890	4	ALKBH5	NM_017758
347359	4	BMP2KL	XM_293293
55172	4	C14ORF104	NM_018139
149466	4	C1orf210	NM_182517
339834	4	CCDC36	NM_178173
1359	4	CPA3	NM_001870
10675	4	CSPG5	NM_006574
27120	4	DKKL1	NM_014419
9715	4	FAM131B	NM_014690
2188	4	FANCF	NM_022725
8514	4	KCNAB2	NM_003636
29995	4	LMCD1	NM_014583
25804	4	LSM4	NM_012321
55777	4	MBD5	NM_018328
4190	4	MDH1	NM_005917
55173	4	MRPS10	NM_018141
8736	4	MYOM1	NM_003803
9688	4	NUP93	NM_014669
5166	4	PDK4	NM_002612
25865	4	PRKD2	NM_016457
51308	4	REEP2	NM_016606
55159	4	RFWD3	NM_018124
6424	4	SFRP4	NM_003014
6628	4	SNRPB	NM_003091
6636	4	SNRPF	NM_003095
202374	4	STK32A	NM_145001
11173	3	ADAMTS7	NM_014272
83592	3	AKR1CL2	NM_031436
308	3	ANXA5	NM_001154
51676	3	ASB2	NM_016150
481	3	ATP1B1	NM_001677
91653	3	BOC	NM_033254

25758	3	C11orf41	XM_039515
55272	3	C15ORF12	NM_018285
727	3	C5	NM_001735
401466	3	C8orf59	XM_376783
2176	3	FANCC	NM_000136
2259	3	FGF14	NM_004115
2558	3	GABRA5	NM_000810
27198	3	GPR81	NM_032554
63897	3	HEATR6	NM_022070
8357	3	HIST1H3H	NM_003536
64768	3	IPPK	NM_022755
3791	3	KDR	NM_002253
3853	3	KRT6A	NM_058242
80216	3	LAK	NM_025144
4130	3	MAP1A	NM_002373
5604	3	MAP2K1	NM_002755
7786	3	MAP3K12	NM_006301
4300	3	MLLT3	NM_004529
51116	3	MRPS2	NM_016034
2660	3	MSTN	NM_005259
4638	3	MYLK	NM_005965
91807	3	MYLK3	NM_182493
4715	3	NDUFB9	NM_005005
4741	3	NEF3	NM_005382
4771	3	NF2	NM_000268
84033	3	OBSCN	XM_290923
9796	3	PHYHIP	NM_014759
5539	3	PPY	NM_002722
6304	3	SATB1	NM_002971
5273	3	SERPINB10	NM_005024
6509	3	SLC1A4	NM_003038
60386	3	SLC25A19	NM_021734
55186	3	SLC25A36	NM_018155
51000	3	SLC35B3	NM_015948
55343	3	SLC35C1	NM_018389
2542	3	SLC37A4	NM_001467
6629	3	SNRPB2	NM_003092
6632	3	SNRPD1	NM_006938
6773	3	STAT2	NM_005419
8677	3	STX10	NM_003765
8464	3	SUPT3H	NM_003599
55116	3	TMEM39B	NM_018056
7224	3	TRPC5	NM_012471
148213	3	ZNF681	NM_138286
139741	2	ACTRT1	NM_138289
9776	2	ATG13	NM_014741
10282	2	BET1	NM_005868
374973	2	C1orf223	XM_371248
22918	2	C1QR1	NM_012072
401089	2	C3orf72	XM_376269
29923	2	C7orf68	NM_013332
766	2	CA7	NM_005182

828	2	CAPS	NM_004058
283316	2	CD163L1	NM_174941
1068	2	CETN1	NM_004066
51287	2	CHCHD8	NM_016565
9469	2	CHST3	NM_004273
1366	2	CLDN7	NM_001307
9685	2	CLINT1	NM_014666
51340	2	CRNKL1	NM_016652
23500	2	DAAM2	NM_015345
8110	2	DPF3	NM_012074
27102	2	EIF2AK1	NM_014413
8507	2	ENC1	NM_003633
51306	2	FAM13B	NM_016603
55120	2	FANCL	NM_018062
2252	2	FGF7	NM_002009
401082	2	FLJ25363	XM_376257
9513	2	FXR2	NM_004860
2620	2	GAS2	NM_005256
8200	2	GDF5	NM_000557
1404	2	HAPLN1	NM_001884
9982	2	HBP17	NM_005130
11077	2	HSF2BP	NM_007031
3597	2	IL13RA1	NM_001560
3777	2	KCNK3	NM_002246
3784	2	KCNQ1	NM_000218
51315	2	KRCC1	NM_016618
319101	2	KRT73	NM_175068
55132	2	LARP1B	NM_018078
729698	2	LOC729698	XM_377887
51320	2	MEX3C	NM_016626
55191	2	NADSYN1	NM_018161
7182	2	NR2C2	NM_003298
4913	2	NTHL1	NM_002528
59277	2	NTN4	NM_021229
5026	2	P2RX5	NM_002561
5194	2	PEX13	NM_002618
8504	2	PEX3	NM_003630
5214	2	PFKP	NM_002627
5232	2	PGK2	NM_138733
55361	2	PI4K2A	NM_018425
55163	2	PNPO	NM_018129
5592	2	PRKG1	NM_006258
387849	2	REP15	XM_370686
9783	2	RIMS3	NM_014747
6429	2	SFRS4	NM_005626
6507	2	SLC1A3	NM_004172
57154	2	SMURF1	NM_020429
2040	2	STOM	NM_004099
94107	2	TMEM203	NM_053045
23043	2	TNIK	XM_039796
200081	2	TXLNA	NM_175852
7311	2	UBA52	NM_003333

54432	2	YIPF1	NM_018982
51538	2	ZCCHC17	NM_016505
9765	2	ZFYVE16	NM_014733
51042	2	ZNF593	NM_015871
154	1	ADRB2	NM_000024
55184	1	C20ORF12	NM_018152
8099	1	CDK2AP1	NM_004642
8208	1	CHAF1B	NM_005441
157807	1	CLVS1	NM_173519
29883	1	CNOT7	NM_013354
1340	1	COX6B1	NM_001863
9785	1	DHX38	NM_014003
55194	1	FAM176B	NM_018166
2215	1	FCGR3B	NM_000570
51291	1	GMIP	NM_016573
10020	1	GNE	NM_005476
2817	1	GPC1	NM_002081
3250	1	HPR	NM_020995
80271	1	ITPKC	NM_025194
9798	1	KIAA0174	NM_014761
3866	1	KRT15	NM_002275
94059	1	LENG9	NM_198988
4043	1	LRPAP1	NM_002337
51338	1	MS4A4A	NM_024021
9788	1	MTSS1	NM_014751
56901	1	NDUFA4L2	NM_020142
338323	1	NLRP14	NM_176822
4831	1	NME2	NM_002512
5030	1	P2RY4	NM_002565
5163	1	PDK1	NM_002610
5290	1	PIK3CA	NM_006218
5352	1	PLOD2	NM_000935
92400	1	RBM18	NM_033117
729708	1	RCTPI1	XM_371261
26575	1	RGS17	NM_012419
6323	1	SCN1A	NM_006920
9805	1	SCRN1	NM_014766
6581	1	SLC22A3	NM_021977
6529	1	SLC6A1	NM_003042
6579	1	SLCO1A2	NM_005075
9779	1	TBC1D5	NM_014744
7004	1	TEAD4	NM_003213
54210	1	TREM1	NM_018643
7743	1	ZNF189	NM_003452
2647	0	BLOC1S1	NM_001487
797	0	CALCB	NM_000728
1351	0	COX8A	NM_004074
57007	0	CXCR7	NM_020311
56940	0	DUSP22	NM_020185
1965	0	EIF2S1	NM_004094
2168	0	FABP1	NM_001443
23416	0	KCNH3	NM_012284

9778	0	KIAA0232	XM_291106
4629	0	MYH11	NM_002474
4668	0	NAGA	NM_000262
2908	0	NR3C1	NM_000176
54212	0	SNTG1	NM_018967
55254	0	TMEM39A	NM_018266

Table 4. Secondary screen results for cell survival

Locus_ID	Accession	Symbol	Alternate Gene_Symbol	# oligos decreased coloc	# oligos decreased survival	# oligos decreased survival AND coloc
22985	NM_014977	ACIN1	ACIN1	4	4	4
10675	NM_006574	CSPG5	CSPG5	4	4	4
54890	NM_017758	FLJ20308	ALKBH5	4	4	4
25804	NM_012321	LSM4	LSM4	4	4	4
55777	NM_018328	MBD5	MBD5	4	4	4
55173	NM_018141	MRPS10	MRPS10	4	4	4
55172	NM_018139	C14orf104	C14ORF104	4	3	3
27120	NM_014419	DKKL1	DKKL1	4	3	3
339834	NM_178173	LOC339834	CCDC36	4	3	3
4190	NM_005917	MDH1	MDH1	4	3	3
149466	NM_182517	MGC52423	C1orf210	4	3	3
8736	NM_003803	MYOM1	MYOM1	4	3	3
9688	NM_014669	NUP93	NUP93	4	3	3
55159	NM_018124	RFWD3	FLJ10520	4	3	3
6628	NM_003091	SNRPB	SNRPB	4	3	3
51308	NM_016606	C5orf19	REEP2	4	2	2
1359	NM_001870	CPA3	CPA3	4	2	2
9715	NM_014690	KIAA0773	FAM131B	4	2	2
29995	NM_014583	LMCD1	LMCD1	4	2	2
347359	XM_293293	LOC347359	BMP2KL	4	2	2
5166	NM_002612	PDK4	PDK4	4	2	2
2188	NM_022725	FANCF	FANCF	4	1	1
8514	NM_003636	KCNAB2	KCNAB2	4	0	0
25865	NM_016457	PRKD2	PRKD2	4	0	0
6424	NM_003014	SFRP4	SFRP4	4	0	0
6636	NM_003095	SNRPF	SNRPF	4	0	0
202374	NM_145001	STK32A	STK32A	4	0	0
51676	NM_016150	ASB2	ASB2	3	4	3
481	NM_001677	ATP1B1	ATP1B1	3	4	3
2259	NM_004115	FGF14	FGF14	3	4	3
5539	NM_002722	PPY	PPY	3	4	3
5273	NM_005024	SERPINB10	SERPINB10	3	4	3
55343	NM_018389	SLC35C1	SLC35C1	3	4	3
6773	NM_005419	STAT2	STAT2	3	4	3
2558	NM_000810	GABRA5	GABRA5	3	3	3
27198	NM_032554	GPR81	GPR81	3	3	3
140446	NM_058242	KRT6A	KRT6A	3	3	3

51000	NM_015948	SLC35B3	SLC35B3	3	3	3
308	NM_001154	ANXA5	ANXA5	3	3	2
55116	NM_018056	FLJ10315	TMEM39B	3	3	2
25758	XM_039515	G2	C11orf41	3	3	2
2660	NM_005259	GDF8	MSTN	3	3	2
80216	NM_025144	LAK	ALPK1	3	3	2
9796	NM_014759	PHYHIP	PHYHIP	3	3	2
60386	NM_021734	SLC25A19	SLC25A19	3	3	2
2542	NM_001467	SLC37A4	SLC37A4	3	3	2
6629	NM_003092	SNRPB2	SNRPB2	3	3	2
148213	NM_138286	LOC148213	ZNF681	3	2	2
401466	XM_376783	LOC401466	C8orf59	3	2	2
6632	NM_006938	SNRPD1	SNRPD1	3	2	2
8357	NM_003536	HIST1H3H	HIST1H3H	3	2	1
4130	NM_002373	MAP1A	MAP1A	3	2	1
51116	NM_016034	MRPS2	MRPS2	3	2	1
4638	NM_005965	MYLK	MYLK	3	2	1
8464	NM_003599	SUPT3H	SUPT3H	3	2	1
63897	NM_022070	ABC1	HEATR6	3	1	1
11173	NM_014272	ADAMTS7	ADAMTS7	3	1	1
83592	NM_031436	AKR1CL2	AKR1CL2	3	1	1
91653	NM_033254	BOC	BOC	3	1	1
55272	NM_018285	C15orf12	C15ORF12	3	1	1
727	NM_001735	C5	C5	3	1	1
3791	NM_002253	KDR	KDR	3	1	1
5604	NM_002755	MAP2K1	MAP2K1	3	1	1
91807	NM_182493	MLCK	MYLK3	3	1	1
4300	NM_004529	MLLT3	MLLT3	3	1	1
4715	NM_005005	NDUFB9	NDUFB9	3	1	1
57729	XM_290923	OBSCN	KIAA1639	3	1	1
6304	NM_002971	SATB1	SATB1	3	1	1
55186	NM_018155	SLC25A36	FLJ10618	3	1	1
4771	NM_000268	NF2	NF2	3	1	0
8677	NM_003765	STX10	STX10	3	1	0
64768	NM_022755	C9orf12	IPPK	3	0	0
2176	NM_000136	FANCC	FANCC	3	0	0
7786	NM_006301	MAP3K12	MAP3K12	3	0	0
4741	NM_005382	NEF3	NEF3	3	0	0
6509	NM_003038	SLC1A4	SLC1A4	3	0	0
7224	NM_012471	TRPC5	TRPC5	3	0	0
283316	NM_174941	CD163L1	M160	2	4	2
55120	NM_018062	FANCL	FANCL	2	4	2
374973	XM_371248	LOC374973	C1orf223	2	4	2
94107	NM_053045	MGC14327	TMEM203	2	4	2
8504	NM_003630	PEX3	PEX3	2	4	2
55163	NM_018129	PNPO	PNPO	2	4	2
6507	NM_004172	SLC1A3	SLC1A3	2	4	2
2040	NM_004099	STOM	STOM	2	4	2
22918	NM_012072	C1QR1	C1QR1	2	3	2
8110	NM_012074	DPF3	DPF3	2	3	2
4913	NM_002528	NTHL1	NTHL1	2	3	2
5194	NM_002618	PEX13	PEX13	2	3	2

51538	NM_016505	PS1D	ZCCHC17	2	3	2
51340	NM_016652	CRNKL1	CRNKL1	2	3	1
9982	NM_005130	HBP17	FGFBP1	2	3	1
387849	XM_370686	REP15	LOC387849	2	3	1
54432	NM_018982	YIPF1	DJ167A19.1	2	3	1
139741	NM_138289	ACTRT1	ACTRT1	2	2	2
9469	NM_004273	CHST3	CHST3	2	2	2
5026	NM_002561	P2RX5	P2RX5	2	2	2
57154	NM_020429	SMURF1	SMURF1	2	2	2
51306	NM_016603	C5orf5	FAM13B	2	2	1
1366	NM_001307	CLDN7	CLDN7	2	2	1
2252	NM_002009	FGF7	FGF7	2	2	1
9513	NM_004860	FXR2	FXR2	2	2	1
29923	NM_013332	HIG2	C7orf68	2	2	1
23043	XM_039796	TNIK	TNIK	2	2	1
7311	NM_003333	UBA52	UBA52	2	2	1
766	NM_005182	CA7	CA7	2	2	0
3784	NM_000218	KCNQ1	KCNQ1OT1	2	2	0
1068	NM_004066	CETN1	CETN1	2	1	1
200081	NM_175852	DKFZp451J0118	TXLNA	2	1	1
55132	NM_018078	FLJ10378	LARP1B	2	1	1
8200	NM_000557	GDF5	GDF5	2	1	1
1404	NM_001884	HAPLN1	HAPLN1	2	1	1
319101	NM_175068	K6IRS3	KRT73	2	1	1
51315	NM_016618	LOC51315	KRCC1	2	1	1
7182	NM_003298	NR2C2	NR2C2	2	1	1
59277	NM_021229	NTN4	NTN4	2	1	1
5214	NM_002627	PFKP	PFKP	2	1	1
5232	NM_138733	PGK2	PGK2	2	1	1
9765	NM_014733	ZFYVE16	ZFYVE16	2	1	1
51042	NM_015871	ZNF593	ZNF593	2	1	1
51287	NM_016565	E2IG2	CHCHD8	2	1	0
11077	NM_007031	HSF2BP	HSF2BP	2	1	0
9776	NM_014741	KIAA0652	ATG13	2	1	0
401089	XM_376269	LOC401089	C3orf72	2	1	0
55361	NM_018425	PI4KII	PI4K2A	2	1	0
51320	NM_016626	RKHD2	MEX3C	2	1	0
10282	NM_005868	BET1	BET1	2	0	0
828	NM_004058	CAPS	CAPS	2	0	0
23500	NM_015345	DAAM2	DAAM2	2	0	0
8507	NM_003633	ENC1	ENC1	2	0	0
9685	NM_014666	ENTH	CLINT1	2	0	0
2620	NM_005256	GAS2	GAS2	2	0	0
27102	NM_014413	HRI	EIF2AK1	2	0	0
3597	NM_001560	IL13RA1	IL13RA1	2	0	0
3777	NM_002246	KCNK3	KCNK3	2	0	0
401082	XM_376257	LOC401082	FLJ25363	2	0	0
729698	XM_377887	LOC729698	LOC402210	2	0	0
55191	NM_018161	NADSYN1	NADSYN1	2	0	0
5592	NM_006258	PRKG1	PRKG1	2	0	0
9783	NM_014747	RIMS3	RIMS3	2	0	0
6429	NM_005626	SFRS4	SFRS4	2	0	0

8208	NM_005441	CHAF1B	CHAF1B	1	4	1
3250	NM_020995	HPR	HPR	1	4	1
54210	NM_018643	TREM1	TREM1	1	4	1
9798	NM_014761	KIAA0174	KIAA0174	1	3	1
94059	NM_198988	LENG9	LENG9	1	3	1
92400	NM_033117	RBM18	RBM18	1	3	1
7004	NM_003213	TEAD4	TEAD4	1	3	1
7743	NM_003452	ZNF189	ZNF189	1	3	1
80271	NM_025194	ITPKC	ITPKC	1	2	1
2215	NM_000570	FCGR3B	FCGR3B	1	2	0
51291	NM_016573	GMIP	GMIP	1	2	0
9788	NM_014751	MTSS1	MTSS1	1	2	0
6323	NM_006920	SCN1A	SCN1A	1	2	0
8099	NM_004642	CDK2AP1	CDK2AP1	1	1	1
1340	NM_001863	COX6B1	COX6B1	1	1	1
9785	NM_014003	DHX38	DHX38	1	1	1
56901	NM_020142	LOC56901	NDUFA4L2	1	1	1
6579	NM_005075	SLCO1A2	SLCO1A2	1	1	1
55184	NM_018152	C20orf12	C20ORF12	1	1	0
3866	NM_002275	KRT15	KRT15	1	1	0
157807	NM_173519	MGC34646	CLVS1	1	1	0
338323	NM_176822	NALP14	NLRP14	1	1	0
4831	NM_002512	NME2	NME2	1	1	0
5163	NM_002610	PDK1	PDK1	1	1	0
5352	NM_000935	PLOD2	PLOD2	1	1	0
26575	NM_012419	RGS17	RGS17	1	1	0
9779	NM_014744	TBC1D5	TBC1D5	1	1	0
154	NM_000024	ADRB2	ADRB2	1	0	0
29883	NM_013354	CNOT7	CNOT7	1	0	0
55194	NM_018166	FLJ10647	FAM176B	1	0	0
10020	NM_005476	GNE	GNE	1	0	0
2817	NM_002081	GPC1	GPC1	1	0	0
729708	XM_371261	LOC729708	RCTPI1	1	0	0
4043	NM_002337	LRPAP1	LRPAP1	1	0	0
51338	NM_024021	MS4A4A	MS4A4A	1	0	0
5030	NM_002565	P2RY4	P2RY4	1	0	0
5290	NM_006218	PIK3CA	PIK3CA	1	0	0
9805	NM_014766	SCRN1	SCRN1	1	0	0
6581	NM_021977	SLC22A3	SLC22A3	1	0	0
6529	NM_003042	SLC6A1	SLC6A1	1	0	0
57007	NM_020311	CMKOR1	CXCR7	0	4	0
2168	NM_001443	FABP1	FABP1	0	4	0
1351	NM_004074	COX8A	COX8A	0	3	0
1965	NM_004094	EIF2S1	EIF2S1	0	2	0
54212	NM_018967	SNTG1	SNTG1	0	2	0
55254	NM_018266	TMEM39A	FLJ10902	0	2	0
797	NM_000728	CALCB	CALCB	0	1	0
56940	NM_020185	DUSP22	DUSP22	0	1	0
2647	NM_001487	BLOC1S1	BLOC1S1	0	0	0
23416	NM_012284	KCNH3	KCNH3	0	0	0
9778	XM_291106	KIAA0232	KIAA0232	0	0	0
4629	NM_002474	MYH11	MYH11	0	0	0

4668	NM_000262	NAGA	NAGA	0	0	0
2908	NM_000176	NR3C1	NR3C1	0	0	0

BIBLIOGRAPHY

Ait-Goughoulte, M., Kanda, T., Meyer, K., Ryerse, J. S., Ray, R. B., and Ray, R. (2008). Hepatitis C virus genotype 1a growth and induction of autophagy. J Virol *82*, 2241-2249.

Al-Zeer, M. A., Al-Younes, H. M., Braun, P. R., Zerrahn, J., and Meyer, T. F. (2009). IFN-gamma-inducible Irga6 mediates host resistance against Chlamydia trachomatis via autophagy. PLoS One *4*, e4588.

Alonso, S., Pethe, K., Russell, D. G., and Purdy, G. E. (2007). Lysosomal killing of Mycobacterium mediated by ubiquitin-derived peptides is enhanced by autophagy. Proc Natl Acad Sci U S A *104*, 6031-6036.

Andrade, R. M., Wessendarp, M., Gubbels, M. J., Striepen, B., and Subauste, C. S. (2006). CD40 induces macrophage anti-Toxoplasma gondii activity by triggering autophagy-dependent fusion of pathogen-containing vacuoles and lysosomes. J Clin Invest *116*, 2366-2377.

Aresta, S., de Tand-Heim, M. F., Beranger, F., and de Gunzburg, J. (2002). A novel Rho GTPase-activating-protein interacts with Gem, a member of the Ras superfamily of GTPases. Biochem J *367*, 57-65.

Baisamy, L., Cavin, S., Jurisch, N., and Diviani, D. (2009). The ubiquitin-like protein LC3 regulates the Rho-GEF activity of AKAP-Lbc. J Biol Chem *284*, 28232-28242.

Barrios-Rodiles, M., Brown, K. R., Ozdamar, B., Bose, R., Liu, Z., Donovan, R. S., Shinjo, F., Liu, Y., Dembowy, J., Taylor, I. W.*, et al.* (2005). High-

throughput mapping of a dynamic signaling network in mammalian cells. Science *307*, 1621-1625.

Bauer, P. O., Wong, H. K., Oyama, F., Goswami, A., Okuno, M., Kino, Y., Miyazaki, H., and Nukina, N. (2009). Inhibition of Rho kinases enhances the degradation of mutant huntingtin. J Biol Chem *284*, 13153-13164.

Berger, Z., Ravikumar, B., Menzies, F. M., Oroz, L. G., Underwood, B. R., Pangalos, M. N., Schmitt, I., Wullner, U., Evert, B. O., O'Kane, C. J., and Rubinsztein, D. C. (2006). Rapamycin alleviates toxicity of different aggregate-prone proteins. Hum Mol Genet *15*, 433-442.

Birmingham, C. L., Smith, A. C., Bakowski, M. A., Yoshimori, T., and Brumell, J. H. (2006). Autophagy controls Salmonella infection in response to damage to the Salmonella-containing vacuole. J Biol Chem *281*, 11374-11383.

Bjorkoy, G., Lamark, T., Brech, A., Outzen, H., Perander, M., Overvatn, A., Stenmark, H., and Johansen, T. (2005). p62/SQSTM1 forms protein aggregates degraded by autophagy and has a protective effect on huntingtin-induced cell death. J Cell Biol *171*, 603-614.

Blanchet, F. P., Moris, A., Nikolic, D. S., Lehmann, M., Cardinaud, S., Stalder, R., Garcia, E., Dinkins, C., Leuba, F., Wu, L.*, et al.* (2010). Human Immunodeficiency Virus-1 Inhibition of Immunoamphisomes in Dendritic Cells Impairs Early Innate and Adaptive Immune Responses. Immunity.

Brabec-Zaruba, M., Berka, U., Blaas, D., and Fuchs, R. (2007). Induction of autophagy does not affect human rhinovirus type 2 production. J Virol *81*, 10815-10817.

Brass, A. L., Dykxhoorn, D. M., Benita, Y., Yan, N., Engelman, A., Xavier, R. J., Lieberman, J., and Elledge, S. J. (2008). Identification of host proteins required for HIV infection through a functional genomic screen. Science *319*, 921-926.

Brass, A. L., Huang, I. C., Benita, Y., John, S. P., Krishnan, M. N., Feeley, E. M., Ryan, B. J., Weyer, J. L., van der Weyden, L., Fikrig, E.*, et al.* (2009). The IFITM proteins mediate cellular resistance to influenza A H1N1 virus, West Nile virus, and dengue virus. Cell *139*, 1243-1254.

Bryan, B., Cai, Y., Wrighton, K., Wu, G., Feng, X. H., and Liu, M. (2005). Ubiquitination of RhoA by Smurf1 promotes neurite outgrowth. FEBS Lett *579*, 1015-1019.

Cadwell, K., Stappenbeck, T. S., and Virgin, H. W. (2009). Role of autophagy and autophagy genes in inflammatory bowel disease. Curr Top Microbiol Immunol *335*, 141-167.

Chan, E. Y., Longatti, A., McKnight, N. C., and Tooze, S. A. (2009). Kinase-inactivated ULK proteins inhibit autophagy via their conserved C-terminal domains using an Atg13-independent mechanism. Mol Cell Biol *29*, 157-171.

Chaturvedi, A., Dorward, D., and Pierce, S. K. (2008). The B Cell Receptor Governs the Subcellular Location of Toll-like Receptor 9 Leading to Hyperresponses to DNA-Containing Antigens. Immunity *28*, 799-809.

Chaumorcel, M., Souque?re, S., Pierron, G., Codogno, P., and Esclatine, A. (2008). Human cytomegalovirus controls a new autophagy-dependent cellular antiviral defense mechanism. Autophagy *4*, 46-53.

Checroun, C., Wehrly, T. D., Fischer, E. R., Hayes, S. F., and Celli, J. (2006). Autophagy-mediated reentry of Francisella tularensis into the endocytic compartment after cytoplasmic replication. Proc Natl Acad Sci U S A *103*, 14578-14583.

Cherry, S., Kunte, A., Wang, H., Coyne, C., Rawson, R. B., and Perrimon, N. (2006). COPI activity coupled with fatty acid biosynthesis is required for viral replication. PLoS Pathog *2*, e102.

Clausen, T. H., Lamark, T., Isakson, P., Finley, K., Larsen, K. B., Brech, A., Overvatn, A., Stenmark, H., Bjorkoy, G., Simonsen, A., and Johansen, T. (2010). p62/SQSTM1 and ALFY interact to facilitate the formation of p62 bodies/ALIS and their degradation by autophagy. Autophagy *6*, 330-344.

Coisy-Quivy, M., Touzet, O., Bourret, A., Hipskind, R. A., Mercier, J., Fort, P., and Philips, A. (2009). TC10 controls human myofibril organization and is activated by the sarcomeric RhoGEF obscurin. J Cell Sci *122*, 947-956.

Cullinane, M., Gong, L., Li, X., Lazar-Adler, N., Tra, T., Wolvetang, E., Prescott, M., Boyce, J. D., Devenish, R. J., and Adler, B. (2008). Stimulation of

autophagy suppresses the intracellular survival of Burkholderia pseudomallei in mammalian cell lines. Autophagy *4*.

De Duve, C., and Wattiaux, R. (1966). Functions of lysosomes. Annu Rev Physiol *28*, 435-492.

Delgado, M. A., Elmaoued, R. A., Davis, A. S., Kyei, G., and Deretic, V. (2008). Toll-like receptors control autophagy. Embo J *27*, 1110-1121.

Dengjel, J., Schoor, O., Fischer, R., Reich, M., Kraus, M., Muller, M., Kreymborg, K., Altenberend, F., Brandenburg, J., Kalbacher, H.*, et al.* (2005). Autophagy promotes MHC class II presentation of peptides from intracellular source proteins. Proc Natl Acad Sci U S A *102*, 7922-7927.

Deretic, V., and Levine, B. (2009). Autophagy, immunity, and microbial adaptations. Cell Host Microbe *5*, 527-549.

Djavaheri-Mergny, M., Amelotti, M., Mathieu, J., Besancon, F., Bauvy, C., Souquere, S., Pierron, G., and Codogno, P. (2006). NF-kappaB activation represses tumor necrosis factor-alpha-induced autophagy. J Biol Chem *281*, 30373-30382.

Dreux, M., Gastaminza, P., Wieland, S. F., and Chisari, F. V. (2009). The autophagy machinery is required to initiate hepatitis C virus replication. Proc Natl Acad Sci U S A *106*, 14046-14051

Dupont, N., Lacas-Gervais, S., Bertout, J., Paz, I., Freche, B., Van Nhieu, G. T., van der Goot, F. G., Sansonetti, P. J., and Lafont, F. (2009). Shigella phagocytic vacuolar membrane remnants participate in the cellular response to

pathogen invasion and are regulated by autophagy. Cell Host Microbe *6*, 137-149.

Duran, J. M., Anjard, C., Stefan, C., Loomis, W. F., and Malhotra, V. (2010). Unconventional secretion of Acb1 is mediated by autophagosomes. J Cell Biol *188*, 527-536.

E, X., Hwang, S., Oh, S., Lee, J. S., Jeong, J. H., Gwack, Y., Kowalik, T. F., Sun, R., Jung, J. U., and Liang, C. (2009). Viral Bcl-2-mediated evasion of autophagy aids chronic infection of gammaherpesvirus 68. PLoS Pathog *5*, e1000609.

English, L., Chemali, M., Duron, J., Rondeau, C., Laplante, A., Gingras, D., Alexander, D., Leib, D., Norbury, C., Lippe, R., and Desjardins, M. (2009). Autophagy enhances the presentation of endogenous viral antigens on MHC class I molecules during HSV-1 infection. Nat Immunol *10*, 480-487.

Fan, W., Tang, Z., Chen, D., Moughon, D., Ding, X., Chen, S., Zhu, M., and Zhong, Q. (2010). Keap1 facilitates p62-mediated ubiquitin aggregate clearance via autophagy. Autophagy *6*.

Farre, J. C., Manjithaya, R., Mathewson, R. D., and Subramani, S. (2008). PpAtg30 tags peroxisomes for turnover by selective autophagy. Dev Cell *14*, 365-376.

Feng, C. G., Zheng, L., Lenardo, M. J., and Sher, A. (2009). Interferon-inducible immunity-related GTPase Irgm1 regulates IFN gamma-dependent host defense, lymphocyte survival and autophagy. Autophagy *5*, 232-234.

Florez-McClure, M. L., Hohsfield, L. A., Fonte, G., Bealor, M. T., and Link, C. D. (2007). Decreased insulin-receptor signaling promotes the autophagic degradation of beta-amyloid peptide in C. elegans. Autophagy *3*, 569-580.

Forshey, B. M., Shi, J., and Aiken, C. (2005). Structural requirements for recognition of the human immunodeficiency virus type 1 core during host restriction in owl monkey cells. J Virol *79*, 869-875.

Fujita, N., Hayashi-Nishino, M., Fukumoto, H., Omori, H., Yamamoto, A., Noda, T., and Yoshimori, T. (2008a). An Atg4B mutant hampers the lipidation of LC3 paralogues and causes defects in autophagosome closure. Mol Biol Cell *19*, 4651-4659.

Fujita, N., Itoh, T., Omori, H., Fukuda, M., Noda, T., and Yoshimori, T. (2008b). The Atg16L complex specifies the site of LC3 lipidation for membrane biogenesis in autophagy. Mol Biol Cell *19*, 2092-2100.

Gal, J., Strom, A. L., Kwinter, D. M., Kilty, R., Zhang, J., Shi, P., Fu, W., Wooten, M. W., and Zhu, H. (2009). Sequestosome 1/p62 links familial ALS mutant SOD1 to LC3 via an ubiquitin-independent mechanism. J Neurochem *111*, 1062-1073.

Garcia-Sastre, A., and Biron, C. A. (2006). Type 1 interferons and the virus-host relationship: a lesson in detente. Science *312*, 879-882.

Geisler, S., Holmstrom, K. M., Skujat, D., Fiesel, F. C., Rothfuss, O. C., Kahle, P. J., and Springer, W. (2010). PINK1/Parkin-mediated mitophagy is dependent on VDAC1 and p62/SQSTM1. Nat Cell Biol *12*, 119-131.

Geng, J., and Klionsky, D. J. (2008). The Atg8 and Atg12 ubiquitin-like conjugation systems in macroautophagy. 'Protein modifications: beyond the usual suspects' review series. EMBO Rep *9*, 859-864.

Gil-Fernandez, C., Ronda-Lain, C., and Rubio-Huertos, M. (1973). Electron microscopic study of Sindbis virus morphogenesis. Arch Gesamte Virusforsch *40*, 1-9.

Griffin, D. E. (2005). Neuronal cell death in alphavirus encephalomyelitis, In Current Topics in Microbiology and Immunology, pp. 57-77.

Gutierrez, M. G., Master, S. S., Singh, S. B., Taylor, G. A., Colombo, M. I., and Deretic, V. (2004). Autophagy is a defense mechanism inhibiting BCG and Mycobacterium tuberculosis survival in infected macrophages. Cell *119*, 753-766.

Gutierrez, M. G., Saka, H. A., Chinen, I., Zoppino, F. C., Yoshimori, T., Bocco, J. L., and Colombo, M. I. (2007). Protective role of autophagy against Vibrio cholerae cytolysin, a pore-forming toxin from V. cholerae. Proc Natl Acad Sci U S A *104*, 1829-1834.

Hamacher-Brady, A., Brady, N. R., and Gottlieb, R. A. (2006). Enhancing macroautophagy protects against ischemia/reperfusion injury in cardiac myocytes. J Biol Chem *281*, 29776-29787.

Hanada, T., Noda, N. N., Satomi, Y., Ichimura, Y., Fujioka, Y., Takao, T., Inagaki, F., and Ohsumi, Y. (2007). The Atg12-Atg5 conjugate has a novel

E3-like activity for protein lipidation in autophagy. J Biol Chem *282*, 37298-37302.

Hara, T., Nakamura, K., Matsui, M., Yamamoto, A., Nakahara, Y., Suzuki-Migishima, R., Yokoyama, M., Mishima, K., Saito, I., Okano, H., and Mizushima, N. (2006). Suppression of basal autophagy in neural cells causes neurodegenerative disease in mice. Nature *441*, 885-889.

Hardwick, J. M., and Levine, B. (2000). Sindbis virus vector system for functional analysis of apoptosis regulators. Methods Enzymol *322*, 492-508.

Harris, J., De Haro, S. A., Master, S. S., Keane, J., Roberts, E. A., Delgado, M., and Deretic, V. (2007). T helper 2 cytokines inhibit autophagic control of intracellular Mycobacterium tuberculosis. Immunity *27*, 505-517.

Hassel, B., Schreff, M., Stube, E. M., Blaich, U., and Schumacher, S. (2003). CALEB/NGC interacts with the Golgi-associated protein PIST. J Biol Chem *278*, 40136-40143.

He, C., and Levine, B. (2010). The Beclin 1 interactome. Curr Opin Cell Biol *22*, 140-149.

He, C., Song, H., Yorimitsu, T., Monastyrska, I., Yen, W. L., Legakis, J. E., and Klionsky, D. J. (2006). Recruitment of Atg9 to the preautophagosomal structure by Atg11 is essential for selective autophagy in budding yeast. J Cell Biol *175*, 925-935.

Helfrich, M. H., and Hocking, L. J. (2008). Genetics and aetiology of Pagetic disorders of bone. Arch Biochem Biophys *473*, 172-182.

Hosokawa, N., Hara, Y., and Mizushima, N. (2006). Generation of cell lines with tetracycline-regulated autophagy and a role for autophagy in controlling cell size. FEBS Lett *580*, 2623-2629.

Hrstka, R., Kroc?ova, Z., C?erny, J., Vojte?s?ek, B., Macela, A., and Stuli?k, J. (2007). Francisella tularensis strain LVS resides in MHC II-positive autophagic vacuoles in macrophages. Folia Microbiologica *52*, 631-636.

Huang, C., Rajfur, Z., Yousefi, N., Chen, Z., Jacobson, K., and Ginsberg, M. H. (2009). Talin phosphorylation by Cdk5 regulates Smurf1-mediated talin head ubiquitylation and cell migration. Nat Cell Biol *11*, 624-630.

Huett, A., Ng, A., Cao, Z., Kuballa, P., Komatsu, M., Daly, M. J., Podolsky, D. K., and Xavier, R. J. (2009). A novel hybrid yeast-human network analysis reveals an essential role for FNBP1L in antibacterial autophagy. J Immunol *182*, 4917-4930.

Hughes, T., and Rusten, T. E. (2007). Origin and evolution of self-consumption: autophagy. Adv Exp Med Biol *607*, 111-118.

Ichimura, Y., Kumanomidou, T., Sou, Y. S., Mizushima, T., Ezaki, J., Ueno, T., Kominami, E., Yamane, T., Tanaka, K., and Komatsu, M. (2008). Structural basis for sorting mechanism of p62 in selective autophagy. J Biol Chem *283*, 22847-22857.

Iwata, A., Riley, B. E., Johnston, J. A., and Kopito, R. R. (2005). HDAC6 and microtubules are required for autophagic degradation of aggregated huntingtin. J Biol Chem *280*, 40282-40292.

Jackson, A. C., Moench, T. R., Trapp, B. D., and Griffin, D. E. (1988). Basis of neurovirulence in Sindbis virus encephalomyelitis of mice. Lab Invest *58*, 503-509.

Jackson, W. T., Giddings, T. H., Jr., Taylor, M. P., Mulinyawe, S., Rabinovitch, M., Kopito, R. R., and Kirkegaard, K. (2005). Subversion of cellular autophagosomal machinery by RNA viruses. PLoS Biol *3*, e156.

Jain, A., Lamark, T., Sjottem, E., Bowitz Larsen, K., Awuh, J. A., Overvatn, A., McMahon, M., Hayes, J. D., and Johansen, T. (2010). p62/SQSTM1 is a target gene for transcription factor NRF2 and creates a positive feedback loop by inducing antioxidant response element-driven gene transcription. J Biol Chem.

Jeong, H., Then, F., Melia, T. J., Jr., Mazzulli, J. R., Cui, L., Savas, J. N., Voisine, C., Paganetti, P., Tanese, N., Hart, A. C*., et al.* (2009). Acetylation targets mutant huntingtin to autophagosomes for degradation. Cell *137*, 60-72.

Jia, K., Hart, A. C., and Levine, B. (2007). Autophagy Genes Protect Against Disease Caused by Polyglutamine Expansion Proteins in Caenorhabditis elegans. Autophagy *3*, in press.

Jia, K., Thomas, C., Akbar, M., Sun, Q., Adams-Huet, B., Gilpin, C., and Levine, B. (2009). Autophagy genes protect against Salmonella typhimurium infection and mediate insulin signaling-regulated pathogen resistance. Proc Natl Acad Sci U S A *106*, 14564-14569.

Johnson, R. T. (1965). Virus Invasion of the Central Nervous System: a Study of Sindbis Virus Infection in the Mouse Using Fluorescent Antibody. Am J Pathol *46*, 929-943.

Johnson, R. T., McFarland, H. F., and Levy, S. E. (1972). Age-dependent resistance to viral encephalitis: studies of infections due to Sindbis virus in mice. J Infect Dis *125*, 257-262.

Johnston, C., Jiang, W., Chu, T., and Levine, B. (2001). Identification of genes involved in the host response to neurovirulent alphavirus infection. J Virol *75*, 10431-10445.

Joubert, P. E., Meiffren, G., Gregoire, I. P., Pontini, G., Richetta, C., Flacher, M., Azocar, O., Vidalain, P. O., Vidal, M., Lotteau, V.*, et al.* (2009). Autophagy induction by the pathogen receptor CD46. Cell Host Microbe *6*, 354-366.

Ju, J. S., Fuentealba, R. A., Miller, S. E., Jackson, E., Piwnica-Worms, D., Baloh, R. H., and Weihl, C. C. (2009). Valosin-containing protein (VCP) is required for autophagy and is disrupted in VCP disease. J Cell Biol *187*, 875-888.

Kadandale, P., Stender, J. D., Glass, C. K., and Kiger, A. A. (2010). Conserved role for autophagy in Rho1-mediated cortical remodeling and blood cell recruitment. Proc Natl Acad Sci U S A.

Kanki, T., Wang, K., Cao, Y., Baba, M., and Klionsky, D. J. (2009). Atg32 is a mitochondrial protein that confers selectivity during mitophagy. Dev Cell *17*, 98-109.

Kawajiri, S., Saiki, S., Sato, S., Sato, F., Hatano, T., Eguchi, H., and Hattori, N. (2010). PINK1 is recruited to mitochondria with parkin and associates with LC3 in mitophagy. FEBS Lett, 12.

Khan, L. A., Yamanaka, T., and Nukina, N. (2008). Genetic impairment of autophagy intensifies expanded polyglutamine toxicity in Caenorhabditis elegans. Biochem Biophys Res Commun *368*, 729-735.

Kim, I., Rodriguez-Enriquez, S., and Lemasters, J. J. (2007). Selective degradation of mitochondria by mitophagy. Arch Biochem Biophys *462*, 245-253.

Kim, P. K., Hailey, D. W., Mullen, R. T., and Lippincott-Schwartz, J. (2008). Ubiquitin signals autophagic degradation of cytosolic proteins and peroxisomes. Proc Natl Acad Sci U S A *105*, 20567-20574.

Kimberlin, D. W. (2007). Management of HSV encephalitis in adults and neonates: diagnosis, prognosis and treatment. Herpes *14*, 11-16.

Kirkin, V., McEwan, D. G., Novak, I., and Dikic, I. (2009). A role for ubiquitin in selective autophagy. Mol Cell *34*, 259-269.

Klionsky, D. J., Abeliovich, H., Agostinis, P., Agrawal, D. K., Aliev, G., Askew, D. S., Baba, M., Baehrecke, E. H., Bahr, B. A., Ballabio, A.*, et al.* (2008). Guidelines for the use and interpretation of assays for monitoring autophagy in higher eukaryotes. Autophagy *4*, 151-175.

Komatsu, M., Kurokawa, H., Waguri, S., Taguchi, K., Kobayashi, A., Ichimura, Y., Sou, Y. S., Ueno, I., Sakamoto, A., Tong, K. I.*, et al.* (2010). The selective

autophagy substrate p62 activates the stress responsive transcription factor Nrf2 through inactivation of Keap1. Nat Cell Biol *12*, 213-223.

Komatsu, M., Waguri, S., Chiba, T., Murata, S., Iwata, J., Tanida, I., Ueno, T., Koike, M., Uchiyama, Y., Kominami, E., and Tanaka, K. (2006). Loss of autophagy in the central nervous system causes neurodegeneration in mice. Nature *441*, 880-884.

Komatsu, M., Waguri, S., Koike, M., Sou, Y. S., Ueno, T., Hara, T., Mizushima, N., Iwata, J., Ezaki, J., Murata, S.*, et al.* (2007). Homeostatic levels of p62 control cytoplasmic inclusion body formation in autophagy-deficient mice. Cell *131*, 1149-1163.

Komatsu, M., Waguri, S., Ueno, T., Iwata, J., Murata, S., Tanida, I., Ezaki, J., Mizushima, N., Ohsumi, Y., Uchiyama, Y.*, et al.* (2005). Impairment of starvation-induced and constitutive autophagy in Atg7-deficient mice. J Cell Biol *169*, 425-434.

Koonin, E. V., Senkevich, T. G., and Dolja, V. V. (2006). The ancient Virus World and evolution of cells. Biol Direct *1*, 29.

Korolchuk, V. I., Menzies, F. M., and Rubinsztein, D. C. (2010). Mechanisms of cross-talk between the ubiquitin-proteasome and autophagy-lysosome systems. FEBS Lett *584*, 1393-1398.

Kraft, C., Deplazes, A., Sohrmann, M., and Peter, M. (2008). Mature ribosomes are selectively degraded upon starvation by an autophagy pathway requiring the Ubp3p/Bre5p ubiquitin protease. Nat Cell Biol *10*, 602-610.

Kroemer, G., and Levine, B. (2008). Autophagic cell death: the story of a misnomer. Nat Rev Mol Cell Biol *9*, 1004-1010.

Ku, B., Woo, J. S., Liang, C., Lee, K. H., Hong, H. S., E, X., Kim, K. S., Jung, J. U., and Oh, B. H. (2008). Structural and biochemical bases for the inhibition of autophagy and apoptosis by viral BCL-2 of murine gamma-herpesvirus 68. PLoS Pathog *4*, e25.

Kubota, H. (2009). Quality control against misfolded proteins in the cytosol: a network for cell survival. J Biochem *146*, 609-616.

Kuma, A., Hatano, M., Matsui, M., Yamamoto, A., Nakaya, H., Yoshimori, T., Ohsumi, Y., Tokuhisa, T., and Mizushima, N. (2004). The role of autophagy during the early neonatal starvation period. Nature *432*, 1032-1036.

Kyei, G. B., Dinkins, C., Davis, A. S., Roberts, E., Singh, S. B., Dong, C., Wu, L., Kominami, E., Ueno, T., Yamamoto, A.*, et al.* (2009). Autophagy pathway intersects with HIV-1 biosynthesis and regulates viral yields in macrophages. J Cell Biol *186*, 255-268.

Lamark, T., Kirkin, V., Dikic, I., and Johansen, T. (2009). NBR1 and p62 as cargo receptors for selective autophagy of ubiquitinated targets. Cell Cycle *8*, 1986-1990.

Lau, A., Wang, X. J., Zhao, F., Villeneuve, N. F., Wu, T., Jiang, T., Sun, Z., White, E., and Zhang, D. D. (2010). A non-canonical mechanism of Nrf2 activation by autophagy deficiency: a direct interaction between Keap1 and p62. Mol Cell Biol.

Layfield, R., and Shaw, B. (2007). Ubiquitin-mediated signalling and Paget's disease of bone. BMC Biochem *8 Suppl 1*, S5.

Lee, H. K., Lund, J. M., Ramanathan, B., Mizushima, N., and Iwasaki, A. (2007). Autophagy-dependent viral recognition by plasmacytoid dendritic cells. Science *315*, 1398-1401.

Lee, H. K., Mattei, L. M., Steinberg, B. E., Alberts, P., Lee, Y. H., Chervonsky, A., Mizushima, N., Grinstein, S., and Iwasaki, A. (2010a). In vivo requirement for Atg5 in antigen presentation by dendritic cells. Immunity *32*, 227-239.

Lee, J. Y., Koga, H., Kawaguchi, Y., Tang, W., Wong, E., Gao, Y. S., Pandey, U. B., Kaushik, S., Tresse, E., Lu, J., *et al.* (2010b). HDAC6 controls autophagosome maturation essential for ubiquitin-selective quality-control autophagy. Embo J *29*, 969-980.

Lee, J. Y., Nagano, Y., Taylor, J. P., Lim, K. L., and Yao, T. P. (2010c). Disease-causing mutations in Parkin impair mitochondrial ubiquitination, aggregation, and HDAC6-dependent mitophagy. Journal of Cell Biology *189*, 671-679.

Lee, Y. R., Lei, H. Y., Liu, M. T., Wang, J. R., Chen, S. H., Jiang-Shieh, Y. F., Lin, Y. S., Yeh, T. M., Liu, C. C., and Liu, H. S. (2008). Autophagic machinery activated by dengue virus enhances virus replication. Virology.

Leib, D. A., Alexander, D. E., Cox, D., Yin, J., and Ferguson, T. A. (2009). Interaction of ICP34.5 with Beclin 1 modulates herpes simplex virus type 1

pathogenesis through control of CD4+ T-cell responses. J Virol *83*, 12164-12171.

Levine, B. (2005). Eating oneself and uninvited guests: autophagy-related pathways in cellular defense.[comment]. Cell *120*, 159-162.

Levine, B. (2007). Cell biology: autophagy and cancer. Nature *446*, 745-747.

Levine, B., Goldman, J. E., Jiang, H. H., Griffin, D. E., and Hardwick, J. M. (1996). Bc1-2 protects mice against fatal alphavirus encephalitis. Proc Natl Acad Sci U S A *93*, 4810-4815.

Li, D. (2006). Selective degradation of the IkappaB kinase (IKK) by autophagy. Cell Res *16*, 855-856.

Li, M. L., Wang, H. L., and Stollar, V. (1997). Complementation of and interference with Sindbis virus replication by full-length and deleted forms of the nonstructural protein, nsP1, expressed in stable transfectants of Hela cells. Virology *227*, 361-369.

Liang, C., Feng, P., Ku, B., Dotan, I., Canaani, D., Oh, B. H., and Jung, J. U. (2006). Autophagic and tumour suppressor activity of a novel Beclin1-binding protein UVRAG. Nat Cell Biol *8*, 688-699.

Liang, X. H., Jackson, S., Seaman, M., Brown, K., Kempkes, B., Hibshoosh, H., and Levine, B. (1999). Induction of autophagy and inhibition of tumorigenesis by beclin 1. Nature *402*, 672-676.

Liang, X. H., Kleeman, L. K., Jiang, H. H., Gordon, G., Goldman, J. E., Berry, G., Herman, B., and Levine, B. (1998). Protection against fatal Sindbis virus encephalitis by beclin, a novel Bcl-2-interacting protein. J Virol *72*, 8586.

Ling, Y. M., Shaw, M. H., Ayala, C., Coppens, I., Taylor, G. A., Ferguson, D. J., and Yap, G. S. (2006). Vacuolar and plasma membrane stripping and autophagic elimination of Toxoplasma gondii in primed effector macrophages. J Exp Med *203*, 2063-2071.

Liu, Y., Schiff, M., Czymmek, K., Talloczy, Z., Levine, B., and Dinesh-Kumar, S. P. (2005). Autophagy regulates programmed cell death during the plant innate immune response. Cell *121*, 567-577.

Maiuri, M. C., Zalckvar, E., Kimchi, A., and Kroemer, G. (2007). Self-eating and self-killing: crosstalk between autophagy and apoptosis. Nat Rev Mol Cell Biol *8*, 741-752.

Manjithaya, R., Anjard, C., Loomis, W. F., and Subramani, S. (2010). Unconventional secretion of Pichia pastoris Acb1 is dependent on GRASP protein, peroxisomal functions, and autophagosome formation. J Cell Biol *188*, 537-546.

Martinez-Vicente, M., and Cuervo, A. M. (2007). Autophagy and neurodegeneration: when the cleaning crew goes on strike. Lancet Neurol *6*, 352-361.

Massey, A. C., Zhang, C., and Cuervo, A. M. (2006). Chaperone-mediated autophagy in aging and disease. Curr Top Dev Biol *73*, 205-235.

Mee, A. P. (1999). Paramyxoviruses and Paget's disease: the affirmative view. Bone *24*, 19S-21S.

Mettenleiter, T. C., Klupp, B. G., and Granzow, H. (2006). Herpesvirus assembly: a tale of two membranes. Curr Opin Microbiol *9*, 423-429.

Mizushima, N., and Klionsky, D. J. (2007). Protein turnover via autophagy: implications for metabolism. Annu Rev Nutr *27*, 19-40.

Mizushima, N., Noda, T., Yoshimori, T., Tanaka, Y., Ishii, T., George, M. D., Klionsky, D. J., Ohsumi, M., and Ohsumi, Y. (1998). A protein conjugation system essential for autophagy. Nature *395*, 395-398.

Mizushima, N., Yamamoto, A., Hatano, M., Kobayashi, Y., Kabeya, Y., Suzuki, K., Tokuhisa, T., Ohsumi, Y., and Yoshimori, T. (2001). Dissection of autophagosome formation using Apg5-deficient mouse embryonic stem cells. J Cell Biol *152*, 657-668.

Mizushima, N., Yamamoto, A., Matsui, M., Yoshimori, T., and Ohsumi, Y. (2004). In vivo analysis of autophagy in response to nutrient starvation using transgenic mice expressing a fluorescent autophagosome marker. Mol Biol Cell *15*, 1101-1111.

Monastyrska, I., Rieter, E., Klionsky, D. J., and Reggiori, F. (2009). Multiple roles of the cytoskeleton in autophagy. Biol Rev Camb Philos Soc *84*, 431-448.

Moscat, J., Diaz-Meco, M. T., and Wooten, M. W. (2007). Signal integration and diversification through the p62 scaffold protein. Trends Biochem Sci *32*, 95-100.

Munz, C. (2010). Antigen processing via autophagy--not only for MHC class II presentation anymore? Curr Opin Immunol *22*, 89-93.

Nakagawa, I., Amano, A., Mizushima, N., Yamamoto, A., Yamaguchi, H., Kamimoto, T., Nara, A., Funao, J., Nakata, M., Tsuda, K.*, et al.* (2004). Autophagy defends cells against invading group A Streptococcus. Science *306*, 1037-1040.

Nakaya, M. A., Habas, R., Biris, K., Dunty, W. C., Jr., Kato, Y., He, X., and Yamaguchi, T. P. (2004). Identification and comparative expression analyses of Daam genes in mouse and Xenopus. Gene Expr Patterns *5*, 97-105.

Narendra, D., Tanaka, A., Suen, D. F., and Youle, R. J. (2008). Parkin is recruited selectively to impaired mitochondria and promotes their autophagy. J Cell Biol *183*, 795-803.

Narendra, D. P., Jin, S. M., Tanaka, A., Suen, D. F., Gautier, C. A., Shen, J., Cookson, M. R., and Youle, R. J. (2010). PINK1 is selectively stabilized on impaired mitochondria to activate Parkin. PLoS Biol *8*, e1000298.

Nazarko, T. Y., Farre, J. C., and Subramani, S. (2009). Peroxisome size provides insights into the function of autophagy-related proteins. Mol Biol Cell *20*, 3828-3839.

Nimmerjahn, F., Milosevic, S., Behrends, U., Jaffee, E. M., Pardoll, D. M., Bornkamm, G. W., and Mautner, J. (2003). Major histocompatibility complex class II-restricted presentation of a cytosolic antigen by autophagy. Eur J Immunol *33*, 1250-1259.

Nixon, R. A. (2007). Autophagy, amyloidogenesis and Alzheimer disease. J Cell Sci *120*, 4081-4091.

Noda, N. N., Ohsumi, Y., and Inagaki, F. (2010). Atg8-family interacting motif crucial for selective autophagy. FEBS Lett *584*, 1379-1385.

Ogawa, M., Yoshimori, T., Suzuki, T., Sagara, H., Mizushima, N., and Sasakawa, C. (2005). Escape of intracellular Shigella from autophagy. Science *307*, 727-731.

Okamoto, K., Kondo-Okamoto, N., and Ohsumi, Y. (2009). Mitochondria-anchored receptor Atg32 mediates degradation of mitochondria via selective autophagy. Dev Cell *17*, 87-97.

Orvedahl, A., Alexander, D., Talloczy, Z., Sun, Q., Wei, Y., Zhang, W., Burns, D., Leib, D. A., and Levine, B. (2007). HSV-1 ICP34.5 confers neurovirulence by targeting the Beclin 1 autophagy protein. Cell Host Microbe *1*, 23-35.

Orvedahl, A., and Levine, B. (2008). Autophagy and viral neurovirulence. Cell Microbiol *10*, 1747-1756.

Orvedahl, A., and Levine, B. (2009a). Autophagy in Mammalian antiviral immunity. Curr Top Microbiol Immunol *335*, 267-285.

Orvedahl, A., and Levine, B. (2009b). Eating the enemy within: autophagy in infectious diseases. Cell Death Differ *16*, 57-69.

Orvedahl, A., MacPherson, S., Sumpter, R., Jr., Talloczy, Z., Zou, Z., and Levine, B. (2010). Autophagy protects against Sindbis virus infection of the central nervous system. Cell Host Microbe *7*, 115-127.

Ozdamar, B., Bose, R., Barrios-Rodiles, M., Wang, H. R., Zhang, Y., and Wrana, J. L. (2005). Regulation of the polarity protein Par6 by TGFbeta receptors controls epithelial cell plasticity. Science *307*, 1603-1609.

Paludan, C., Schmid, D., Landthaler, M., Vockerodt, M., Kube, D., Tuschl, T., and Munz, C. (2005). Endogenous MHC class II processing of a viral nuclear antigen after autophagy. Science *307*, 593-596.

Pandey, U. B., Nie, Z., Batlevi, Y., McCray, B. A., Ritson, G. P., Nedelsky, N. B., Schwartz, S. L., DiProspero, N. A., Knight, M. A., Schuldiner, O.*, et al.* (2007). HDAC6 rescues neurodegeneration and provides an essential link between autophagy and the UPS. Nature *447*, 859-863.

Pankiv, S., Clausen, T. H., Lamark, T., Brech, A., Bruun, J. A., Outzen, H., Overvatn, A., Bjorkoy, G., and Johansen, T. (2007). p62/SQSTM1 binds directly to Atg8/LC3 to facilitate degradation of ubiquitinated protein aggregates by autophagy. J Biol Chem *282*, 24131-24145.

Pattingre, S., Tassa, A., Qu, X., Garuti, R., Liang, X. H., Mizushima, N., Packer, M., Schneider, M. D., and Levine, B. (2005). Bcl-2 antiapoptotic proteins inhibit Beclin 1-dependent autophagy. Cell *122*, 927-939.

Pertz, O. (2010). Spatio-temporal Rho GTPase signaling - where are we now? J Cell Sci *123*, 1841-1850.

Pickford, F., Masliah, E., Britschgi, M., Lucin, K., Narasimhan, R., Jaeger, P. A., Small, S., Spencer, B., Rockenstein, E., Levine, B., and Wyss-Coray, T. (2008). The autophagy-related protein beclin 1 shows reduced expression in early Alzheimer disease and regulates amyloid beta accumulation in mice. J Clin Invest *118*, 2190-2199.

Pohl, C., and Jentsch, S. (2009). Midbody ring disposal by autophagy is a post-abscission event of cytokinesis. Nat Cell Biol *11*, 65-70.

Ponpuak, M., Davis, A. S., Roberts, E. A., Delgado, M. A., Dinkins, C., Zhao, Z., Virgin, H. W. t., Kyei, G. B., Johansen, T., Vergne, I., and Deretic, V. (2010). Delivery of cytosolic components by autophagic adaptor protein p62 endows autophagosomes with unique antimicrobial properties. Immunity *32*, 329-341.

Py, B. F., Lipinski, M. M., and Yuan, J. (2007). Autophagy limits Listeria monocytogenes intracellular growth in the early phase of primary infection. Autophagy *3*, 117-125.

Pyo, J. O., Jang, M. H., Kwon, Y. K., Lee, H. J., Jun, J. I., Woo, H. N., Cho, D. H., Choi, B., Lee, H., Kim, J. H.*, et al.* (2005). Essential roles of Atg5 and FADD in autophagic cell death: dissection of autophagic cell death into vacuole formation and cell death. J Biol Chem *280*, 20722-20729.

Qing, G., Yan, P., Qu, Z., Liu, H., and Xiao, G. (2007). Hsp90 regulates processing of NF-kappaB2 p100 involving protection of NF-kappaB-inducing kinase (NIK) from autophagy-mediated degradation. Cell Res *17*, 520-530.

Qing, G., Yan, P., and Xiao, G. (2006). Hsp90 inhibition results in autophagy-mediated proteasome-independent degradation of IkappaB kinase (IKK). Cell Res *16*, 895-901.

Raine, C. S., Feldman, L. A., Sheppard, R. D., and Bornstein, M. B. (1969). Ultrastructure of measles virus in cultures of hamster cerebellum. J Virol *4*, 169-181.

Rajcani, J., Andrea, V., and Ingeborg, R. (2004). Peculiarities of herpes simplex virus (HSV) transcription: an overview. Virus Genes *28*, 293-310.

Ralston, S. H., and Helfrich, M. H. (1999). Are paramyxoviruses involved in Paget's disease? A negative view. Bone *24*, 17S-18S.

Ralston, S. H., Langston, A. L., and Reid, I. R. (2008). Pathogenesis and management of Paget's disease of bone. Lancet *372*, 155-163.

Ravikumar, B., Acevedo-Arozena, A., Imarisio, S., Berger, Z., Vacher, C., O'Kane, C. J., Brown, S. D., and Rubinsztein, D. C. (2005). Dynein mutations impair autophagic clearance of aggregate-prone proteins. Nat Genet *37*, 771-776.

Ravikumar, B., Duden, R., and Rubinsztein, D. C. (2002). Aggregate-prone proteins with polyglutamine and polyalanine expansions are degraded by autophagy. Hum Mol Genet *11*, 1107-1117.

Reggiori, F., Monastyrska, I., Shintani, T., and Klionsky, D. J. (2005). The actin cytoskeleton is required for selective types of autophagy, but not nonspecific autophagy, in the yeast Saccharomyces cerevisiae. Mol Biol Cell *16*, 5843-5856.

Rice, C. M., and Strauss, J. H. (1982). Association of sindbis virion glycoproteins and their precursors. J Mol Biol *154*, 325-348.

Sahai, E., Garcia-Medina, R., Pouyssegur, J., and Vial, E. (2007). Smurf1 regulates tumor cell plasticity and motility through degradation of RhoA leading to localized inhibition of contractility. J Cell Biol *176*, 35-42.

Sanjuan, M. A., Dillon, C. P., Tait, S. W., Moshiach, S., Dorsey, F., Connell, S., Komatsu, M., Tanaka, K., Cleveland, J. L., Withoff, S., and Green, D. R. (2007). Toll-like receptor signalling in macrophages links the autophagy pathway to phagocytosis. Nature *450*, 1253-1257.

Schmid, D., Pypaert, M., and Munz, C. (2007). Antigen-loading compartments for major histocompatibility complex class II molecules continuously receive input from autophagosomes. Immunity *26*, 79-92.

Seibenhener, M. L., Babu, J. R., Geetha, T., Wong, H. C., Krishna, N. R., and Wooten, M. W. (2004). Sequestosome 1/p62 is a polyubiquitin chain binding protein involved in ubiquitin proteasome degradation. Mol Cell Biol *24*, 8055-8068.

Shames, S. R., Auweter, S. D., and Finlay, B. B. (2009). Co-evolution and exploitation of host cell signaling pathways by bacterial pathogens. Int J Biochem Cell Biol *41*, 380-389.

Shelly, S., Lukinova, N., Bambina, S., Berman, A., and Cherry, S. (2009). Autophagy is an essential component of Drosophila immunity against vesicular stomatitis virus. Immunity *30*, 588-598.

Shi, C. S., and Kehrl, J. H. (2010). TRAF6 and A20 regulate lysine 63-linked ubiquitination of Beclin-1 to control TLR4-induced autophagy. Sci Signal *3*, ra42.

Shvets, E., Fass, E., Scherz-Shouval, R., and Elazar, Z. (2008). The N-terminus and Phe52 residue of LC3 recruit p62/SQSTM1 into autophagosomes. J Cell Sci *121*, 2685-2695.

Singh, S. B., Davis, A. S., Taylor, G. A., and Deretic, V. (2006). Human IRGM induces autophagy to eliminate intracellular mycobacteria. Science *313*, 1438-1441.

Sir, D., Tian, Y., Chen, W. L., Ann, D. K., Yen, T. S., and Ou, J. H. (2010). The early autophagic pathway is activated by hepatitis B virus and required for viral DNA replication. Proc Natl Acad Sci U S A *107*, 4383-4388.

Smith, J. D., and de Harven, E. (1978). Herpes simplex virus and human cytomegalovirus replication in WI-38 cells. III. Cytochemical localization of lysosomal enzymes in infected cells. J Virol *26*, 102-109.

Strauss, J. H., and Strauss, E. G. (1994). The alphaviruses: gene expression, replication, and evolution. Microbiol Rev *58*, 491-562.

Su, T., Suzui, M., Wang, L., Lin, C. S., Xing, W. Q., and Weinstein, I. B. (2003). Deletion of histidine triad nucleotide-binding protein 1/PKC-interacting protein in mice enhances cell growth and carcinogenesis. Proc Natl Acad Sci U S A *100*, 7824-7829.

Sumpter, R., Jr., and Levine, B. (2010). Autophagy and innate immunity: Triggering, targeting and tuning. Semin Cell Dev Biol.

Takeshige, K., Baba, M., Tsuboi, S., Noda, T., and Ohsumi, Y. (1992). Autophagy in yeast demonstrated with proteinase-deficient mutants and conditions for its induction. J Cell Biol *119*, 301-311.

Takeuchi, O., and Akira, S. (2010). Pattern recognition receptors and inflammation. Cell *140*, 805-820.

Talloczy, Z., Jiang, W., Virgin, H. W. t., Leib, D. A., Scheuner, D., Kaufman, R. J., Eskelinen, E. L., and Levine, B. (2002). Regulation of starvation- and virus-induced autophagy by the eIF2alpha kinase signaling pathway. Proc Natl Acad Sci U S A *99*, 190-195.

Talloczy, Z., Virgin, H. W. t., and Levine, B. (2006). PKR-Dependent Autophagic Degradation of Herpes Simplex Virus Type 1. Autophagy *2*, 24-29.

Tang, H., Da, L., Mao, Y., Li, Y., Li, D., Xu, Z., Li, F., Wang, Y., Tiollais, P., Li, T., and Zhao, M. (2009). Hepatitis B virus X protein sensitizes cells to

starvation-induced autophagy via up-regulation of beclin 1 expression. Hepatology *49*, 60-71.

Tanida, I., Fukasawa, M., Ueno, T., Kominami, E., Wakita, T., and Hanada, K. (2009). Knockdown of autophagy-related gene decreases the production of infectious hepatitis C virus particles. Autophagy *5*, 937-945.

Tanida, I., Sou, Y. S., Ezaki, J., Minematsu-Ikeguchi, N., Ueno, T., and Kominami, E. (2004). HsAtg4B/HsApg4B/autophagin-1 cleaves the carboxyl termini of three human Atg8 homologues and delipidates microtubule-associated protein light chain 3- and GABAA receptor-associated protein-phospholipid conjugates. J Biol Chem *279*, 36268-36276.

Taylor, M. P., and Kirkegaard, K. (2007). Modification of cellular autophagy protein LC3 by poliovirus. J Virol *81*, 12543-12553.

Taylor, R. M., Hurlbut, H. S., Work, T. H., Kingston, J. R., and Frothingham, T. E. (1955). Sindbis virus: a newly recognized arthropodtransmitted virus. Am J Trop Med Hyg *4*, 844-862.

Tellinghuisen, T. L., Hamburger, A. E., Fisher, B. R., Ostendorp, R., and Kuhn, R. J. (1999). In vitro assembly of alphavirus cores by using nucleocapsid protein expressed in Escherichia coli. J Virol *73*, 5309-5319.

Tellinghuisen, T. L., and Kuhn, R. J. (2000). Nucleic acid-dependent cross-linking of the nucleocapsid protein of Sindbis virus. J Virol *74*, 4302-4309.

Thurston, T. L., Ryzhakov, G., Bloor, S., von Muhlinen, N., and Randow, F. (2009). The TBK1 adaptor and autophagy receptor NDP52 restricts the proliferation of ubiquitin-coated bacteria. Nat Immunol *10*, 1215-1221.

Tresse, E., Salomons, F. A., Vesa, J., Bott, L. C., Kimonis, V., Yao, T. P., Dantuma, N. P., and Taylor, J. P. (2010). VCP/p97 is essential for maturation of ubiquitin-containing autophagosomes and this function is impaired by mutations that cause IBMPFD. Autophagy *6*, 217-227.

Tsukada, M., and Ohsumi, Y. (1993). Isolation and characterization of autophagy-defective mutants of Saccharomyces cerevisiae. FEBS Lett *333*, 169-174.

Tyler, K. L. (2004). Herpes simplex virus infections of the central nervous system: encephalitis and meningitis, including Mollaret's. Herpes *11 Suppl 2*, 57A-64A.

Verpooten, D., Ma, Y., Hou, S., Yan, Z., and He, B. (2009). Control of TANK-binding kinase 1-mediated signaling by the gamma(1)34.5 protein of herpes simplex virus 1. J Biol Chem *284*, 1097-1105.

Wang, H. R., Ogunjimi, A. A., Zhang, Y., Ozdamar, B., Bose, R., and Wrana, J. L. (2006). Degradation of RhoA by Smurf1 ubiquitin ligase. Methods Enzymol *406*, 437-447.

Wang, H. R., Zhang, Y., Ozdamar, B., Ogunjimi, A. A., Alexandrova, E., Thomsen, G. H., and Wrana, J. L. (2003). Regulation of cell polarity and protrusion formation by targeting RhoA for degradation. Science *302*, 1775-1779.

Webber, J. L., and Tooze, S. A. (2010). Coordinated regulation of autophagy by p38alpha MAPK through mAtg9 and p38IP. Embo J *29*, 27-40.

Wei, Y., Pattingre, S., Sinha, S., Bassik, M., and Levine, B. (2008). JNK1-mediated phosphorylation of Bcl-2 regulates starvation-induced autophagy. Mol Cell *30*, 678-688.

Wilson, M. I., Gill, D. J., Perisic, O., Quinn, M. T., and Williams, R. L. (2003). PB1 domain-mediated heterodimerization in NADPH oxidase and signaling complexes of atypical protein kinase C with Par6 and p62. Mol Cell *12*, 39-50.

Wong, J., Zhang, J., Si, X., Gao, G., Mao, I., McManus, B. M., and Luo, H. (2008). Autophagosome Supports Coxsackievirus B3 Replication In Host Cells. J Virol.

Xu, Y., Jagannath, C., Liu, X. D., Sharafkhaneh, A., Kolodziejska, K. E., and Eissa, N. T. (2007). Toll-like receptor 4 is a sensor for autophagy associated with innate immunity. Immunity *27*, 135-144.

Yamaguchi, K., Ohara, O., Ando, A., and Nagase, T. (2008). Smurf1 directly targets hPEM-2, a GEF for Cdc42, via a novel combination of protein interaction modules in the ubiquitin-proteasome pathway. Biol Chem *389*, 405-413.

Yano, T., Mita, S., Ohmori, H., Oshima, Y., Fujimoto, Y., Ueda, R., Takada, H., Goldman, W. E., Fukase, K., Silverman, N.*, et al.* (2008). Autophagic control

of listeria through intracellular innate immune recognition in drosophila. Nat Immunol *9*, 908-916.

Yorimitsu, T., and Klionsky, D. J. (2007). Eating the endoplasmic reticulum: quality control by autophagy. Trends Cell Biol *17*, 279-285.

Yoshikawa, Y., Ogawa, M., Hain, T., Yoshida, M., Fukumatsu, M., Kim, M., Mimuro, H., Nakagawa, I., Yanagawa, T., Ishii, T.*, et al.* (2009). Listeria monocytogenes ActA-mediated escape from autophagic recognition. Nat Cell Biol *11*, 1233-1240.

Yousefi, S., Perozzo, R., Schmid, I., Ziemiecki, A., Schaffner, T., Scapozza, L., Brunner, T., and Simon, H. U. (2006). Calpain-mediated cleavage of Atg5 switches autophagy to apoptosis. Nat Cell Biol *8*, 1124-1132.

Yu, L., Wan, F., Dutta, S., Welsh, S., Liu, Z., Freundt, E., Baehrecke, E. H., and Lenardo, M. (2006). Autophagic programmed cell death by selective catalase degradation. Proc Natl Acad Sci U S A *103*, 4952-4957.

Zhang, H., Monken, C. E., Zhang, Y., Lenard, J., Mizushima, N., Lattime, E. C., and Jin, S. (2006). Cellular autophagy machinery is not required for vaccinia virus replication and maturation. Autophagy *2*, 91-95.

Zhao, Z., Fux, B., Goodwin, M., Dunay, I. R., Strong, D., Miller, B. C., Cadwell, K., Delgado, M. A., Ponpuak, M., Green, K. G.*, et al.* (2008). Autophagosome-independent essential function for the autophagy protein Atg5 in cellular immunity to intracellular pathogens. Cell Host Microbe *4*, 458-469.

Zhao, Z., Thackray, L. B., Miller, B. C., Lynn, T. M., Becker, M. M., Ward, E., Mizushima, N. N., Denison, M. R., and Virgin, H. W. t. (2007). Coronavirus replication does not require the autophagy gene ATG5. Autophagy *3*, 581-585.

Zheng, Y. T., Shahnazari, S., Brech, A., Lamark, T., Johansen, T., and Brumell, J. H. (2009). The adaptor protein p62/SQSTM1 targets invading bacteria to the autophagy pathway. J Immunol *183*, 5909-5916.

Zhou, D., and Spector, S. A. (2008). Human immunodeficiency virus type-1 infection inhibits autophagy. Aids *22*, 695-699.

Zhu, H., Kavsak, P., Abdollah, S., Wrana, J. L., and Thomsen, G. H. (1999). A SMAD ubiquitin ligase targets the BMP pathway and affects embryonic pattern formation. Nature *400*, 687-693.